

# **ECONOMIC GEOLOGY OF ALTERED SERPENTINITES IN THE BURKS MOUNTAIN COMPLEX, COLUMBIA COUNTY, GEORGIA**

**Mark D. Cocker**



**GEORGIA DEPARTMENT OF NATURAL RESOURCES  
ENVIRONMENTAL PROTECTION DIVISION  
GEORGIA GEOLOGIC SURVEY**

**BULLETIN 123**



**ECONOMIC GEOLOGY OF ALTERED SERPENTINITES  
IN THE BURKS MOUNTAIN COMPLEX,  
COLUMBIA COUNTY, GEORGIA**

**Mark D. Cocker**

**Georgia Department of Natural Resources  
Joe D. Tanner, Commissioner**

**Environmental Protection Division  
Harold F. Reheis, Director**

**Georgia Geologic Survey  
William H. McLemore, State Geologist**

**Atlanta  
1991**

**BULLETIN 123**



## TABLE OF CONTENTS

|   | Page |
|---|------|
| ABSTRACT .....  | 1    |
| INTRODUCTION .....  | 1    |
| Purpose .....   | 1    |
| Location .....  | 1    |
| Topography .....  | 3    |
| Exposure .....  | 3    |
| Vegetation .....  | 3    |
| Previous studies .....                                      | 3    |
| Field and laboratory techniques .....                       | 3    |
| Acknowledgements .....                                      | 4    |
| REGIONAL GEOLOGY .....                                      | 4    |
| LOCAL GEOLOGY .....   | 4    |
| Kiokee belt .....   | 4    |
| Serpentinites .....   | 8    |
| Multilithic breccia .....                                   | 10   |
| Coastal Plain sedimentary rocks .....                       | 10   |
| STRUCTURAL GEOLOGY .....                                    | 10   |
| METAMORPHISM .....  | 17   |
| Kiokee Belt .....   | 17   |
| Serpentinite .....  | 17   |
| METASOMATIC ALTERATION OF SERPENTINITE .....                | 17   |
| WEATHERING OF SERPENTINITE AND TALC .....                   | 28   |
| ECONOMIC GEOLOGY .....                                      | 28   |
| Talc .....  | 28   |
| Serpentine .....  | 37   |
| Chromium .....  | 37   |
| Rare earth elements, vanadium and titanium .....            | 37   |
| Nickel .....  | 38   |
| Cobalt .....  | 38   |
| Corundum .....  | 38   |
| Asbestos .....  | 38   |
| Platinum group elements .....                               | 39   |
| Quartz vein mineralization (base and precious metals) ..... | 39   |
| DISCUSSION AND CONCLUSIONS .....                            | 39   |
| Origin of the mineral deposits .....                        | 39   |
| Economic geology of the mineral deposits .....              | 40   |
| REFERENCES CITED .....                                      | 40   |
| APPENDICES .....  | 43   |
| I. Whole Rock Chemistry - Talc .....                        | 45   |
| II. Trace Element Geochemistry .....                        | 46   |
| III. Drilling Results .....                                 | 48   |
| IV. Drill Logs .....  | 58   |

## LIST OF ILLUSTRATIONS

| Figure  | Page |
|---|------|
| 1. Location map of the Burks Mountain complex and project area .....                                      | 2    |
| 2. Generalized geologic map of the Pollards Corner area .....   | 5    |
| 3. Geologic map of the talc prospect .....  | 6    |
| 4. Ground magnetic map of the project area .....  | 9    |
| 5. Cross section B-B' .....   | 11   |
| 6. Long section A-A' .....  | 12   |
| 7. Photomicrograph of lizardite .....   | 13   |
| 8. Normative olivine and enstatite versus height above base of the serpentinite .....                     | 14   |
| 9. Multilithic breccia .....  | 15   |
| 10. Talc boulder field .....  | 15   |
| 11. Histogram of stream orientations .....  | 16   |
| 12. Composite histogram of dips of all veins (in core) .....  | 18   |
| 13. Composite histogram of brittle structure orientations(surface) .....                                  | 19   |
| 14. Chlorite, foliated talc and massive talc alteration .....   | 21   |
| 15. Chlorite, talc, talc + carbonate metasomatic alteration .....   | 21   |
| 16. Photomicrograph of magnetite destruction in talc .....  | 22   |
| 17. Modal magnetite - talc diagram .....  | 23   |
| 18. Photomicrograph of silicified serpentinite .....  | 24   |
| 19. SiO <sub>2</sub> and MgO, Fe <sub>2</sub> O <sub>3</sub> and FeO versus serpentinite alteration ..... | 25   |
| 20. Al <sub>2</sub> O <sub>3</sub> and CaO versus serpentinite alteration .....                           | 26   |
| 21. Na <sub>2</sub> O and K <sub>2</sub> O, and TiO <sub>2</sub> versus serpentinite alteration .....     | 27   |
| 22. SiO <sub>2</sub> -MgO content of talc .....   | 30   |
| 23. Weathering index versus GE brightness .....   | 31   |
| 24. Total Fe content versus GE brightness .....   | 32   |
| 25. Oxidation ratio versus GE brightness .....  | 33   |
| 26. Distribution of Ni, Cr, and Co in serpentinite from DDH PC 87-5 .....                                 | 34   |
| 27. Map of potential talc ore zones .....   | 35   |
| 28. Long section (A-A') of potential talc ore zones .....   | 36   |
| 29. Recovery DDH PC87-1 .....   | 49   |
| 30. Recovery DDH PC87-2 .....   | 50   |
| 31. Recovery DDH PC87-3 .....   | 51   |
| 32. Recovery DDH PC87-4 .....   | 52   |
| 33. Recovery DDH PC87-5 .....   | 53   |
| 34. Recovery DDH PC88-1 .....   | 54   |
| 35. Recovery DDH PC88-2 .....   | 55   |
| 36. Recovery DDH PC88-3 .....   | 56   |
| 37. Recovery DDH PC88-4 .....   | 57   |
| 38. Graphic Log DDH PC87-1 .....  | 60   |
| 39. Graphic Log DDH PC87-2, DDH PC87-3, and DDH PC87-6 .....  | 64   |
| 40. Graphic Log DDH PC87-4 .....  | 68   |
| 41. Graphic Log DDH PC87-5 .....  | 73   |
| 42. Graphic Log DDH PC88-1, DDH PC88-3, and DDH PC88-4 .....  | 79   |
| 43. Graphic Log DDH PC88-2 .....  | 83   |

# ECONOMIC GEOLOGY OF ALTERED SERPENTINITES IN THE BURKS MOUNTAIN COMPLEX, COLUMBIA COUNTY, GEORGIA

by

Mark D. Cocker

## ABSTRACT

This report focuses on the evaluation of the economic potential of serpentinites and associated talc mineralization located south and southeast of Pollards Corner, Columbia County, Georgia. The investigation consisted of field mapping, a ground magnetic survey, logging of drill core, whole-rock and trace-element geochemistry, petrography and x-ray diffraction analyses. The serpentinites are fragments of an elongate complex of mafic/ultramafic rocks called the Burks Mountain complex (Sacks and others, 1989). The Burks Mountain complex principally consists of serpentinite, derived from a harzburgite protolith, with minor occurrences of metagabbro and metabasalt. This complex is conformably enclosed within gently to moderately dipping, middle to upper amphibolite facies gneisses and schists of the Kiokee belt.

Talc formed by the alteration of a serpentinitized meta-harzburgite located south of Burks Mountain. Retrograde greenschist facies metamorphism, probably during the waning stages of the Alleghanian orogeny, pervasively altered the meta-harzburgite to a lizardite serpentinite. Subsequent fracturing of the serpentinite opened channelways for hydrous, siliceous, and CO<sub>2</sub>-bearing fluids to form talc selvages around serpentinite clasts and along fractures in the serpentinite. The most extensive fracturing occurred along the upper contact of the serpentinite forming a multilithic breccia.

Similar talc mineralization occurs around the base of a serpentinite at Burks Mountain and may underlie that serpentinite. Large portions of this Burks Mountain serpentinite body are fractured, silicified and quartz veined.

Potentially economic mineral deposits in the study area include mainly talc and serpentinite. Talc mineralization is evident as talc boulder fields. These boulder fields were formed by the weathering and removal of less-resistant materials from the underlying, talc-bearing, multilithic breccia. The estimated grade of the talc-bearing breccia is 25 percent talc and

calculated tonnages are on the order of 7.3 million tons. Drilled intercepts suggest that additional talc is localized along the upper and lower boundaries and adjacent to fractures in the underlying serpentinite. An open-pit configuration, little overburden, and anticipated easy mining and ore separation favor a low-cost production. Development of additional talc-mineralized zones in other nearby serpentinites would further reduce the cost of a processing operation. Drilling in the underlying serpentinite also encountered significant intervals of unweathered, massive serpentinite suitable for dimension stone and other industrial purposes. Open-pit mining of the talc deposit would expose the serpentinite so that it could be developed.

Economic concentrations of Ni, Cr, Pt, Pd, Au, Ag, Cu, Pb, and Zn were searched for but not encountered. Enrichment of V, Ti and rare earth elements is found in layered magnetite and ilmeno-hematite which occur in the upper part of the northern serpentinite. The extent of this mineralization is unknown.

## INTRODUCTION

### Purpose

The purpose of this investigation is to describe the talc mineralization near Pollards Corner, Georgia, and to discuss its origin, and economic potential. Potential metallic mineralization associated with the host serpentinite also is considered.

### Location

The area covered by this investigation is located 2.2 miles (3.5 km) ESE of Pollards Corner in Columbia County, Georgia (Fig. 1). The northwestern corner of the project area is located approximately 82°15'W and 33°37'30"N in the northwestern corner of the Evans 7.5' quadrangle. Reconnaissance studies extended west into the northeast corner of the Appling 7.5' quadrangle.

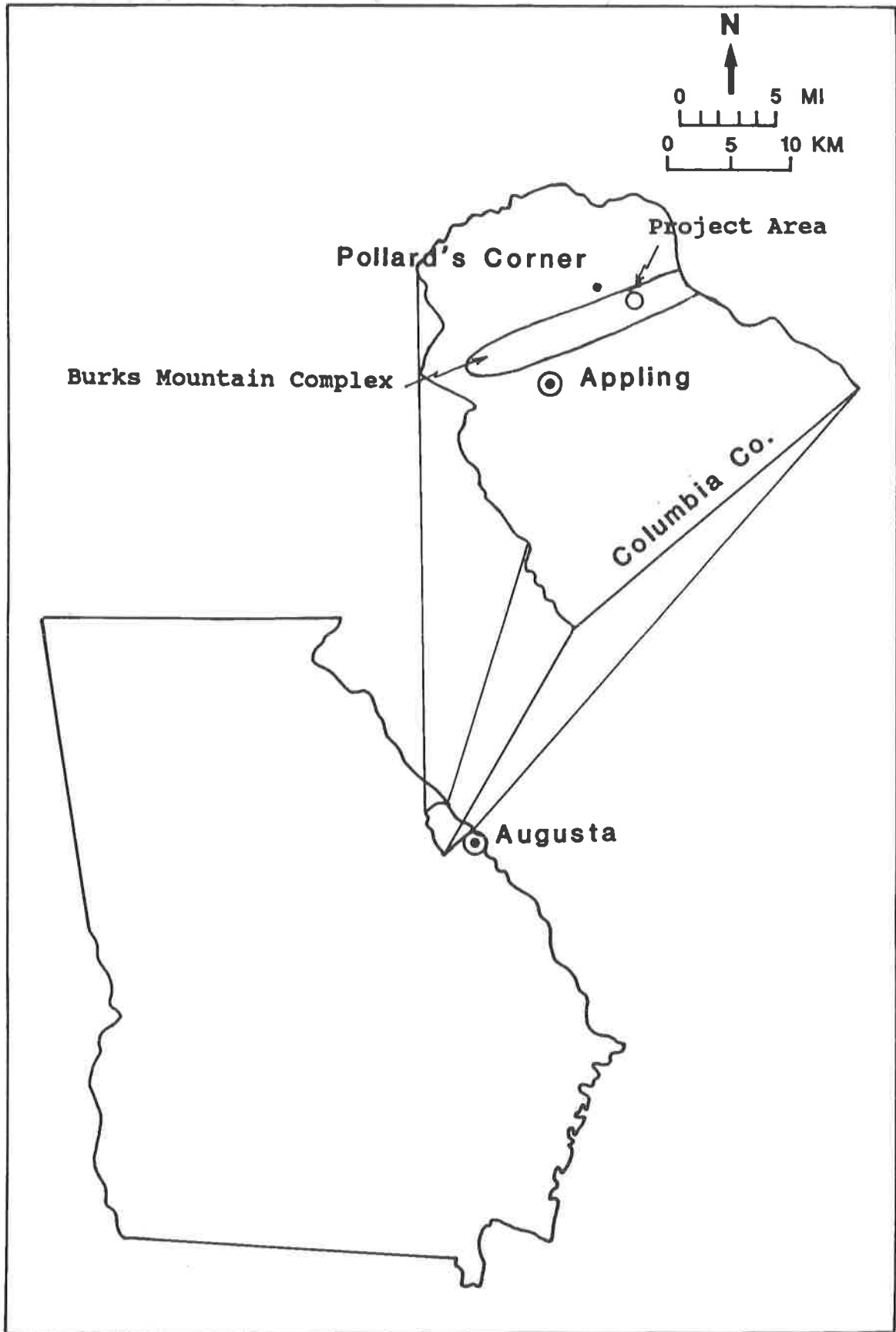


Figure 1. Location map of the Burks Mountain complex and project area



Access to the area is via Georgia Hwy #304/ U.S. Hwy #221 or Georgia Hwy #104 to Pollards Corner and via the paved Old Petersburg Road or the graded dirt Old Middleton Road to the village of Rosemont at the western end of Burks Mountain.

### Topography

Elevation of the project area generally ranges from 250 to 350 feet (76 to 107 m). The ground surface is gently rolling to flat. Along the northern edge of the project area, the western end of Burks Mountain abruptly rises 180 feet (55 m) above the surrounding area to a maximum elevation of 535 feet (163 m).

### Exposure

Rocks in the project area are exposed along: three major roadcuts on Old Petersburg Road; steep-sided gullies and creeks; and on the upper slopes of Burks Mountain. In addition, outcrops of highly resistant rocks are scattered in fields and forested areas. The high average annual rainfall of 48.5 inches (LeGrand and Furcron, 1956) significantly aids in the chemical and physical degradation of less resistant rocks.

### Vegetation

Forests of the Southern Pinelands, consisting of pines and mixed hardwoods, cover approximately 50 percent of the project area with the remainder consisting of open pasture.

### Previous studies

The earliest documentation of the economic geology of the ultramafic rocks (talc) near Pollards Corner is by Hopkins (1914). Later, LeGrand and Furcron (1956) described the mining of serpentinite for the production of magnesium sulfate from Dixie Mountain (Burks Mountain).

High metal prices in the early 1960's sparked renewed interest in the Burks Mountain complex serpentinites. The J.M. Huber Corporation tested the nickel and chrome potential of the serpentinites with four core holes in the vicinity of Dixie Mountain and at least one core hole approximately 1/2 mile southeast of Pollard's Corner. Worthington (1964) examined the nickel, chrome and platinum potential of the serpentinites as part of a regional (Appalachian) exploration program. McLemore (1965) mapped an area of over 35 square miles around the Pollards Corner area and noted the occurrence of talc in the present study area.

Hurst and others (1966) mapped the geology of Columbia County and evaluated the mineral resource potential of the area through a detailed soil geochemistry survey over the serpentinites.

Recent studies include an investigation of ultramafic rocks in Georgia as part of the Georgia Geologic Survey's Accelerated Minerals Program (Vincent and others, 1990), and analysis of the Burks Mountain complex with regards to regional studies of the Modoc Fault Zone and the Kiokee Belt (Sacks and others, 1989).

### Field and Laboratory Techniques

The current investigation involved detailed geologic mapping of an area less than one square mile in size on a scale of 1"=200 feet (1:2400) using an enlarged topographic base. Roadcuts were mapped in greater detail on a scale of 1"=50 feet (1:600). As an aid in 1:2400 scale mapping and to establish stations for a detailed ground magnetic survey, a grid was established using tape and Brunton compass (Cocker, 1991a).

Drilling was done with the Georgia Geologic Survey's Failing CF-15 drill rig using conventional wire-line drilling methods. Further information on the drilling program is included in Appendix III - Drilling Results.

Drill core was logged in detail (1"=10 feet) to obtain information on lithology, structure, alteration, veining, and drilling recovery. The core was then sampled for geochemical analysis, petrography and x-ray diffraction studies. Rock-chip geochemical samples were collected from selected outcrops and float during the field mapping phase (Cocker, 1991b). X-ray diffraction analysis (XRD) determined the mineralogy of the serpentinite, and identified talc, chlorite, calcite, dolomite and magnesite (Cocker, 1991b).

Petrographic studies consisted of mineral identification, modal analyses and textural descriptions using standard transmitted- and reflected-light microscopy. Twenty-three standard thin sections and 6 polished thin sections of fresh, unweathered drill core samples and 12 standard thin sections of surface samples collected by Vincent and others (1990) were examined in detail. Further details are given by Cocker (1991b).

Whole-rock analyses of core and surface samples included SiO<sub>2</sub>, Al<sub>2</sub>O<sub>3</sub>, Fe<sub>2</sub>O<sub>3</sub>, FeO, MgO, CaO, Na<sub>2</sub>O, K<sub>2</sub>O, TiO<sub>2</sub>, P<sub>2</sub>O<sub>5</sub>, MnO and Loss-on-Ignition (LOI). Selected samples were analyzed for Au, Ag, Cu, Pb, Zn, As, Hg, Pt, Pd, Co, Ni, Cr, Sr, V and Ba. Inductively coupled argon plasma spectrometry (ICAP) was used for SiO<sub>2</sub>, Al<sub>2</sub>O<sub>3</sub>, MgO, CaO, Na<sub>2</sub>O, K<sub>2</sub>O, TiO<sub>2</sub>, P<sub>2</sub>O<sub>5</sub>, and MnO, Sr, V and Ba. Dichromatic

titration was used for Fe<sup>+2</sup> and Fe<sup>+3</sup>. Loss-on-ignition (LOI) was measured by gravimetric analysis. Ni, Cr, Co, Rb, Cu, Pb, Zn, Ag, Au and As were measured by atomic absorption (AA). Fire assay and ICP were used for Pt and Pd analysis. Samples were sent to Skyline Labs., Inc. (Wheat Ridge, CO) for standard whole-rock analyses and for trace-element analyses. Selected samples were analyzed by Bondar-Clegg, Inc. (Lake-wood, CO) for rare earth elements (REE) using instrumental neutron activation analysis (INAA) and x-ray fluorescence (XRF).

Ten samples of talc-rich rock were analyzed by Georgia Kaolin Company (courtesy of S. Pickering, Jr.) for GE brightness. These samples are from the surface and drill core. Samples were crushed to -100 mesh and ball milled for one hour.

Various abbreviations are used in this report to refer to drill hole or sample locations. Drill holes are designated by DDH (diamond drill hole), PC (Pollards Corner), 87 or 88 (the year drilled), followed by 1 to 6 (the drill hole number for that year). Core samples refer to the year and hole number (e.g. 87-1) and the depth from which it was collected (e.g. 234 feet). Surface samples are either given a grid number (e.g. E100, 70W) or a sample line number (e.g. D137).

#### Acknowledgements

The author gratefully acknowledges Mr. J. Dan Smith of Augusta, Georgia for his permission to conduct the investigation on his property and for his continued interest in the work. The brightness tests performed by Georgia Kaolin Company under the direction of Sam Pickering, Jr. are also appreciated. The author wishes to express thanks to all the reviewers for their criticisms and comments of early versions of this document. These include Drs. Gilles O. Allard and James A. Whitney of the University of Georgia and Dr. Paul E. Sacks of the United States Geological Survey.

### REGIONAL GEOLOGY

The talc deposits of the Pollards Corner area are associated with serpentinites which form part of an elongate grouping of mafic/ultramafic rocks called the Burks Mountain complex (Sacks and others, 1987; Sacks and others, 1989). The Burks Mountain complex is conformably enclosed within gently to moderately dipping, middle to upper amphibolite facies gneisses and schists of the Kiokee belt located in the southeasternmost part of the Piedmont Province of Georgia.

The Burks Mountain complex consists princi-

pally of serpentinite, metagabbro, talc and several types of amphibolite. This complex is interpreted as a suite of metamorphosed and locally altered harzburgite, cumulate wherlite or olivine clinopyroxenite, cumulate gabbro and anorthositic gabbro, rodingite and possibly mafic volcanic rocks (Sacks and others, 1989). It extends from Columbia County in Georgia into South Carolina (Fig. 2) for a total strike length of over 20 miles (33 km). The Burks Mountain complex is roughly parallel to the regional strike and concordant with regional foliation of the Kiokee belt.

The Kiokee belt consists of a sequence of migmatitic micaceous quartzo-feldspathic gneiss, locally interlayered with amphibole-biotite schist, and biotite-muscovite schist. Migmatitic gneiss and sillimanite schist indicate that middle to upper amphibolite facies metamorphism was attained in the Kiokee belt (Secor and others, 1986a; Secor, 1987; Maher, 1978, 1987; Sacks and others, 1989).

The Kiokee belt and the adjacent Carolina slate belt to the north and Belair belt to the south may have accumulated in association with one or more subduction-related volcanic arcs (530-580 Ma) developed adjacent to the African continent (Whitney and others, 1978; Feiss, 1982; Rogers, 1982; Secor and others, 1983, 1986b; Shelley and others, 1988; Higgins and others, 1988). These belts were accreted to North America by the Late Ordovician (Kish and others, 1979; Vick and others, 1987; Sacks and others, 1989), and metamorphosed and emplaced into their present position during the Alleghanian orogeny (Secor and others, 1986a and 1986b; Dallmeyer and others, 1986; and Secor, 1987).

### LOCAL GEOLOGY

#### Kiokee Belt

Within the project area (Fig.3), the Burks Mountain complex principally consists of two large masses of serpentinite enclosed in an interlayered sequence of migmatitic, biotite-quartz-feldspar gneiss, plus hornblende-biotite gneiss and schist with minor metaquartzite. These serpentinites (referred to as the northern and southern serpentinites) strike northeast and dip gently to moderately southeast. Abundant quartz-feldspar granite dikes intrude the metamorphic rocks and are cut in turn by numerous, thin, quartz-feldspar pegmatites. The petrology and petrochemistry of the felsic and mafic rocks of the Kiokee belt in this area are discussed in detailed by Cocker (1991b).

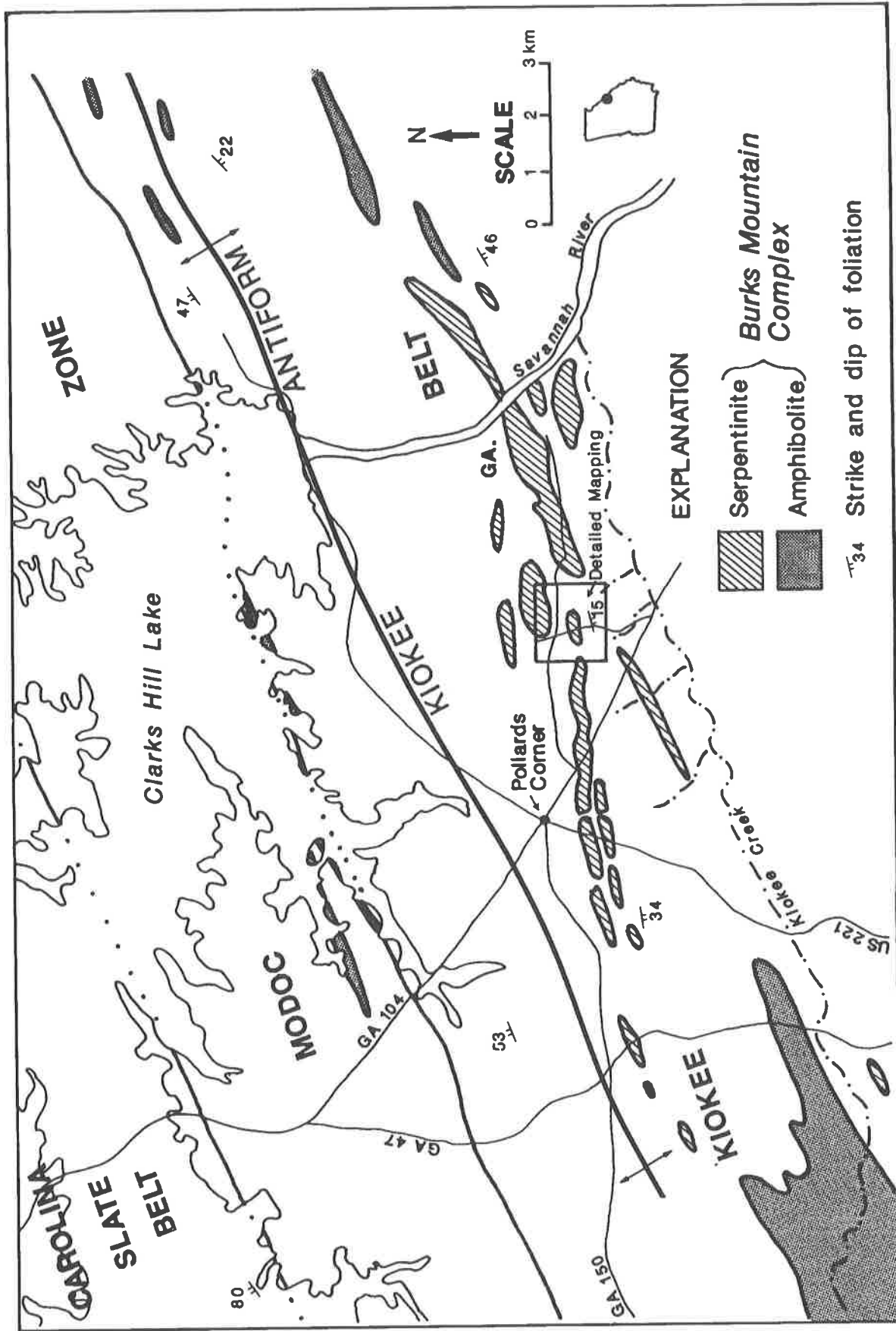


Figure 2. Generalized Geologic Map of the Pollards Corner Area. (Modified from Georgia Geologic Survey, 1976; Sacks and others, 1989).

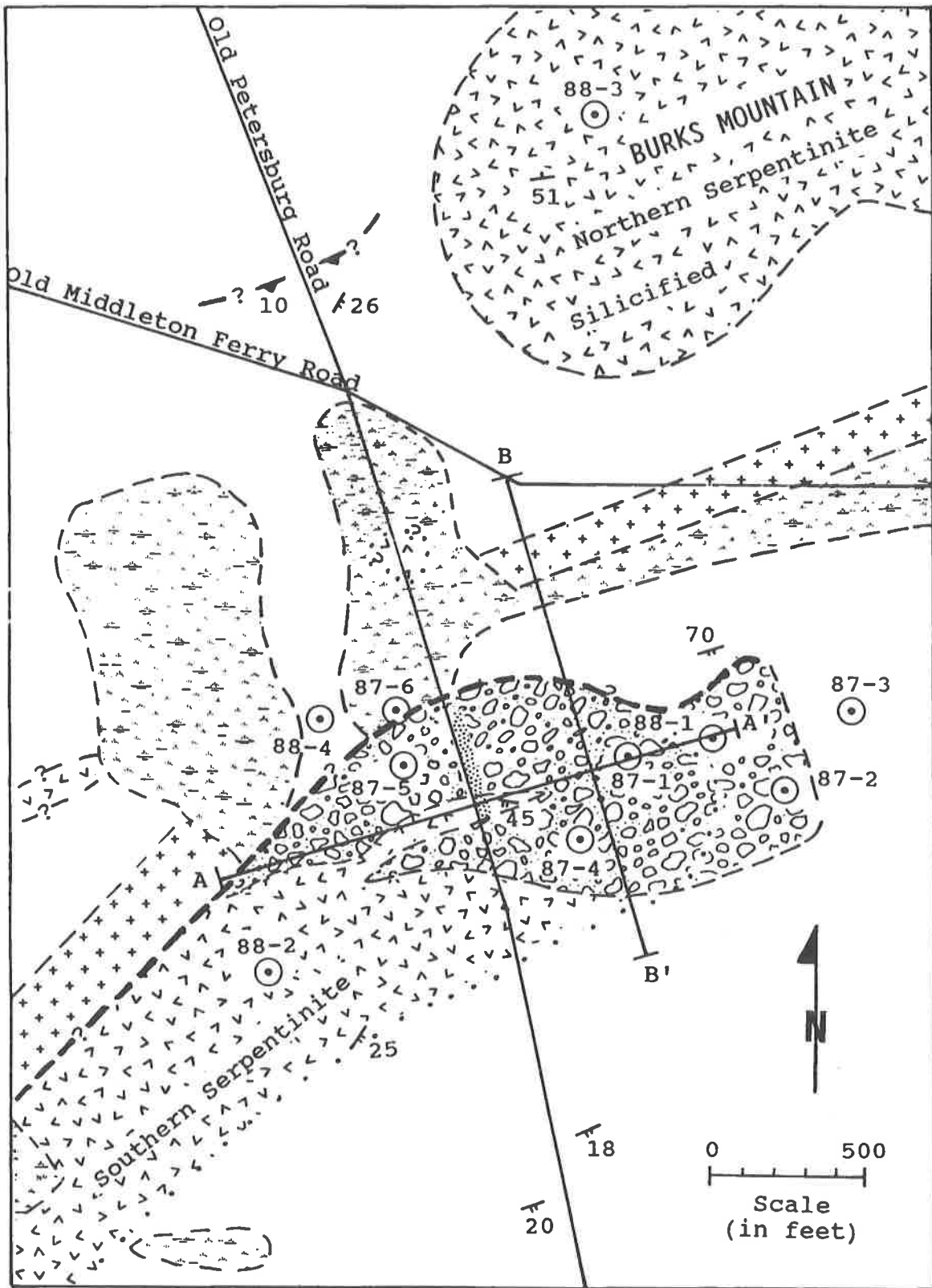


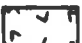





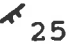
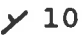





Figure 3. Geologic map of the talc prospect. Map shows the locations of drill holes and sections A-A' and B-B'.

## EXPLANATION

-  Cretaceous/Tertiary undifferentiated
-  Multilithic breccia
-  Serpentinite
-  Permo-Carboniferous granite
-  Migmatitic biotite amphibole gneiss
-  Contact (dashed where uncertain; dotted where concealed)
-  Fault (inferred from ground magnetic data and drill holes)
-  Low angle fault (thrust ?)
-  25 Strike and dip of foliation
-  10 Strike and dip of centimeter-scale igneous layering
-  87-1 Diamond drill hole
-  Line of section
-  Roadcut

## Serpentinites (Burks Mountain complex)

Exposures of the two serpentinites differ markedly because the northern serpentinite is considerably more resistant to weathering than the southern serpentinite. The pervasively silicified northern serpentinite is considerably more resistant to weathering than adjacent gneisses and granites and forms the western end of Burks Mountain. The southern serpentinite is not exposed but is overlain by a multilithic breccia, containing mainly serpentinite clasts. The breccia is exposed in a long roadcut on the Old Petersburg Road approximately 1400 feet (425 m) south of the Old Middleton Ferry Road. Talc boulders derived by weathering of the multilithic breccia, drill data, and a ground magnetic survey define the subsurface aspect of the southern serpentinite.

The serpentinites appear to be concordant or nearly concordant to the enclosing regional foliation which dips from 10 to 30°SE (Fig. 3). A ground magnetic survey and drill hole data (Cocker, 1989a, and 1991 b) indicate that the southern serpentinite strikes N64°E (Fig. 4). Drilled intercepts show the southern serpentinite to range from 95 to 145 feet (29 to 44 m) thick with an average thickness of 117 feet (36 m). The serpentinite is underlain by Kiokee gneisses, granite and amphibolites and is overlain in DDH PC 88-2 by similar lithologies. In other drill holes, the serpentinite is overlain by the multilithic breccia (Cocker, 1991 b).

The typical Burks Mountain serpentinite as observed in 41 thin sections is composed of 65-85 percent, mesh-textured lizardite (Fig. 7). In addition to the lizardite, other minerals include disseminated, coarse-grained chromite/magnetite (1-5 percent), and very fine-grained, secondary magnetite "dust" (0-4 percent) that is concentrated along the mesh-texture rims in lizardite. The least altered serpentinite usually contains 5-25 percent secondary carbonate, talc, chlorite, and quartz (Cocker, 1989a and 1991b). The serpentinite mineralogy consists of three temporally distinct assemblages: 1) primary minerals (Cr-spinels - altered to magnetite) which are relicts from the original ultramafic body; 2) metamorphic minerals (anthophyllite, tremolite, lizardite, olivine, enstatite (altered to talc or lizardite), talc, chlorite, Fe-Cr spinel, magnetite) which formed during regional metamorphism; and 3) secondary minerals (talc, chlorite, magnetite, carbonate minerals, quartz) which formed after regional metamorphism as alteration products of primary and metamorphic minerals (Cocker, 1989a, 1989b, 1991a and b).

The original composition of the serpentinite is inferred to be a harzburgite based on preserved pri-

mary textures (Sacks and others, 1989; Cocker, 1991 b) and geochemistry (Cocker, 1989a, 1989c, and 1991 b). Other, relatively uncommon, ultramafic rocks in the Burks Mountain complex are interpreted as olivine-clinopyroxene cumulates (wehrlites) with possible relict igneous layering (Sacks and others, 1989).

Variations in the concentrations of SiO<sub>2</sub>, MgO, MnO, Fe<sub>2</sub>O<sub>3</sub>, and CaO principally reflect primary igneous differentiation trends. Normative enstatite increases from 17 percent at the base to 53 percent near the top, forsterite declines from 67 percent to 37 percent, and diopside declines from 13 percent to 0 percent (Fig. 8). SiO<sub>2</sub> increases upward from 38 weight percent to 41-42 weight percent reflecting a decrease in SiO<sub>2</sub>-poor olivine (Mg<sub>2</sub>SiO<sub>4</sub>) and an increase in SiO<sub>2</sub>-richer enstatite (MgSiO<sub>3</sub>). MgO exhibits a gradual increase upward from 35 to 36.5-37 weight percent. A slight upward decrease in Fe<sub>2</sub>O<sub>3</sub> from 6-7.5 weight percent to about 5 weight percent may reflect a decrease in the overall magnetite/chromite content of the original igneous body. An upward decrease in CaO from 3.5 weight percent to 0.08 weight percent may result from a decrease in primary Ca-pyroxene (Cocker, 1989a, 1989c, and 1991b).

The trace elements, Co, Ni, and Cr, tend to increase toward the base of the serpentinite. Because Ni and Co show a similar variation trend with each other and with normative olivine, they probably are substituting in the olivine structure. The Cr content does not appear to show a similar trend and is probably more dependent on the variation in the amount of magmatic chromite in the serpentinite (Cocker, 1991 (b)).

Significant enrichment of TiO<sub>2</sub>, Fe<sub>2</sub>O<sub>3</sub>, V, and rare earth elements (REE's) occurs in magnetite and ilmenite-hematite-rich layers in the northern Burks Mountain serpentinite. While the southern serpentinite contains about 0.01 weight percent TiO<sub>2</sub>, the Fe-Ti rich layers in the northern serpentinite are enriched to 9.2 weight percent; V is enriched from 5-15 ppm to 750 ppm; and Fe<sub>2</sub>O<sub>3</sub> is enriched from 5.89 weight percent to 38.2 weight percent. The Cr content of these layers is very low (<0.01 weight percent) (Cocker, 1989c and 1991b). The V content of the Burks Mountain serpentinite and talc is on the order of 5-15 ppm and 5-20 ppm respectively. Vanadium is concentrated in pyroxenes of dunites and harzburgites, in massive chromite rather than in disseminated chromite (Challis, 1965), and in the later crystallizing titanomagnetites or high Ti-norites as in the Stillwater (Helz, 1985) and Bushveld layered mafic intrusions (Reynolds, 1985). REE's in the Burks Mountain serpentinite are generally below detection limits but increase significantly in

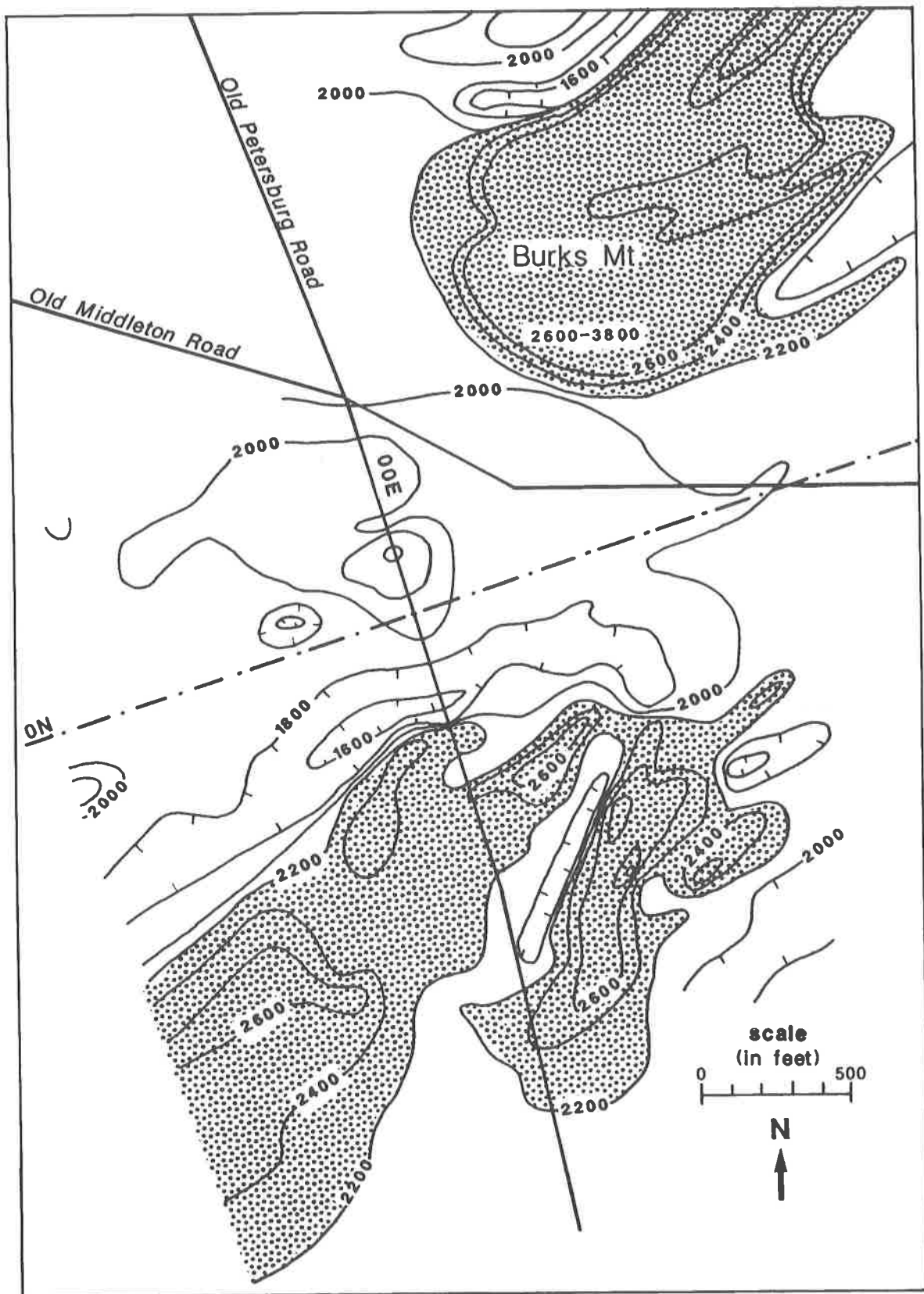


Figure 4. Ground magnetic map of the project area ( contour interval 200 gammas). The ground magnetic readings greater than 2200 gammas are shaded. These areas are underlain at or near the surface by magnetic serpentinite.

the magnetite-rich layers (Cocker, 1989c).

### Multilithic Breccia (Burks Mountain complex)

Multilithic breccia (Figs. 3, 5 and 6) is exposed in the Old Petersburg Road roadcut and is penetrated in at least four of the drill holes. Drill intercepts of the multilithic breccia range from a minimum of 85 feet (26 m) in DDH PC 88-1 to a maximum of 137 feet (42 m) in DDH PC 87-5. Average thickness is 76 feet (23 m). The breccia thickens to the west but disappears between DDH PC 87-5 and DDH PC 88-2. Talc clasts located several hundred feet west of DDH PC 87-5 indicate the breccia probably extends under that area. A three-point solution on the basal contact of the breccia with the serpentinite defines a strike of N39°W dipping 10°SW (Cocker, 1989a and 1991b). The down-dip extent of the breccia was not drilled.

The multilithic breccia (Fig. 9) consists of generally small (<0.5 to 5 m), subrounded to rounded serpentinite clasts with minor (<20 percent) mafic rocks, gneiss and kaolinized granite clasts enclosed in and supported by a matrix of coarsely crystalline chlorite. Ultramafic clasts are rimmed by foliated talc. Complete replacement of the smaller serpentinite clasts by talc is common, although serpentinite-cored clasts are present (Cocker, 1989a, 1989b, and 1991b).

The breccia matrix, composed of coarse-grained chlorite, is friable and poorly consolidated. The chlorite is frequently washed out during drilling leaving a chaotic mixture of clasts in the drill core. Surface weathering removes the chlorite and decomposed gneiss, granite and serpentinite clasts leaving the inert talc clasts as a surface residuum of subrounded to rounded pebbles, cobbles and boulders (Fig. 10). Areas underlain by multilithic breccia are covered by this residual talc.

The multilithic breccia provides important evidence concerning the relative timing of regional metamorphism, serpentinitization, serpentinite brecciation, and alteration to talc, carbonate and chlorite. The presence of Kiokee gneiss and kaolinized granite as clasts within the breccia conclusively indicate that the Kiokee gneiss and granite formed prior to the brittle deformation and brecciation of the serpentinite. Also, serpentinitization occurred prior to brecciation. Alteration of the serpentinite to talc, carbonate and chlorite along fractures and in breccia clasts occurred subsequent to brecciation and hence after regional high-grade and retrograde metamorphism (Cocker, 1989a and 1991b).

### Coastal Plain sedimentary rocks

Numerous outcrops of arkosic sandstones and conglomeratic sandstones occur unconformably overlying gneisses, schists and granites over much of the mapped area (Cocker, 1991b). These clastic rocks dip at a shallow angle to the south. The maximum observed thickness in outcrop is about 8 feet (2.6 m). These sandstones are similar to clastic rocks described as belonging to the Cretaceous-age Gaillard Formation (Huddleston, personal communication, 1991) or the previously described Tuscaloosa Formation (Eargle, 1955; LeGrand and Furcron, 1956; and O'Connor and Prowell, 1976); they may be as young as middle Eocene (Tschudy and Patterson, 1975; and O'Connor and Prowell, 1976).

## STRUCTURAL GEOLOGY

Brittle deformation of the serpentinite is critical to the development of the talc mineralization. In this part of the Kiokee belt, brittle deformation appears complex and is probably multistage. Brittle deformation of the serpentinite is manifested as faults, multilithic breccias, talc, chlorite and carbonate veining, and open-space quartz veining. Granite and pegmatite dikes intrude and preserve earlier brittle structures in the surrounding Kiokee rocks. Moderately to steeply dipping talc veins are common in outcrop and in drill core; 22 percent of the 41 veins in drill core dip 60-65° (in non-oriented core, only dip angles of structures are measurable). Dips of fractures containing coarse-grained chlorite are concentrated (49 percent of the 37 fractures) in the range 40-60° (Cocker, 1991b). White to creamy carbonate veins in serpentinite are locally abundant in drill core but are virtually absent in surface exposures due to weathering. Carbonate veins tend to dip from 50-65° (55 percent of the 33 veins in drill core).

Brecciated rock in the drill core which is not accompanied by alteration or mineralization is referred to in this report as dry brittle fracturing. Measurable dry brittle fracture surfaces are rare to absent. This fracturing is the youngest recognized brittle deformation, because there is no alteration or mineralization, and it affects all other brittle fractures. Long intervals of fractured core suggests that this fracturing is more extensive than is indicated by surface geologic mapping.

Topographic expression of this fracturing may be seen as lineament trends. A major concentration (30 percent) of the orientations of stream segments greater than 600 m long (Fig. 11) strike from N25-55°W with the greatest concentration (up to 22 streams per 5° interval) between N35-50°W (Cocker, 1991b). These



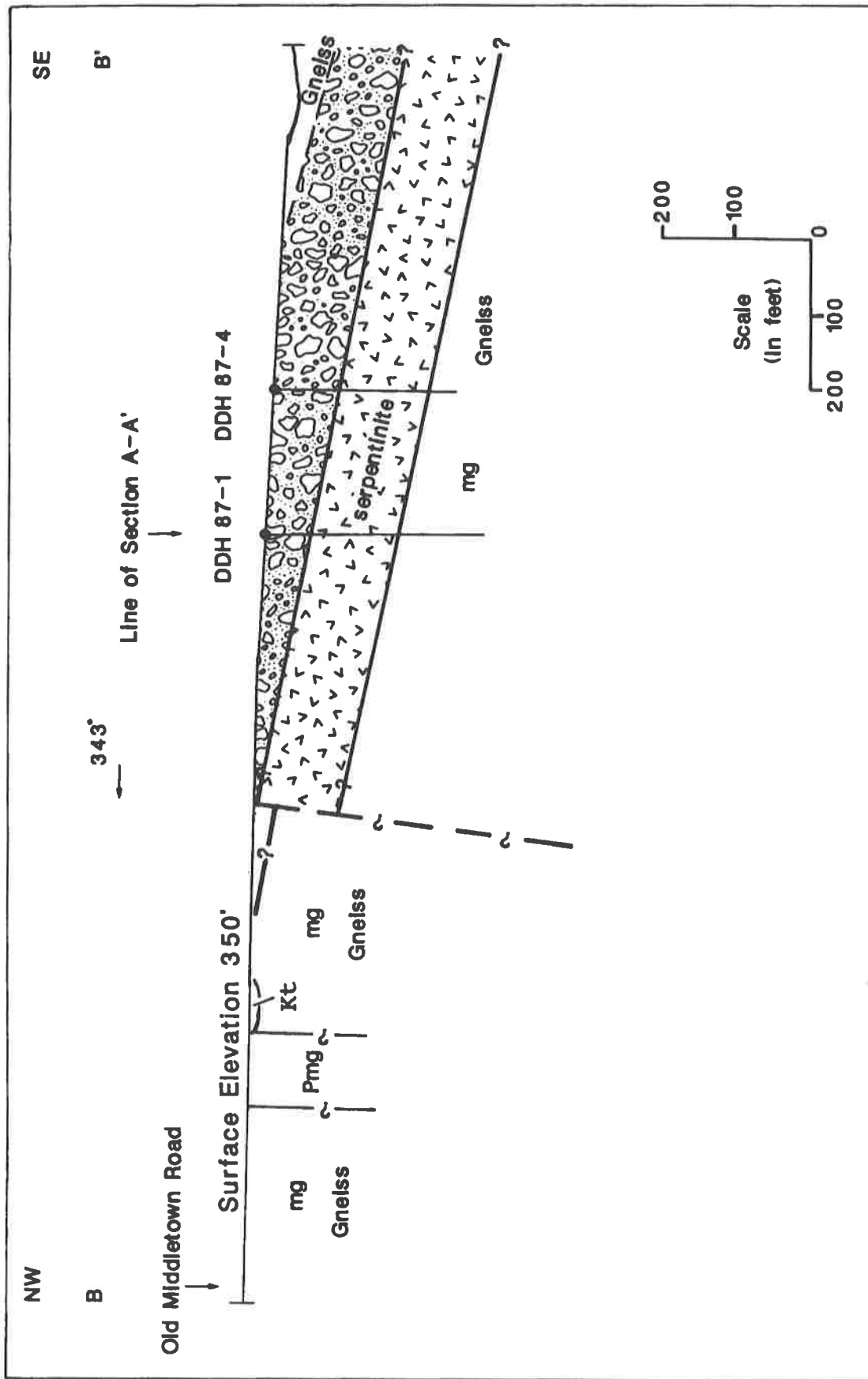


Figure 5. Cross section B-B'. This section was constructed from the surface geology and the geology projected from DDH's 87-1 and 87-4 into the section. This section is oriented at 90° to the long section A-A'. The existence of the fault on the north side of the serpentinite is inferred from the ground magnetic sections (Cocker, unpublished).

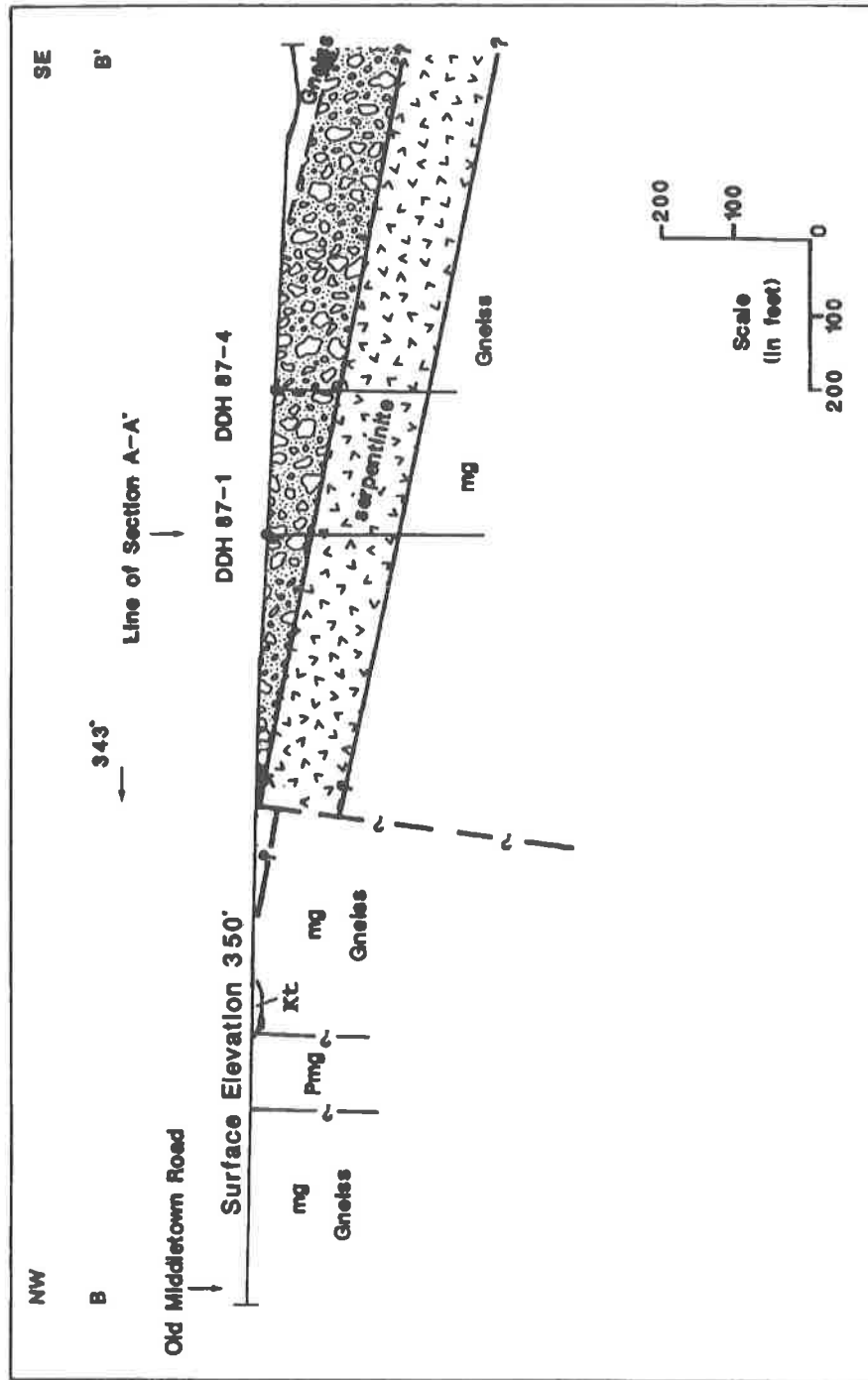
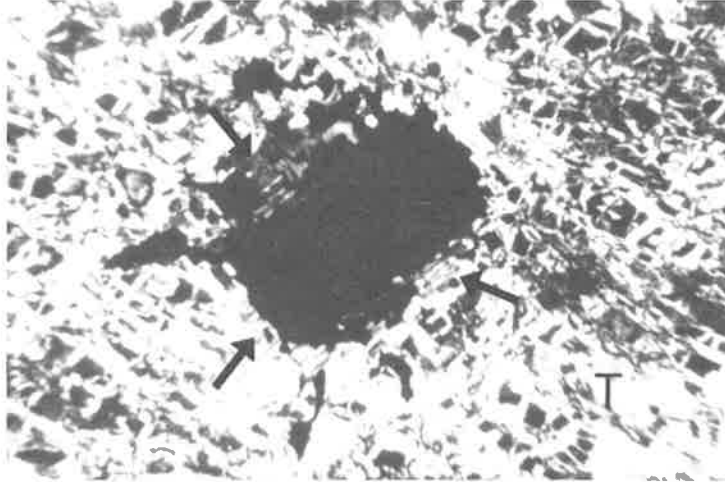


Figure 6. Long section A-A'. This section shows the distribution of the multilithic breccia relative to the underlying southern serpentinite as determined from drill hole data. DDH's 87-4, 87-5, and 88-2 are projected into the section. The existence and attitude of the fault between DDH's 87-5 and 88-2 is inferred from the ground magnetics and the apparent displacement of the serpentinite in this section.



**Figure 7.** Photomicrograph of lizardite. Pictured is the typical mesh-texture of the lizardite in the Burks Mountain serpentinites. Large, black grain in center is a magmatic spinel altered to Cr-magnetite with a rim of chlorite (shown by arrows). Patchy talc (T) is disseminated in the lizardite. Sample is PC 87-4-185. Width of field of view is 2.65 mm.

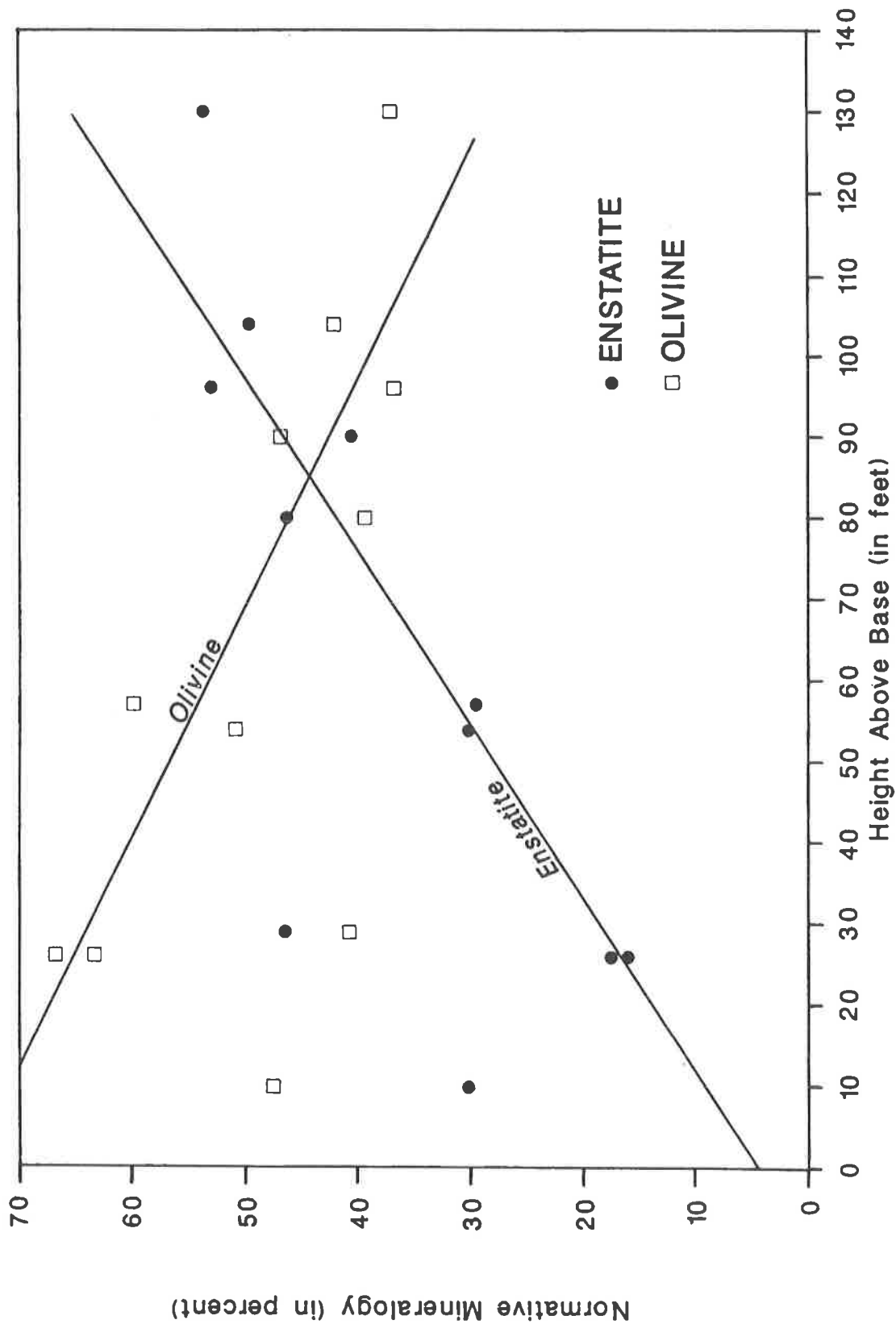
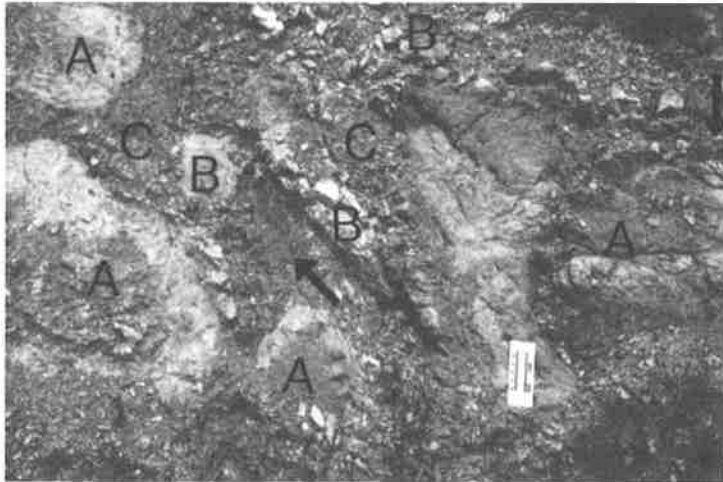


Figure 8. Normative olivine and enstatite versus height above base of the serpentinite. Trend lines suggest a continual change in composition from the base towards the top of the serpentinite and are inferred to represent igneous differentiation. Samples are from DDH's 87-1, 87-4, 87-5 and 88-2. Closely spaced pairs are from different drill holes and reinforce the concept of changing composition at similar horizons during cooling of the magma. The samples at 10 and 26 feet lie off from the main trends. These may contain some talc which has a higher



**Figure 9.** Multilithic breccia. Clasts include: large, rounded clasts of serpentinite with talc-altered rims (A); smaller, rounded clasts completely replaced by talc (B); small, rounded clasts of Kiokee gneiss (shown by arrows); and coarse-grained chlorite matrix (C). View is along Old Petersburg Road about 160 feet south of north end of roadcut. Location of roadcut shown in Figure 3. Scale is 10 cm (4 inches).



**Figure 10.** Talc boulder field. Talc boulders are rounded clasts weathered out of the underlying multilithic breccia. Location is approximately 600 feet east of the multilithic breccia roadcut on the Old Petersburg Road (Figure 3). Hammer in center of picture is about 1 foot long.

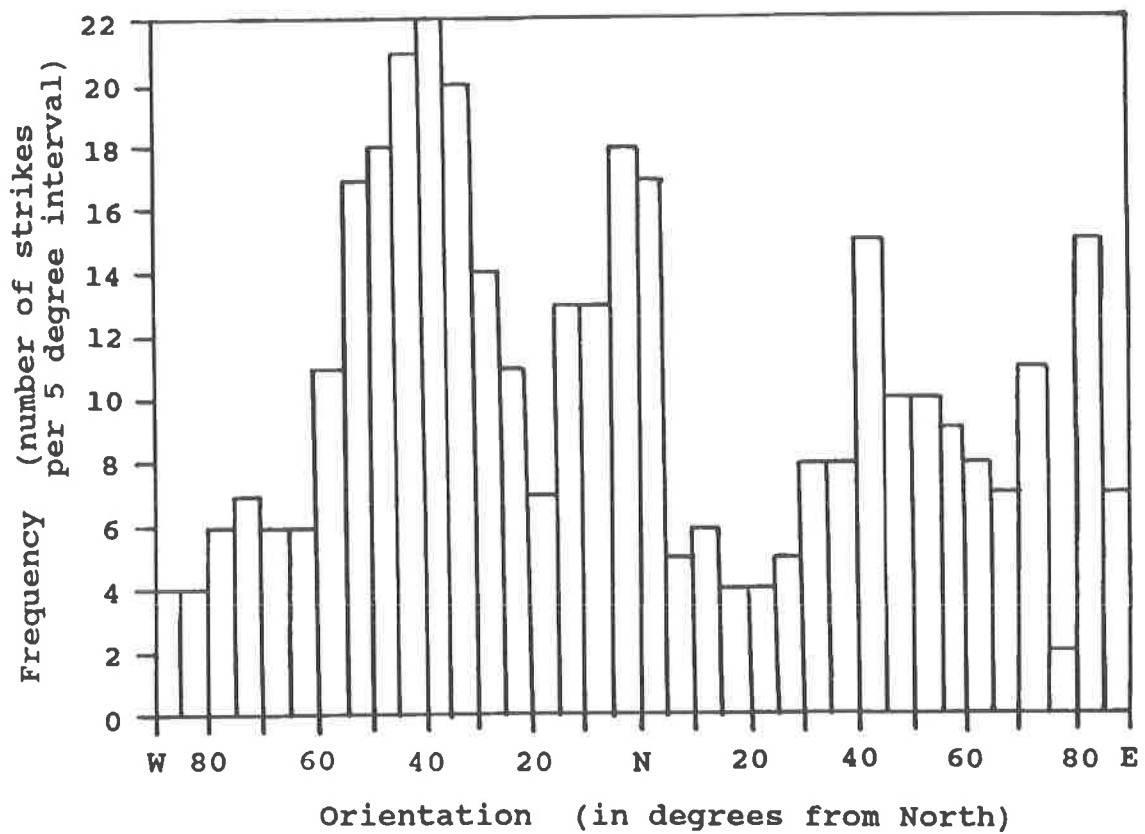


Figure 11. Histogram of stream orientations. Orientations were compiled from all stream segments (total = 371) at least 1000 feet long within an area 30,000 feet east to west and 10,000 feet north to south centered on the project area (Cocker, 1991b). The concentration of orientations from N25°W to N55°W may be influenced by N25°W to N40°W brittle fractures.

stream lineations are parallel to a series of small vertical faults, striking at about N40°W, which cross-cut the Modoc Fault (Howell and Pirkle, 1976).

The composite distribution of dips (Fig. 12) measured from 137 veins of quartz, carbonate, chlorite and talc shows a crude bell-shaped distribution with 35 percent of the veins forming the apex falling in the 50 to 65° range. The composite distribution of strike orientations (Fig. 13) of all brittle structures (including dikes, faults, veins and abrupt breaks in magnetic anomalies) shows concentrations between N25-70°W, N25-40°E and N60-75°E (Cocker, 1991b).

Brittle deformation occurred after serpentinitization and was accompanied during earlier stages by influx of "metamorphic/ hydrothermal" solutions which altered serpentinite adjacent to the fractures and deposited various minerals in the fractures. Geologic relations indicate the following sequence of brittle deformation:

- 1) brittle fracturing and brecciation of the serpentinite, with development of talc along fractures and rimming breccia clasts, and accompanied by chlorite within the fractures;
- 2) multistage fracturing accompanied by introduction of silica;
- 3) multistage fracturing accompanied by carbonate veining;
- 4) faulting and fracturing with little or no associated veining or alteration.

## METAMORPHISM

### Kiokee Belt

Alleghanian-age, upper amphibolite facies metamorphism of the Kiokee belt is attributed to a major thermal event. It is recorded as muscovite + sillimanite-bearing schists and gneisses and migmatitic gneisses (Maher, 1978, 1987; Secor and others, 1986a; Dallmeyer and others, 1986; Secor and others, 1986b; Secor, 1987; Sacks and others, 1989).

The development of the epidote-amphibolite facies metamorphic assemblages overprinting higher-grade metamorphic assemblages in this part of the Kiokee belt is indicative of retrograde metamorphism as suggested by McLemore (1965). Retrograde metamorphism could result from the release of fluids during thrusting of the Kiokee belt rocks onto the North American craton (Armstrong and Dick, 1974; Frazier and Schwimmer, 1987). A younger, lower-grade, zeolite facies metamorphism produced zeolites in fractures (McLemore, 1965).

### Serpentinite

Petrographic evidence suggests that an olivine + enstatite + spinel harzburgite was, in part, metamorphosed to the assemblage enstatite + olivine + tremolite + anthophyllite + Cr-magnetite + chlorite. This assemblage is indicative of metamorphic grade approximately equivalent to the sillimanite-muscovite facies (Cocker, 1989a and 1991b). Antigorite or chrysotile did not develop during prograde metamorphism suggesting that the harzburgite was relatively anhydrous at that time. The absence of antigorite or chrysotile textures, indicates that serpentinitization did not occur under prograde metamorphic conditions or in an ultramafite undergoing stress (Wicks and O'Hanley, 1988).

Retrograde, metamorphism of meta-harzburgite produced lizardite serpentinite. Mesh-textured lizardite (Fig. 7) is pseudomorphic after olivine, orthopyroxene (bastite) (Sacks and others, 1989), anthophyllite, and tremolite (Cocker, 1989a and 1991b). Lizardite is the only serpentine mineral identified in thin sections or in XRD analyses of core samples. The mesh-texture of the lizardite is attributed to serpentinitization in a static environment (MacDonald, 1984; Wicks and O'Hanley, 1988; Cocker, 1991b). Conditions prevailing during the formation of lizardite include: low temperatures, <200-250°C, low pressures, <2.5 kb, and low P(H<sub>2</sub>O), <300 bars (Wicks and O'Hanley, 1988; Cocker, 1989a and 1991b).

## METASOMATIC ALTERATION OF SERPENTINITE

Circulation of fluids between the country rock and the serpentinite metasomatically altered the serpentinite to nearly monomineralic zones of talc, chlorite, and quartz. Although spatial and temporal overlap of alteration phases has obscured some textural and mineralogical relations, the following alteration zoning is present: 1) a core of "fresh" serpentinite containing locally abundant disseminated patches of talc, carbonate and chlorite; 2) fine-grained chlorite; 3) talc + carbonate; 4) massive talc; 5) foliated talc; 6) coarse chlorite; 7) altered country rock; 8) fresh country rock (gneiss, granite or amphibolite). Alteration of the country rocks involved chloritization, biotitization and perhaps albitization (Cocker, 1989a and 1991b). This zonation is similar to metasomatic alteration sequences commonly developed at ultramafic-country rock contacts in New England (Chidester, 1962; Jahns, 1967; Sanford, 1982).

Alteration of the serpentinite is best developed in fractures cutting the serpentinite, along the

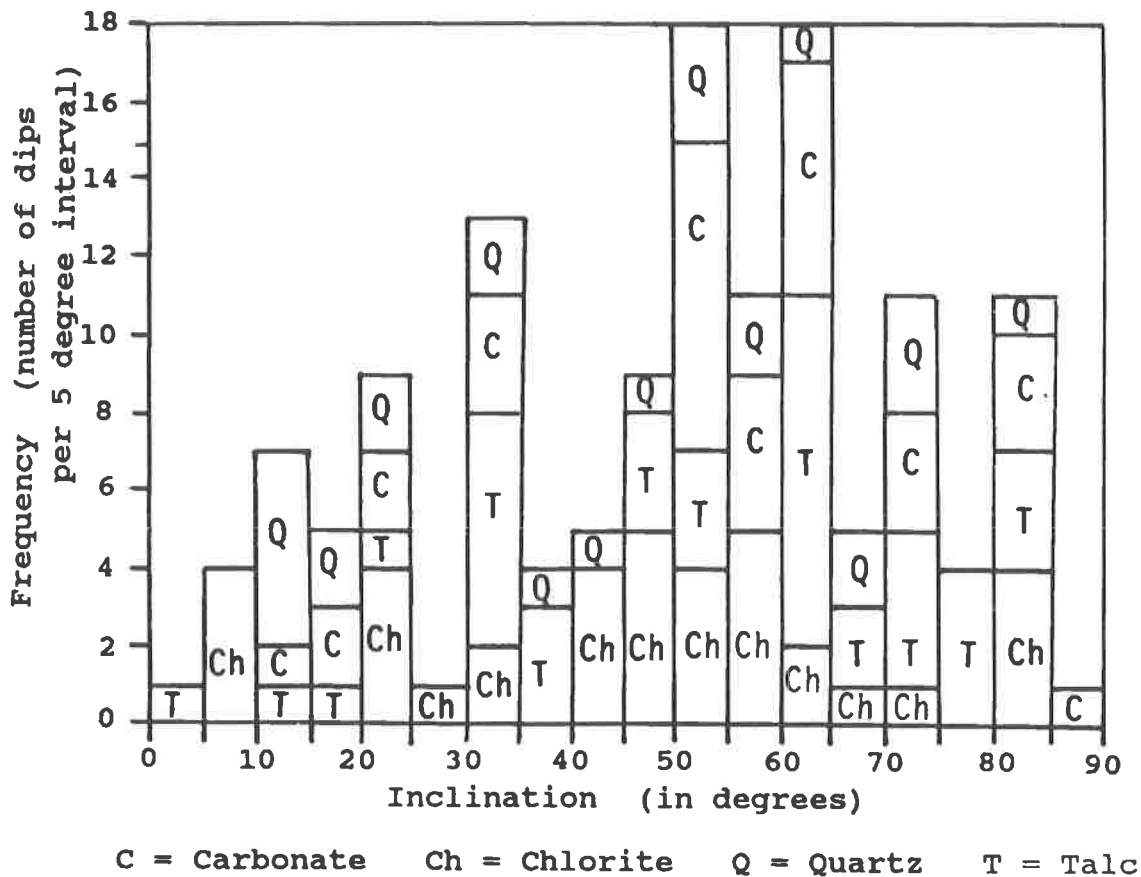


Figure 12. Composite histogram of dips of all veins (in core). Angles of veins measured relative to core axis were recalculated to dips from horizontal. Total number of veins, which is used loosely to include mineralized fractures, is 137. This includes 78 talc (T) +/-chlorite (Ch), 26 quartz (Q), and 33 carbonate (C) veins. More than a third (35 percent) of the veins dip 50-65°.



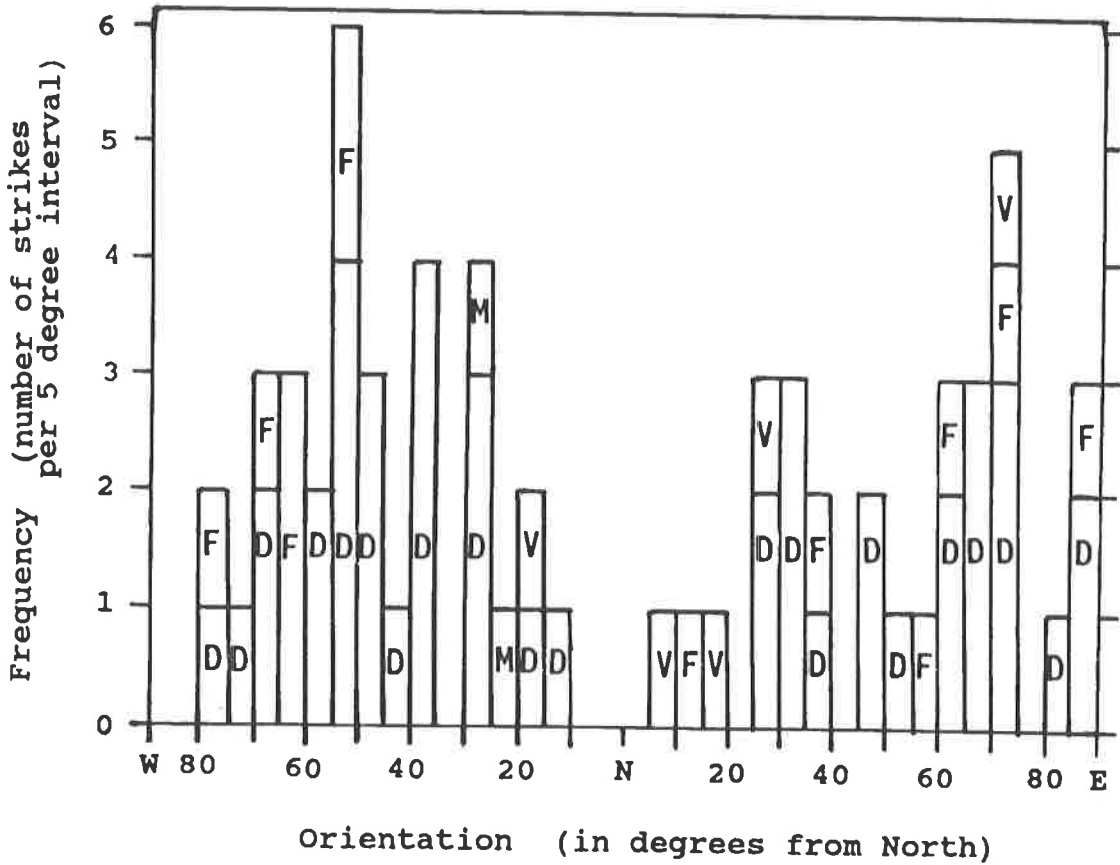


Figure 13. Composite histogram of brittle structure orientations (surface). Structures are concentrated from N25-70°W, N25-40°E and N60-75°E. The northwest trend overlaps the stream orientation trend in Figure 37. Orientations are from unpublished field data (Cocker, 1988) and abrupt breaks in magnetic anomalies from the ground magnetic survey. Total number of orientations is 63 and includes dikes (D), faults (F), veins (V) and the geophysical data (M).

contacts with the country rock, and around the serpentinite clasts in the multilithic breccia. The carbonates, magnesite, dolomite and calcite, are most abundant in rocks with relatively low talc (<25 modal percent) and at 30-50 modal percent lizardite (Cocker, 1991b). They replace lizardite, talc and chlorite and form veins cutting lizardite, talc and chlorite. Coarse, platy talc forming a fibrous, cross-fiber texture, about 1 cm wide, occurs along fractures and edges of ultramafic clasts in the multilithic breccia (Fig. 14). Massive talc extends beyond the fibrous talc from fractures or clast rims into the serpentine (Fig. 15). Talc generally replaces lizardite, enstatite, tremolite and anthophyllite. Steatization (the formation of talc and various carbonates) destroys the fine-grained secondary magnetite occurring as rims around the lizardite mesh texture (Fig. 16). A decrease in modal magnetite with increasing talc (Fig. 17) and the absence of fine-grained magnetite in talc that has replaced lizardite implies dissolution of the fine-grained magnetite during steatization. The larger magnetite and/or ferritchromite masses are not visibly affected (Fig. 16). Coarse-grained chlorite (derived from the alteration of talc and/or crushed serpentinite?) fills fractures and forms the matrix of the multilithic breccia replacing talc and to a lesser extent lizardite, tremolite and anthophyllite. In drill core and outcrop this chlorite forms massive, coarse-grained, non-foliated, platy intergrowths and is particularly susceptible to weathering and washout by drilling fluids because the chlorite plates are loosely held together.

Silicification and quartz veining are widespread in the northern serpentinite and are locally developed in the southern serpentinite. Quartz veins cut across talc, chlorite, and serpentine, with quartz generally replacing these minerals. Quartz completely replaces all lizardite leaving only the metamorphic and secondary magnetite (Fig. 18) preserving the lizardite mesh-texture. The intensity of silicification is directly related to the density of quartz veining indicating that silicification and quartz veining are probably simultaneous and directly related. Veining is multistage as indicated by: 1) banded quartz veins; 2) quartz veins cross-cutting other quartz veins; and 3) vein mineralogy changing with decreasing age from quartz to chalcedony to opal. Crustiform vein quartz is common, indicating open-space filling (Cocker, 1991b).

Metasomatism within relatively unaltered serpentinite is suggested by the geochemical distribution of several oxides. These include an increase in  $\text{CO}_2$  content towards the base of the serpentinite, and slight decreases in  $\text{Al}_2\text{O}_3$ , and slight increases in  $\text{Na}_2\text{O}$ ,  $\text{K}_2\text{O}$  and  $\text{FeO}$  from the center to the margins of the

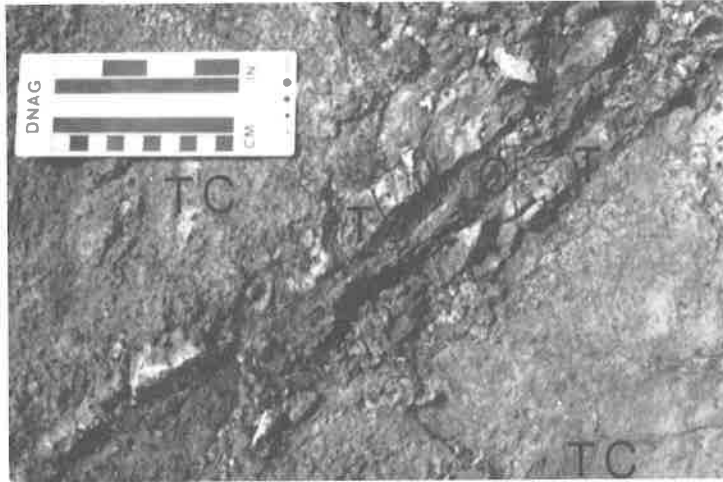
serpentinite (Cocker, 1991b). The extremely small Al-content of the serpentinite suggests that most of this component, required to form the abundant chlorite in fractures and breccias, must have come from the country rock.

More pronounced metasomatism occurs in the major and trace element chemistry of the talc, chlorite and silicified serpentinite.  $\text{SiO}_2$  increases from 38.3 average weight percent in serpentinite to 42.2 average weight percent in chlorite; to 47.5 average weight percent in talc; and to 90.4 weight percent in silicified serpentinite (Fig. 19). Similarly,  $\text{MgO}$  decreases from 36.3 average weight percent in serpentinite to 27.7 average weight percent in chlorite, to 28.2 average weight percent in talc, and to 1.8 weight percent in silicified serpentinite (Fig. 19). Concentrations of  $\text{Al}_2\text{O}_3$ ,  $\text{TiO}_2$ ,  $\text{Na}_2\text{O}$ , and  $\text{K}_2\text{O}$  are very low in serpentinite, talc, silicified serpentinite and silicified talc but are significantly enriched in chlorite (Figs. 20 and 21).  $\text{Al}_2\text{O}_3$  increases from generally less than 0.5 weight percent up to 12.3 weight percent in chlorite.  $\text{TiO}_2$  increases dramatically from 0.01 weight percent in serpentinite and talc up to 5.1 weight percent in chlorite.  $\text{Na}_2\text{O}$  and  $\text{K}_2\text{O}$  increase from less than 0.05 weight percent in serpentinite up to 0.1 weight percent  $\text{Na}_2\text{O}$  in talc and up to 0.28 weight percent  $\text{Na}_2\text{O}$  and 0.75 weight percent  $\text{K}_2\text{O}$  in chlorite. The normal  $\text{CaO}$  content of the serpentinite is generally less than 3 weight percent but increases up to 8.5 weight percent (average 4.06 weight percent) in talc, and up to 4.2 weight percent in silicified talc. Dissolution of secondary magnetite during steatization (Fig. 16) reduced the  $\text{Fe}_2\text{O}_3$  content from 5.89 average weight percent in serpentinite to 3.05 average weight percent in talc (Fig. 19). The  $\text{Fe}_2\text{O}_3$  content in chlorite is similar to that in serpentinite (Cocker, 1989a, 1989b, 1991a and b).

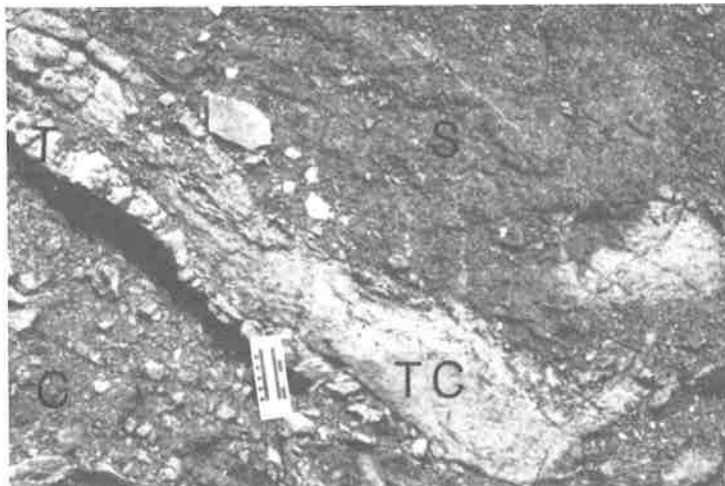
The leaching action of fluids circulating through the multilithic breccia depleted Co, Ni and Cr from serpentinite adjacent to and within the breccia (above 110 feet in DDH PC87-5). Co, Ni and Cr are reduced approximately in half from serpentinite to talc to chlorite (Cocker, 1991b).

Conditions prevailing during the metasomatic alteration of lizardite to talc, carbonate and chlorite include low temperatures, <200-250°C, low pressures, <2.5 kb, and low  $\text{P}(\text{H}_2\text{O})$ , <300 bars (Wicks and O'Hanley, 1988; Cocker, 1989a and 1991b). Alteration of the lizardite to carbonate, talc and chlorite probably resulted from fracturing and brecciation leading to, or resulting from, a decrease in pressure plus the introduction of  $\text{CO}_2$ ,  $\text{SiO}_2$  and  $\text{Al}_2\text{O}_3$  (Cocker, 1989a, 1989b, 1991a and b).

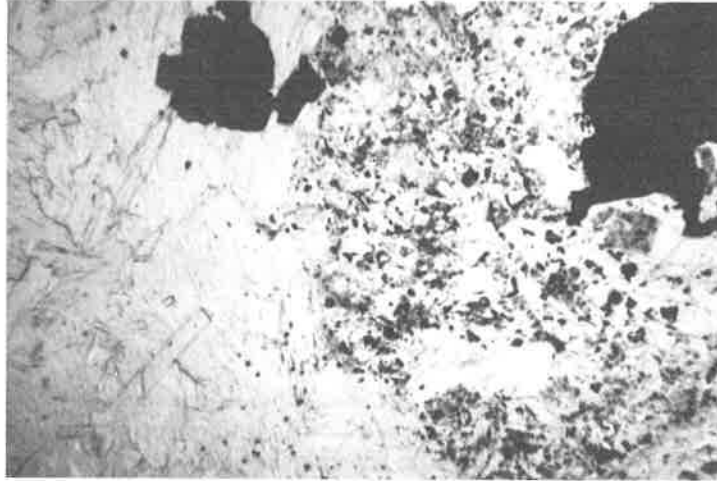
Silicification involves significant addition of silica and removal of most other oxides. The intimate



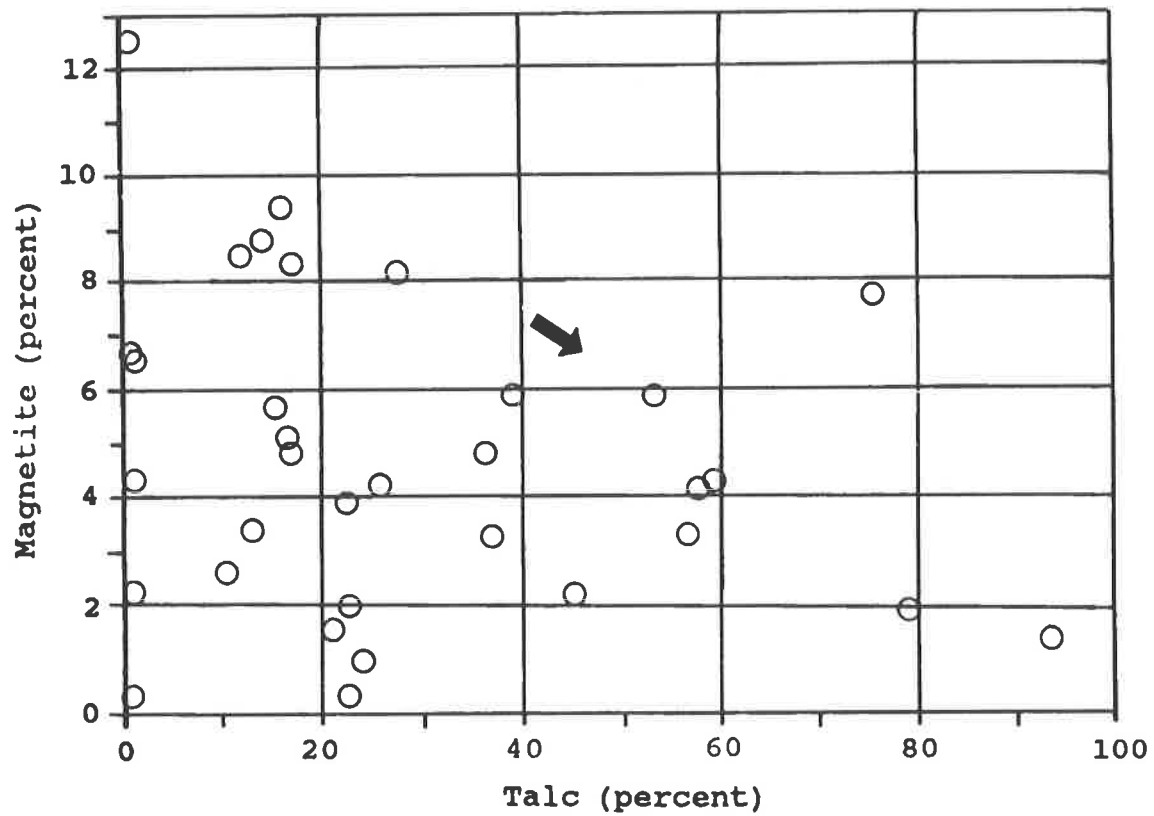
**Figure 14.** Chlorite, foliated talc, and massive talc alteration. Closeup view of alteration adjacent to edge of serpentinite clast in multilithic breccia with coarse-grained chlorite (C); foliated talc rim (T); massive talc + carbonate (TC); and serpentinite with patchy talc (S). Scale is 10 cm (4 inches). View is along the Old Petersburg Road at about 118 feet south of the north end of the roadcut. Location of roadcut



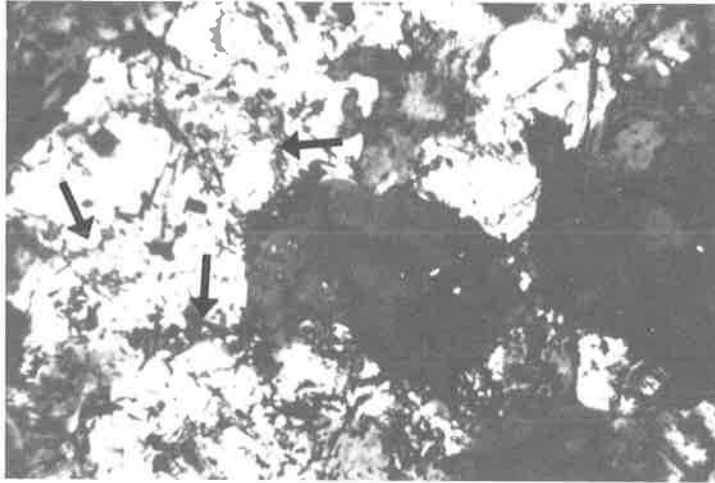
**Figure 15.** Chlorite, talc, talc + carbonate metasomatic alteration. Outcrop shows alteration of large serpentinite clast in multilithic breccia with coarse-grained breccia matrix (C); foliated talc rim (T); massive talc + carbonate (TC); and serpentinite with patchy talc (S). Talc alteration extends along fractures. Scale is 10 cm (4 inches). View is along the Old Petersburg Road at about 134-140 feet south of the north end of the roadcut. Location of the roadcut is shown in Figure 3.



**Figure 16. Photomicrograph of magnetite destruction in talc.** Right half of picture is lizardite serpentinite plus fine-grained (black specs) magnetite derived from olivine and enstatite during serpentinization. Left half contains coarse-bladed talc that has replaced the lizardite and most of the secondary magnetite. Large black grains in upper center and upper right are magmatic spinels altered to Cr-magnetites during prograde metamorphism. The Cr-magnetite in the talc is not visibly affected by steatization. Sample is PC87-4-67. Width of field of view is 2.65 mm.



**Figure 17. Modal magnetite - talc diagram.** Diagram illustrates an overall decrease in total modal magnetite with increasing modal talc in serpentinite. The few percent magnetite in +60 percent talc is primary, magmatic Cr-magnetite. The scatter in the abundance of magnetite may be attributed to the distribution of Cr-magnetite.



**Figure 18. Photomicrograph of silicified serpentinite.** Outline of lizardite mesh-texture is preserved by the fine-grained secondary magnetite (shown by arrows). Remainder of section is quartz. Sample is AP5. Width of field of view is 1.13 mm.

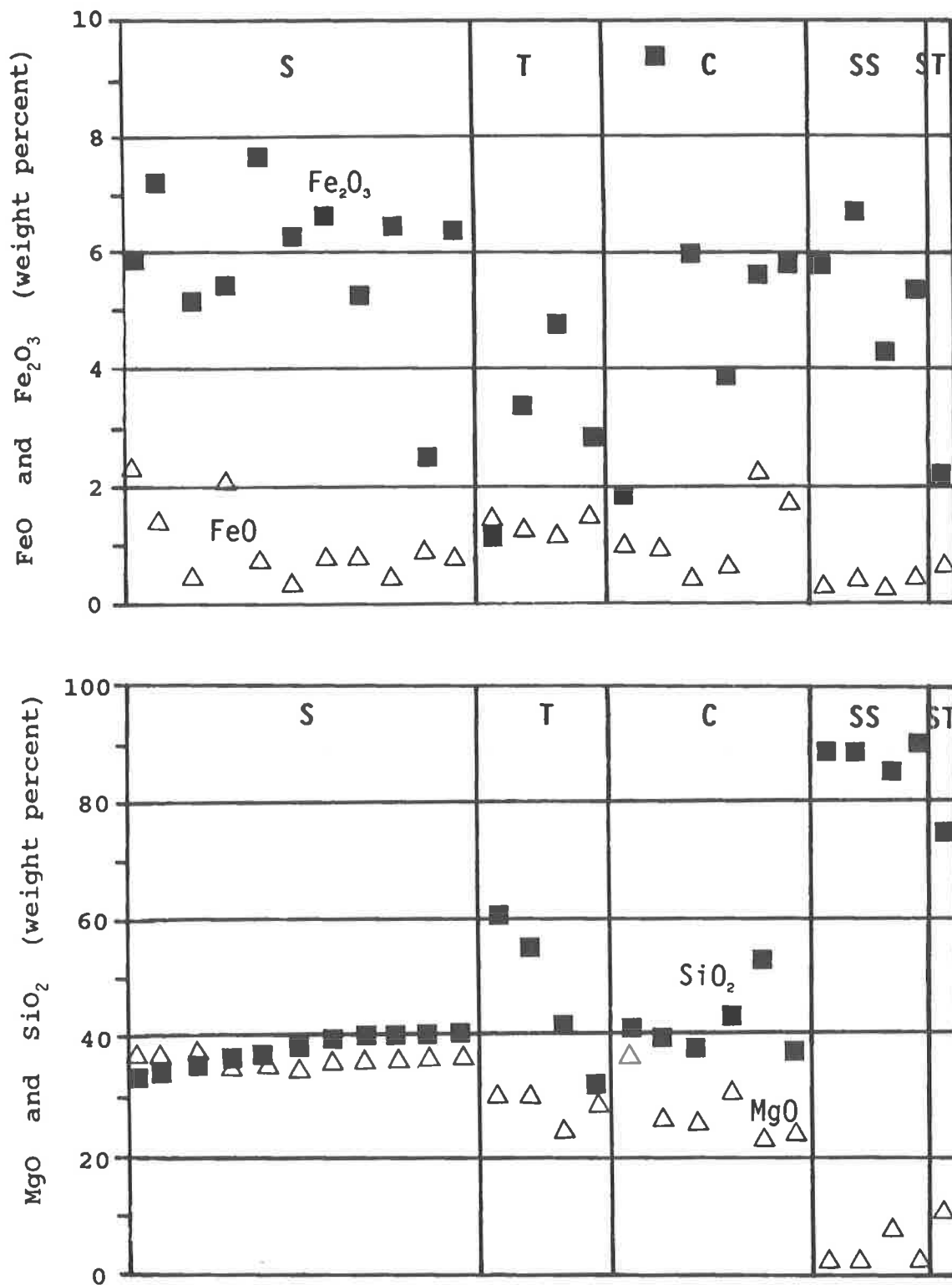


Figure 19. SiO<sub>2</sub> and MgO, Fe<sub>2</sub>O<sub>3</sub> and FeO versus serpentine alteration type. SiO<sub>2</sub> and Fe<sub>2</sub>O<sub>3</sub> are depicted by solid squares and MgO and FeO are shown by open triangles. Weight percent of each oxide is plotted versus the principal rock type. Each rock type is essentially a monomineralogic alteration "assemblage". Variations in compositions of each rock type are due principally to trace amounts of other minerals such as talc, chlorite and carbonate in serpentine. S = lizardite serpentine, T = talc, C = chlorite, SS = silicified serpentine, ST = silicified talc.





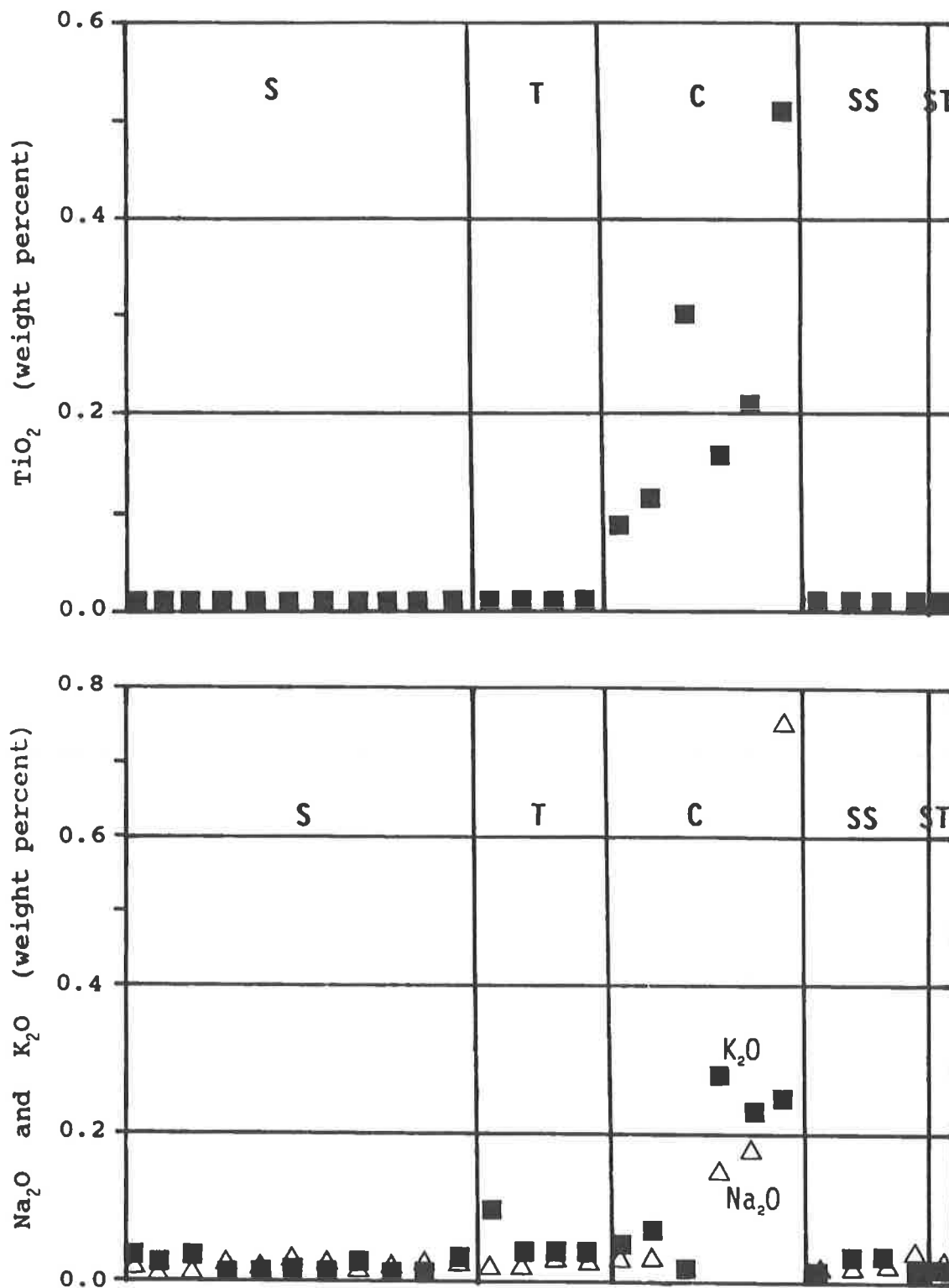


Figure 21. Na<sub>2</sub>O and K<sub>2</sub>O, and TiO<sub>2</sub> versus serpentinite alteration type. K<sub>2</sub>O and TiO<sub>2</sub> are shown by solid squares, and Na<sub>2</sub>O is depicted by open triangles. Weight percent of each oxide is plotted versus the principal rock type. Each rock type is essentially a monomineralic alteration "assemblage". Variations in compositions of each rock type are due principally to trace amounts of other minerals such as talc, chlorite and carbonate in serpentinite. S = lizardite serpentinite, T = talc, C = chlorite, SS = silicified serpentinite, ST = silicified talc.

association of multistage quartz veining with the silicification of Burks Mountain serpentinites is similar to other occurrences of extensive silicification and quartz veining documented as being hydrothermal in origin. The source of the hydrothermal silica-bearing solutions is presently unknown, but constraints on the conditions at the time of silicification can be estimated. Petrographic and field relations (Cocker, 1989a, and 1991b) demonstrate that silicification occurred after steatization and at low temperatures and pressures. Phase relations in the system serpentine + quartz also suggest that conditions of silicification were under relatively low temperatures. Estimated maximum temperatures and pressures at the time of silicification are 300°C and <3 kb. (Cocker, 1989a and, 1991b).

## WEATHERING OF SERPENTINITE AND TALC

The northern and southern serpentinites differ markedly in their susceptibility to weathering. The northern mass is resistant to weathering principally because of its extensive silicification. Weathering of partially silicified serpentinite produced a type of pseudogossan boxwork consisting of resistant quartz veins, resistant silicified layers, and oxidized, pitted serpentinite. Where it is exposed as clasts in the multilithic breccia (the Old Petersburg Road roadcut), the southern serpentinite illustrates the strong degree of weathering typical of a serpentinite in the Georgia Piedmont. A weathered serpentinite clast (sample D139) from the Old Petersburg Road roadcut is apparently depleted in MgO, FeO, CaO, and Ni, and enriched in Al<sub>2</sub>O<sub>3</sub>, Na<sub>2</sub>O, K<sub>2</sub>O, Cr, TiO<sub>2</sub>, and Fe<sub>2</sub>O<sub>3</sub> (Cocker, 1991b). The weathering of the serpentinite and breccia was facilitated by ground-water movement through abundant fractures in the serpentinite and through the coarse chlorite surrounding the breccia clasts.

Under the same weathering conditions, talc seems to be relatively stable. Talc appears fresh in outcrop and forms a surficial residual deposit over the multilithic breccia. Talc's resistance to weathering and the susceptibility to weathering and erosion of chlorite, gneiss and serpentinite clasts of the multilithic breccia result in the concentration of subangular to rounded pebbles, cobbles and boulders of talc at the surface (Fig. 10). The concentration of surficial talc might suggest a greater abundance of talc than drill results indicate. Core holes collared on the surficial talc result in: 1) poor drill core recovery, 2) a mixture of talc and gneiss clasts in the core, and 3) occasionally recovered coarse-grained chlorite.

Talc appears to be stable under intense tropi-

cal weathering conditions in Nigeria (Akpanika and others, 1987) and under subtropical conditions in Winterboro, Alabama (Blount and Vassiliou, 1980). At Winterboro, deep weathering of an illite plus quartz-bearing dolomite-hosted talc deposit released talc from the dolomite and concentrated the talc within a mixture of yellow, red and brown clays.

## ECONOMIC GEOLOGY

The present investigation focussed on two primary commodities (talc and serpentine/serpentinite) because they are present in potentially economic tonnages. Serpentine and talc are important in industry for their physical and chemical properties. Other commodities were investigated because they have either been reported as occurring or have the potential for occurring in the Burks Mountain ultramafites. These commodities are primarily metals which normally occur in ultramafites (Ni, Cr, Pt, etc.) or may be introduced through hydrothermal processes (Au, Ag, Pb, Zn, etc.). These commodities are discussed in approximate order of abundance or importance.

### Talc

Talc's distinct physical and chemical properties are important for its industrial usage. Because talc is defined both as a mineral and as an industrial rock composed of one or more minerals, these properties can vary considerably. The mineral talc is a hydrous magnesium silicate, with an ideal formula of Mg<sub>6</sub>Si<sub>8</sub>O<sub>20</sub>(OH)<sub>4</sub>, and a stoichiometric composition of 63.36 weight percent silica, 31.89 weight percent magnesia, and 4.75 weight percent water (Roe, 1975). Although Fe<sup>+2</sup> may substitute for as much as 10 percent of the Mg, most talc compositions fall in the range of 1-4 mole percent Fe-talc end-member in isochemically metamorphosed ultramafic rocks (Evans and Guggenheim, 1988). Industrial talc is a rock composed mainly of magnesium-rich silicate minerals with the mineral talc being an important constituent. Other minerals that commonly may occur in industrial talc include: serpentine, tremolite, chlorite, anthophyllite and diopside. Less common are quartz, calcite, dolomite, and magnesite (Brown, 1973). Industrial talc generally is ground to a powder which is inert and light-colored but has a wide range of hardness and particle shapes because of differences in the physical properties of the various contained minerals. This greatly increases the versatility of industrial talc. The two major varieties of industrial talc are steatite and soapstone. Steatite is massive talc of high purity suit-

able for electrical insulator manufacture and fillers. Soapstone refers to impure varieties of massive talc (Roe, 1975; and Roe and Olson, 1983). Soapstone is also used in art carvings, stoves and laboratory furniture.

The surface occurrences of talc boulder fields (Fig. 10) associated with the Burks Mountain serpentinites (McLemore, 1965 and Vincent and others, 1990) suggest potentially economic concentrations of near-surface talc. Surface mapping, ground magnetics, and logging of drill holes indicate that the talc boulder fields are an in-situ weathering residuum of a multilithic breccia above the serpentinite (Cocker, 1989b and 1991a).

A reasonable estimation of the talc potential in the multilithic breccia is inhibited by generally poor recovery of drilled talc intercepts caused by the friable nature of the chloritic breccia matrix. Estimation of the talc content from the exposure of the multilithic breccia in the Old Petersburg Road cut suggests a potential grade of 25 percent talc in the breccia.

Talc used for a particular purpose must meet certain quality standards which are peculiar for that particular purpose. Laboratory testing of the Burks Mountain talc for the wide variety of uses of talc is beyond the scope of this investigation. Selected samples were tested for two of the more important factors: chemical composition and GE brightness. GE brightness is an industry standard test relating the brightness of a powdered test sample to that of an industry standard powder. Values range from 0 to 100 with 100 being the ideal brightness.

Chemical analyses indicate that talc samples from the Burks Mountain complex (Appendix I) are similar in composition to talc analyses reported from numerous mines in the United States and worldwide (Fig. 22). Mineralogical impurities in the Burks Mountain talc are chlorite, lizardite, magnetite, dolomite, magnesite, anthophyllite and quartz.

Measurements of GE brightness range from 36.9 in weathered talc boulders to 67.7 in unweathered, drill intercepts (Cocker, 1991a). A plot of GE brightness versus weathering index (Fig. 23) shows the strong influence of weathering on the brightness of talc. Entirely unweathered talc, having a weathering index of approximately 90, would have a GE brightness of approximately 80. Iron content (Fig. 24) exerts a strong control on GE brightness. Removal of anhydrous Fe-oxides (principally by magnetic separation) would increase the GE brightness to approximately 75. Oxidation of Fe-oxides probably is the principal cause of GE brightness reduction in weathered samples as suggested (Cocker, 1991a) by a plot of oxidation ratios versus GE brightness (Fig. 25).

The size or volume of this talc deposit is de-

rived from measurement of its thickness and its areal extent. An approximate thickness of the multilithic breccia is derived from drill intercepts; a more accurate thickness is not attainable because of poor recovery. A maximum thickness of 137 feet (42 m) is indicated in DDH PC 87-5 (Fig. 41) and a minimum thickness of 85 feet (26 m) is present in DDH PC 88-1 (Fig. 42). Thicknesses of 20-30 feet (6-9 m) are suggested in DDH PC 87-2 (Fig. 39) and DDH PC 87-3 (Fig. 39), although very poor recoveries limit this interpretation (Figures 33, 34, 30 and 31 respectively). Average thickness in the confirmed intercepts is 76 feet (23 m). The breccia thickens to the west but disappears between DDH PC 87-5 and DDH PC 88-2 (Fig. 6). Talc boulders several hundred feet west of DDH PC 87-5 indicate the breccia probably extends under that area (Cocker, 1991a). The down-dip extent of the breccia was not tested (Fig. 5).

Based on the drill intercepts (Figs. 5, 6 and 28) and the mapped surface distribution of the breccia and talc float (Fig. 3 and 27), a tonnage was calculated for the talc-bearing breccia. The breccia was divided into two segments based on drill intercepts (Fig. 28). The east segment is 900 feet long by 600 feet wide by 70 feet thick. The west segment is 600 feet long by 600 feet wide by 130 feet thick. Calculated volumes for these two segments are  $3.78 \times 10^7 \text{ ft}^3$  and  $4.68 \times 10^7 \text{ ft}^3$  respectively. A tonnage factor equal to  $11.64 \text{ ft}^3/\text{ton}$  was calculated using a specific gravity of 2.75 for the breccia. The specific gravity of the breccia is an approximate value because of the diverse lithologic composition of the clasts. It is derived from the average specific gravities of talc (2.75), serpentine (2.78), granite (2.64), and gneiss (2.80) (Telford and others, 1976). At a total volume of  $8.46 \times 10^7 \text{ ft}^3$ ,  $7.268 \times 10^6$  tons of talc ore are possible to probable (Cocker, 1991a).

The shallow dip of the breccia, its surface exposure and little to no significant overburden suggest that the talc deposit is amenable to an open pit mining operation. The poorly consolidated nature of the breccia should allow for easy removal (use of front-end loaders) and easy separation of talc clasts from matrix. The open-pit configuration, little overburden, and anticipated easy mining and ore separation favor a low-cost production. The presence of additional ore zones along the Burks Mountain complex would further reduce the cost of a processing operation.

Additional occurrences similar to that described here, were briefly examined during the course of this study. A large exposure of soapstone south of Phinizy (Hopkins, 1914), approximately 5 miles (8 km) west of this investigation, consists of numerous rounded talc boulders scattered in cultivated fields and forested areas. Additionally, numerous rounded talc boulders are located around the base of Burks

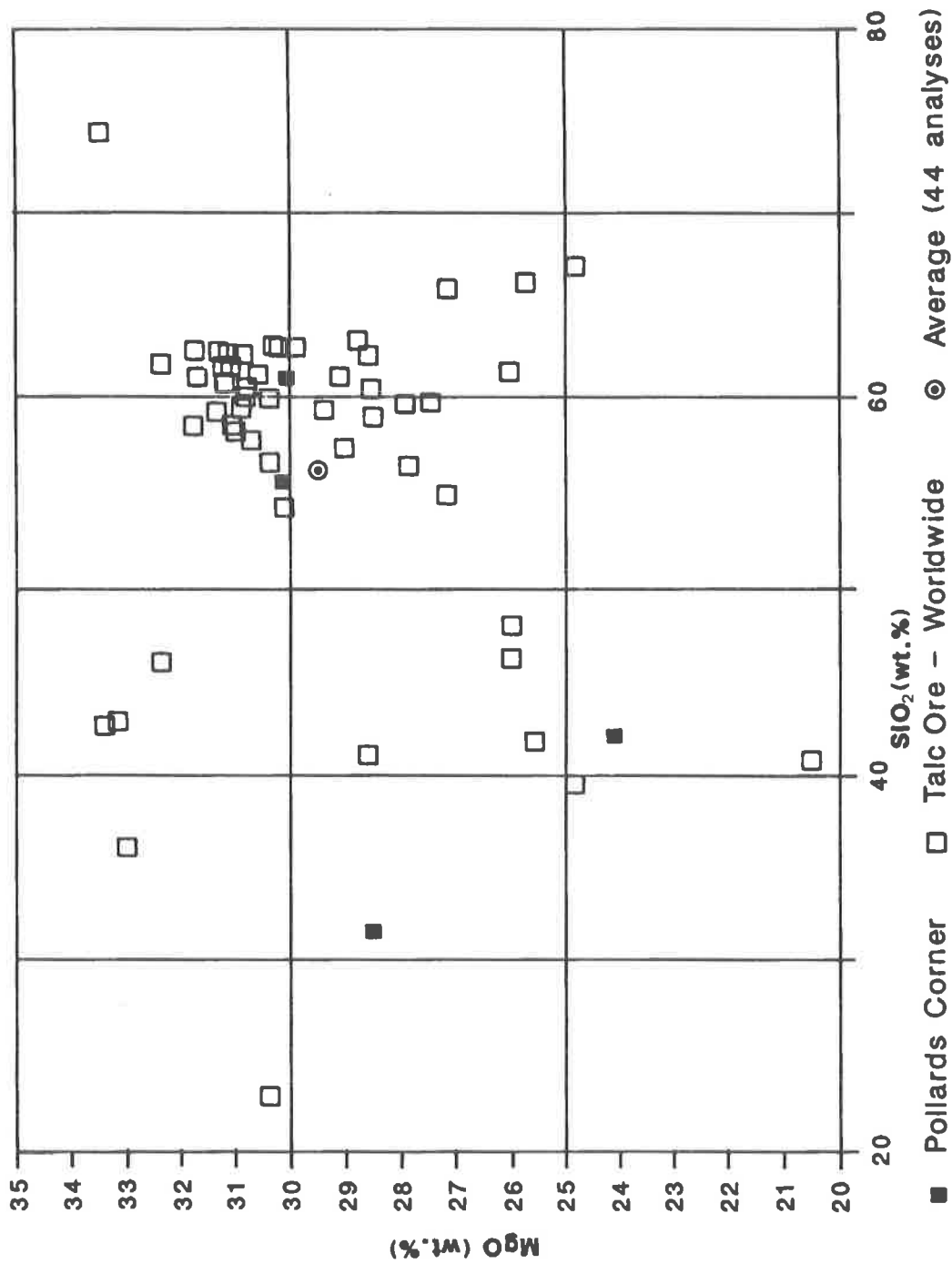
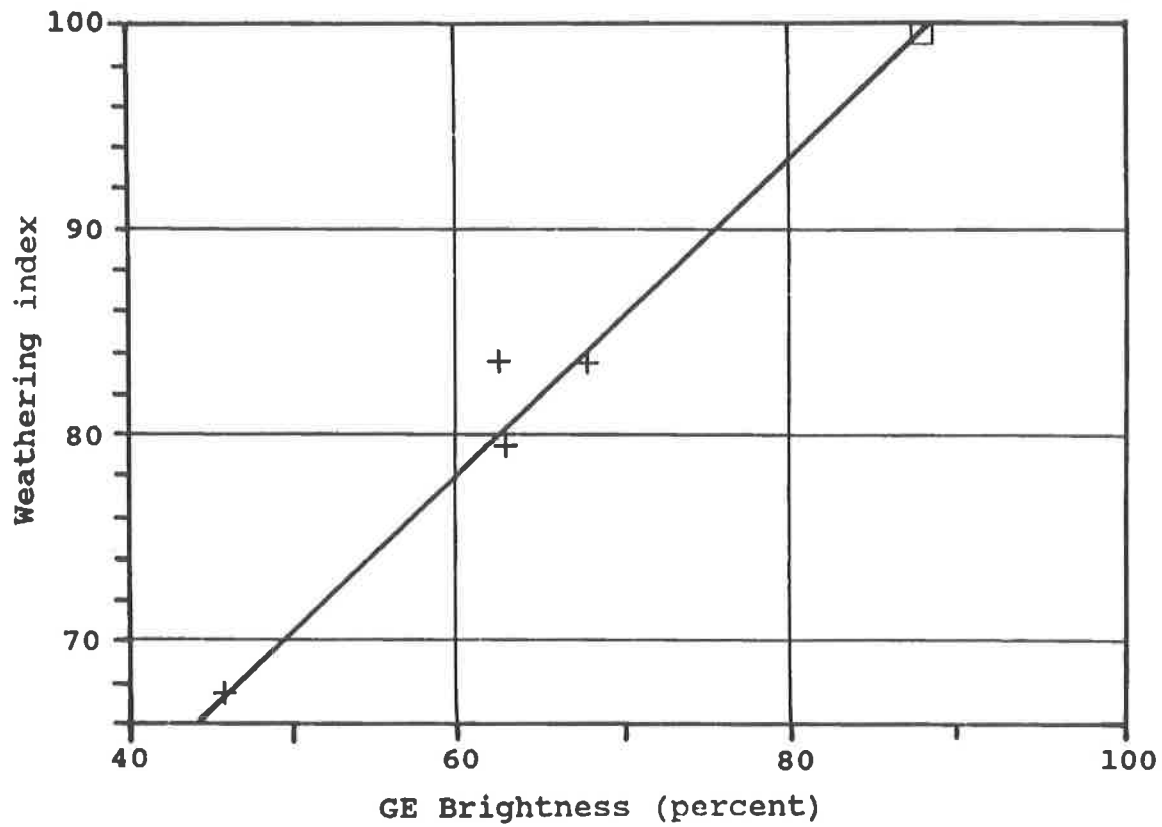
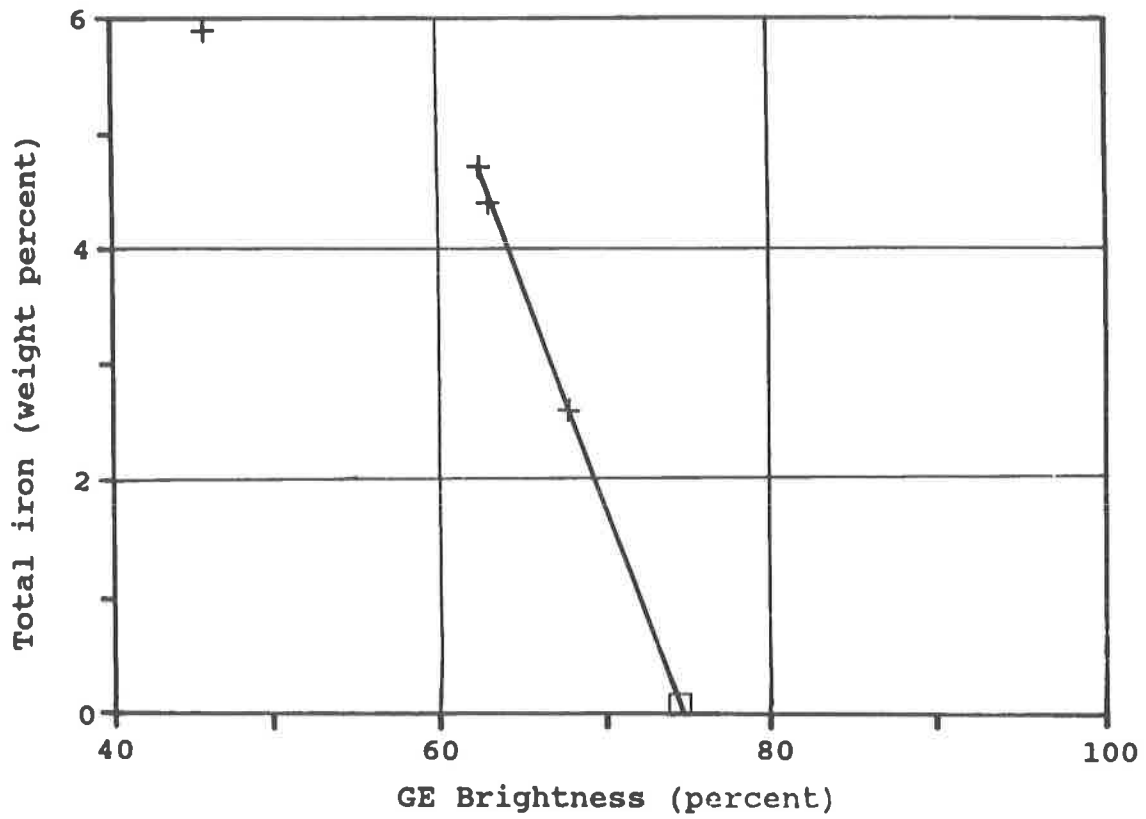


Figure 22.  $\text{SiO}_2$ -MgO content of talc.  $\text{SiO}_2$ -MgO compositions of 4 talc samples from this study are plotted along with 40 analyses of talc published in the literature. Average talc composition of all the samples is shown by the circle. Two of the Burks Mountain talc samples are similar in composition to the large concentration of analyses at 31 weight percent MgO and 60 weight percent  $\text{SiO}_2$ . The two talc samples from the Burks Mountain complex that are lower in  $\text{SiO}_2$  contain carbonates which reduced the relative  $\text{SiO}_2$  content.



**Figure 23.** Weathering index versus GE brightness. A plot of the weathering index (see section in text on weathering of talc) against GE brightness suggests a trend line A-A'. Entirely fresh/unweathered talc (shown by open square) should have a weathering index of about 86-90 giving a



**Figure 24.** Total Fe content versus GE brightness. A plot of total Fe (weight percent) suggests complete removal of Fe would give a GE brightness of approximately 75 (shown by open square).

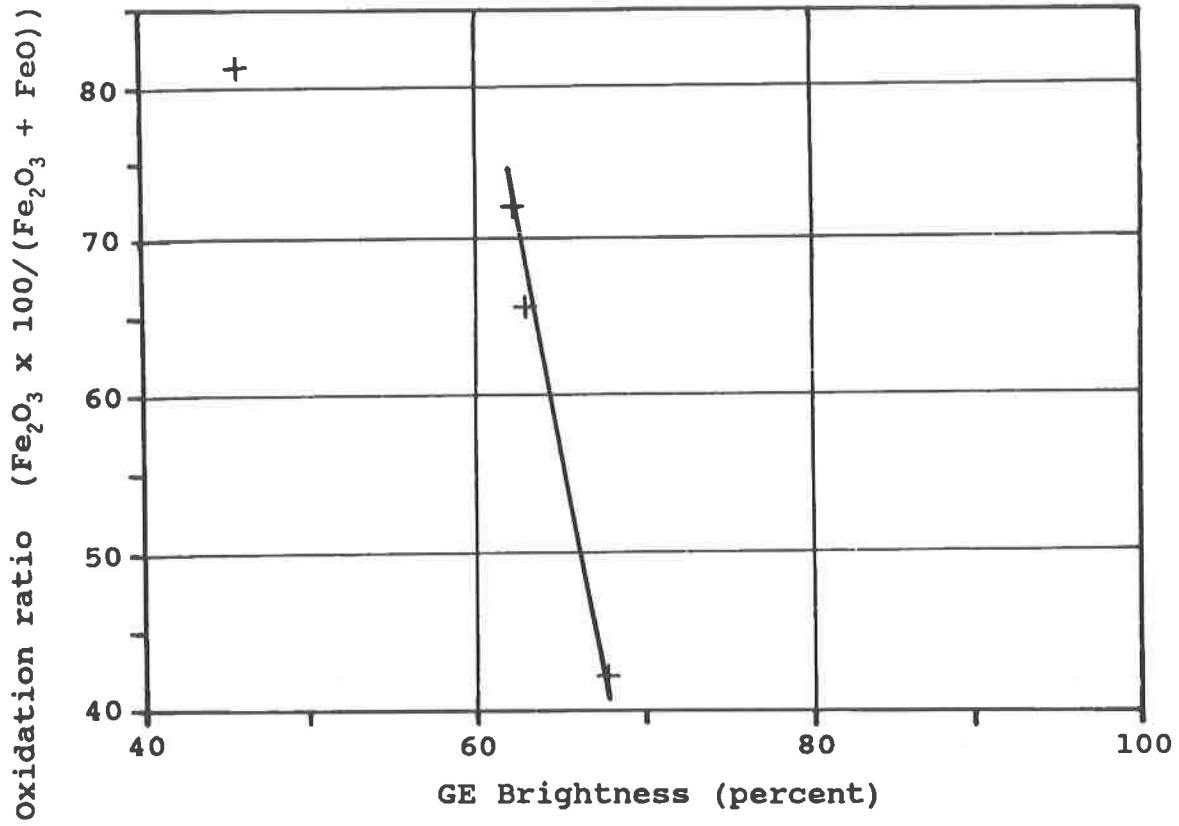


Figure 25.

**Oxidation ratio versus GE brightness.** An increase in the oxidation ratio indicates increased oxidation of Fe. An increase in oxidation decreases the GE brightness. Increasing oxidation indicates increasing weathering.

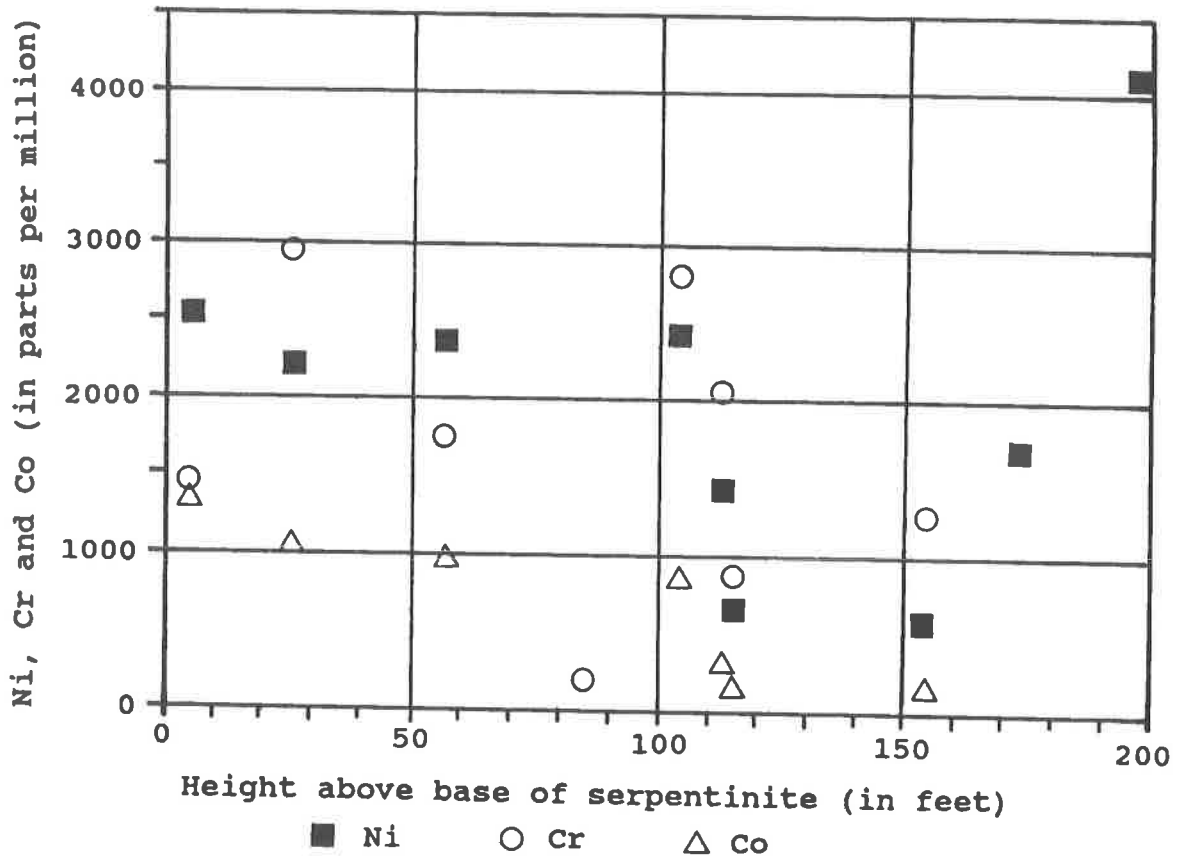


Figure 26. Distribution of Ni, Cr, and Co in serpentinite from DDH PC 87-4. Ni and Co increase towards the base while Cr increases erratically towards the base.



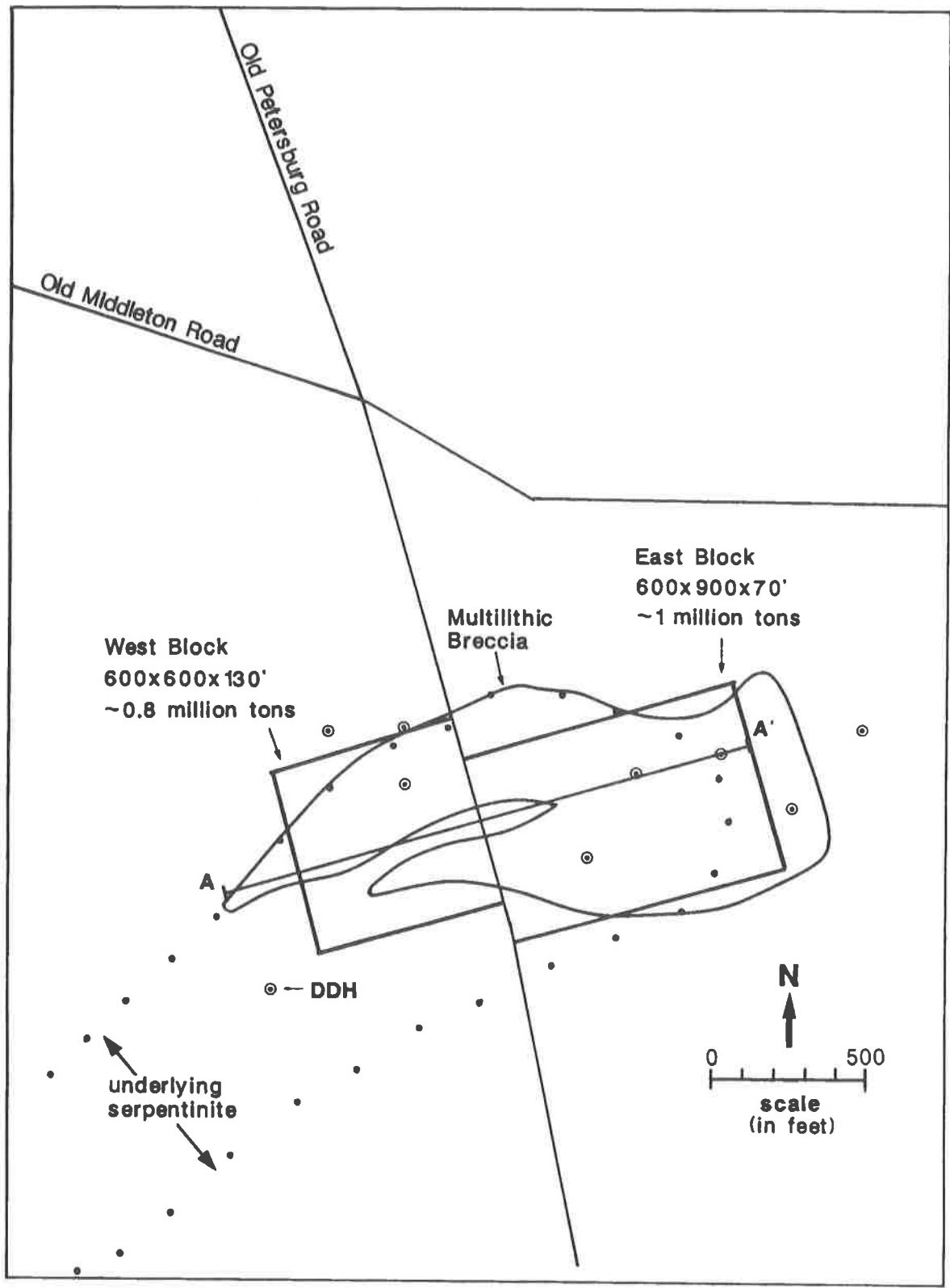


Figure 27. Map of potential talc ore zones. Map is of the same area as in Figure 4. Only the multilithic breccia and the southern serpentinite are shown. DDH's and long section A-A' as in Figure 4. Two potential ore zones in the multilithic breccia are blocked out and calculated tonnages are shown.

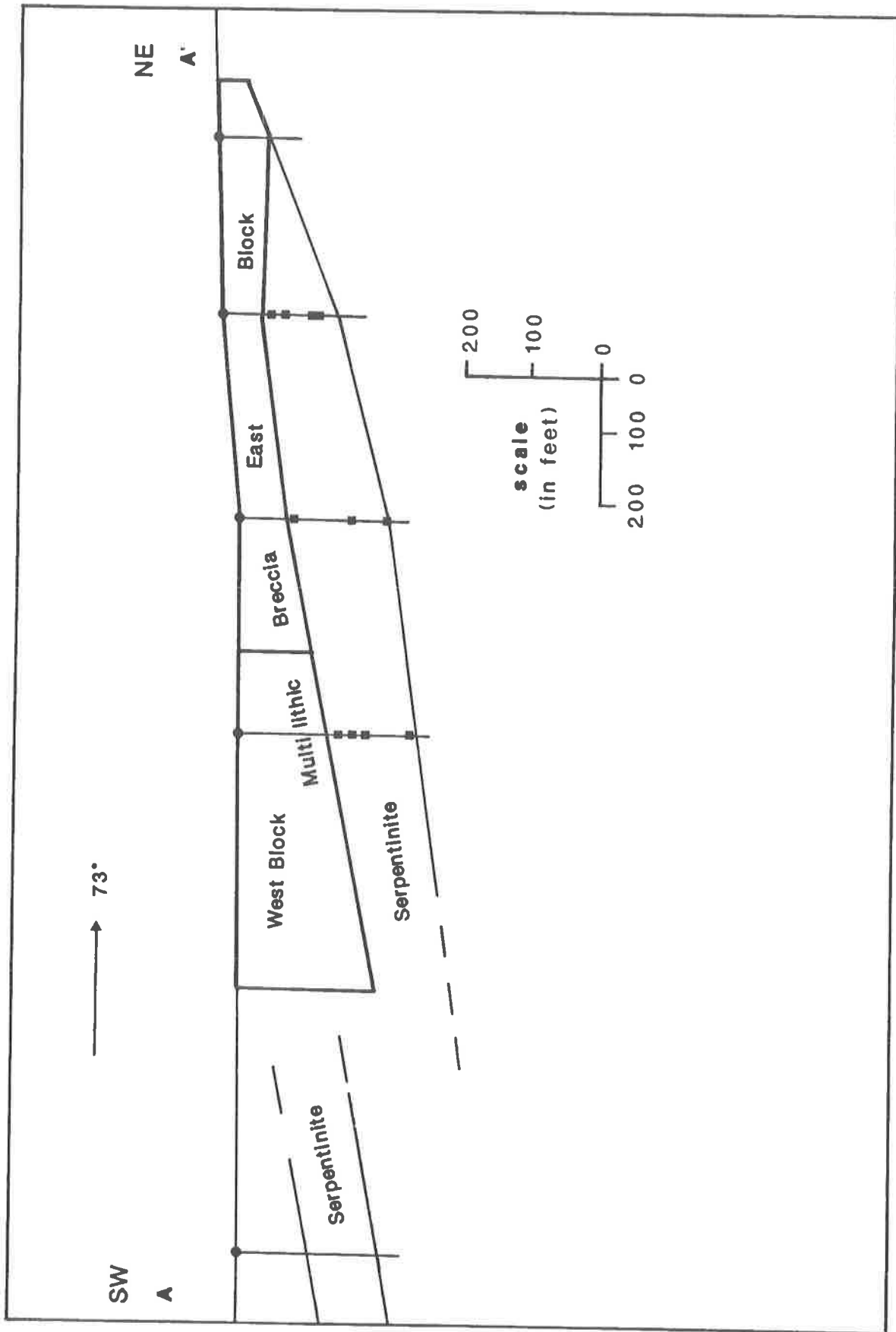


Figure 28. Long section A-A' of potential ore zones. Geology as in Figure 6. Ore blocks as in Figure 27. Talc intercepts in drill holes within the serpentinite are shown as black squares.

Mountain. Local concentrations of talc boulders may be due to the general lack of talus from the higher slopes of Burks Mountain rather than an actual increase in the extent of talc mineralization.

Massive talc is also present within the 95-145 feet (29-44 m) thick serpentinite underlying the breccia. Core intercepts suggest that talc is localized along the upper and lower boundaries and adjacent to fractures in the serpentinite. Because the talc mineralization dips more steeply ( $30-84^{\circ}$ ) than the upper and lower contacts of the serpentinite, the fracture-controlled talc mineralization may extend deeper into the serpentinite (Cocker, 1991a). Talc mineralization, which favors replacement of enstatite over olivine, should increase upwards, because the serpentinite is more enstatite normative towards the top.

The serpentinite which crops out on the upper slopes of Burks Mountain contains only minor amounts of apparently, fracture-related talc mineralization. In addition, widespread and pervasive quartz veining and silicification of this serpentinite also replaced and diluted the observed talc mineralization. The talc around the base of Burks Mountain and perhaps underlying Burks Mountain may be of economic interest.

### Serpentine

Massive serpentine/serpentinite has two primary uses: 1) as a high grade source of magnesia, and 2) as a decorative stone known as "verde antique". Other uses include lab furniture (although synthetics are showing strong competition) and as art carvings. The International Minerals Chemical Corporation mined serpentinite from a small quarry on the southern slope of Dixie Mountain. (eastern end of Burks Mountain) for about five years beginning in 1940 or 1941. Processing of crushed serpentinite in an Augusta plant produced crude epsom salt ( $MgSO_4$ ). The process involved digestion of the serpentinite with sulfuric acid, removal of gelatinous silica by filtering, and crystallization of the salt from the filtrate. A recovery of 95 percent of the average MgO content of 35-38 percent was attained in tests run by the Georgia Department of Mines, Mining and Geology (LeGrand and Furcron, 1956). Hurst and others (1966) suggest that the high cost of the mineral lease was the reason for cessation of this operation. The MgO content of 11 samples of fresh serpentinite from drill core (Cocker, 1991b) ranges from 35.10 to 37.50 weight percent with an average of 36.26 weight percent MgO.

Continuous drill intercepts of massive, fresh serpentinite suggest that the southern serpentinite could be a potential source of "verde antique". Drilling results indicate that the serpentinite becomes more

massive and less broken west of the Old Petersburg Road. Shallow depth of overburden and a gently dipping configuration of the serpentinite are compatible with an open pit operation. Drill intercepts indicate that the serpentinite is a 95-145 feet (24-44 m) thick mass. A pronounced magnetic anomaly (+1000 gammas) indicates the serpentinite (Fig. 4) dips to the southeast and extends to the southwest beneath overlying Kiokee gneiss. Faulting, in addition to up-plunge thinning, truncates the serpentinite to the northeast approximately 1000 feet (300 m) east of the road (Cocker, 1989a and 1991a).

### Chromium

Mafic and ultramafic bodies are generally anomalously high in chromium and host all the world's known chromite deposits. A soil geochemical survey identified Cr anomalies containing values up to 600-800 ppm in the Burks Mountain complex (Hurst and others, 1966). Hurst and others describe veins and pods of chromite, up to 3 inches thick, south of Dixie Mountain (eastern end of Burks Mountain) and chromite grains, less than 1/8 inch in diameter, disseminated throughout the serpentinite. Although not confirmed, the present results suggest that the chromite is probably magnetite.

In the present study, the Cr content of serpentinites and talc averaged 2350 ppm and 2150 ppm, respectively. Thirty surface and drill hole rock samples contain 100 to 4600 ppm Cr. Samples collected from the surface to a depth of 4 feet in DDH PC 88-1 suggest that the maximum concentration (supergene enrichment?) of Cr occurs at a depth of 1 foot in soils.

### Rare earth elements, vanadium and titanium

Magnetite and ilmeno-hematite intergrowths, containing highly anomalous rare earth elements (REE's), vanadium and titanium, occur as layered and vein-like segregations in the upper part of the northern serpentinite on Burks Mountain (Cocker, 1990). The high  $TiO_2$  (9.2 weight percent) and V (750 ppm) content is similar to values reported from massive magmatic magnetite occurring in the upper stratigraphic levels of layered mafic intrusions such as the Bushveld (Reynolds, 1985) and Stillwater complexes. In addition, Ce (180 ppm), Dy (28 ppm), Eu (8.3 ppm), Ho (4.6 ppm), La (273 ppm), Lu (1.90 ppm), Nd (170 ppm), Sc (120 ppm), Sm (38.90 ppm), Tb (5.1 ppm), Yb (12.0 ppm), and Y (180 ppm) are exceedingly elevated relative to crustal abundances and to abundances in other samples from the Burks Mountain complex and Kiokee rocks (Cocker, 1989c). The REE's are enriched 10x to

+100x relative to standard chondrite normative abundances (Cocker, 1989c). REE's are similar in concentration to those in a high-Ti norite in the Stillwater Complex (Helz, 1985). REE analyses from the high-Ti-V magnetite layers of the Bushveld and Stillwater are not available in the literature, but REE's are speculated to be concentrated in these layers (Reynolds, 1985). Concentration of the magnetite and ilmeno-hematite, which form 30-40 percent by volume of the Burks Mountain rock, would yield approximately 24 percent  $TiO_2$  and 2000 ppm V. The lateral extent of this anomalous magnetite and ilmeno-hematite is unknown. An attempt to drill test (DDH 88-3) this occurrence was unsuccessful because of caving and loss of circulation in broken and silicified serpentinite.

### Nickel

Ultramafic bodies are normally anomalously high in nickel, but, in most cases, the nickel content is generally too low to be considered economic. Also, partitioning of Ni into olivine during magmatic crystallization makes Ni difficult to extract. In humid regions, intense weathering of ultramafic rocks leaches Mg and concentrates silica and Ni in a laterite overlying the bedrock. Deposits of nickeliferous silicates, garnierite, and nickeliferous iron-oxides are mined in New Caledonia, Oregon, Cuba, Indonesia, and Brazil. Ni grades in these deposits range from 0.8 to 5 weight percent (Rice, 1957).

In the early 1960's, a regional exploration program for Ni indicated that anomalous Ni concentrations are associated with the ultramafic rocks of the Burks Mountain complex (Worthington, 1964). Two samples contained 0.256 and 0.462 weight percent Ni. A soil geochemical survey (Hurst and others, 1966) confirmed the anomalous Ni content and delineated areas of high Ni concentrations coincident with the ultramafites. This soil geochemical sampling program consisted of 2299 samples collected from a uniform depth of one foot and analyzed by x-ray spectrography. Ni concentrations, shown as counts/sec, range from 3000 to 5000 over the Burks Mountain complex. Quantitative analyses are not provided. A subsequent drilling program by the J.M. Huber Corporation tested one of the anomalies on Dixie Mountain. Although results are unavailable, grades are presumed to be uneconomic because no further exploration is indicated.

Nickel content of serpentinites analyzed during this study range from 2000 to 2700 ppm with an average of 2210 ppm. Concentrations tend to increase towards the base of the serpentinite (Fig. 26). A decrease in Ni with increasing alteration (2150 ppm in

talc and 900 to 1650 ppm in silicified serpentinite) suggests the removal of Ni during alteration of the serpentinite to talc or quartz. Samples collected from the surface to a depth of 4 feet in DDH PC 88-1 suggest that Ni is leached in the upper 2 feet and slightly supergene enriched at a depth of 3 feet. Ni is also depleted in weathered outcrop (1900 ppm). The lack of significant primary or supergene Ni enrichment in any of the results indicates that the Ni is presently subeconomic.

### Cobalt

Concentrations of Co in drill core samples range from 15 to 135 ppm and increase towards the base of the serpentinite. As discussed earlier, Co increases with increasing Ni. Significant concentrations of Co are not known at Burks Mountain.

### Corundum

Corundum is reported by McLemore (1965) and Hurst and others (1966) as occurring in the serpentinites along their contacts with the enclosing gneisses. Most corundum crystals are less than 1/4" across and brown or gray in color although some are up to 3/4" long and deep blue in color suggesting the possibility of gem quality sapphires (Hurst and others, 1966). No follow-up studies are known, and no corundum was observed during the present investigation.

### Asbestos

Asbestos minerals are generally fibrous Mg-silicates commonly associated with serpentinites. The most common asbestos minerals are chrysotile serpentine, tremolite-actinolite, and brucite. Although Hopkins (1914) and McLemore (1965) identified a fibrous vein mineral as chrysotile, this study found no chrysotile in core or in outcrop, and no chrysotile has been positively identified (by petrography or x-ray diffraction) from the Burks Mountain complex. Physical, structural and chemical conditions necessary for development of cross-fiber chrysotile asbestos as outlined by Wicks and O'Hanley (1988), do not appear to have been attained in any of the serpentinites of the Burks Mountain complex (Cocker, 1989a, 1989b, and 1991b). A cross-fiber/foliated texture commonly developed in the serpentinite adjacent to fractures and rimming clasts is primarily coarse-bladed talc with minor chlorite. Physical and chemical conditions (discussed earlier) do not appear favorable for either the formation of economic concentrations of fibrous Mg-silicates or for their preservation from destructive

alteration. Petrographic studies (Cocker, 1991b) indicate that talc and lizardite replaced most of the earlier anthophyllite and tremolite, and suggest that these fibrous Mg-silicates are probably of little consequence.

#### Platinum group elements (PGE's)

Most primary economic deposits of platinum group elements (PGE's) occur in mafic/ultramafic bodies. The world's supply comes mainly from South Africa and the Soviet Union with only one deposit (the Stillwater J-M (Howland) reef) currently being mined in the United States. Surface and drill core samples were analyzed for the two most common and usually most abundant PGE's, platinum and palladium. The samples contained no PGE's over the detection limit of 0.1 ppm.

#### Quartz vein mineralization (base and precious metals)

Extensive quartz veining and silicification, particularly in the northern serpentinite, indicates significant hydrothermal activity accompanied by introduction of large volumes of silica. Cross-cutting relationships, grain size variations, degree of crystallinity, and alteration envelopes suggest a rather complex period of fracturing and veining. Veins range from small and simple, 1-3 mm wide, to large and composite, up to 15 cm wide, with at least 10 distinct episodes of vein filling. In many mining districts, base and precious metal mineralization is associated with quartz veining. Eleven quartz-veined or silicified serpentinite outcrops were sampled and analyzed for the more commonly encountered base metals plus gold and silver.

Geochemical results (Appendix II) show less than 10 ppm Cu, less than 5 ppm Pb, 35 ppm or less Zn, less than 2 ppm As and generally less than 0.02 ppm Au and 0.05 ppm Ag. One sample (DDH PC-1-74) contains 0.03 ppm Au and 5.8 ppm Ag which are clearly anomalous. The lack of additional anomalous samples is not encouraging. The extremely low values are at background levels and indicate either no anomalous primary concentrations or significant depletion through weathering.

Mercury is weakly anomalous (0.02-0.04 ppm) and may be related to the silicification and quartz veining. A similar association of quartz veining, serpentinites and Hg mineralization is common in the California Coast Range serpentinites (Bailey and Everhart, 1964). Values are considered too low for potentially economic Hg concentrations. Because the area has been subjected to intense and prolonged

weathering since quartz veining occurred, higher concentrations of Hg may have been leached from the near-surface.

High-grade copper (assay of about 15 percent copper) in the form of chalcopyrite is reported to have been drilled about 1/2 mile southeast of Pollards Corner by the J.M. Huber Corporation. Results of a geochemical survey revealed no strongly anomalous copper in surface samples from the vicinity of the drill hole suggesting that the occurrence may be rather restricted (Hurst and others, 1966).

## DISCUSSION AND CONCLUSIONS

### Origin of the mineral deposits

The following paragenesis outlines a sequence of events critical to the formation of the presently observed mineral deposits and mineralization. Circumstances surrounding some of these events are presently uncertain but may be better understood when current studies are completed (Maher and Sacks, personal communication, 1989).

- 1) emplacement of the Burks Mountain ultramafites into the Kiokee Belt rocks subsequent to penetrative deformation;
- 2) prograde metamorphism of an ultramafite of harzburgite composition to an upper amphibolite grade- assemblage of enstatite + olivine + chlorite +/- tremolite +/- anthophyllite + ferritchromite or Cr-magnetite;
- 3) retrograde metamorphism of olivine, enstatite, anthophyllite and tremolite to lizardite serpentinite plus secondary magnetite;
- 4) fracturing of the serpentinite and enclosing Kiokee rocks;
- 5) influx of CO<sub>2</sub>, which may be accompanied by SiO<sub>2</sub> and/or loss of MgO through a fracture system resulting in alteration of lizardite to carbonate + talc; CO<sub>2</sub> addition may extend beyond #6;
- 6) influx of Al<sub>2</sub>O<sub>3</sub> along fractures and breccias to form coarse-grained chlorite from talc and lizardite; this may accompany or overlap #5;
- 7) replacement of talc, serpentinite, amphibole and chlorite by quartz +/- chalcedony during numerous periods of silica veining and pervasive silicification;
- 8) further fracturing of serpentinite and Kiokee gneisses during Late Jurassic extensional tectonics(?).

## Economic geology of the mineral deposits

The talc, serpentinite and the REE-Ti-V-bearing magnetite layers are the most important resources identified in this part of the Burks Mountain complex. Samples were tested for other potentially economic elements (Ni, Cr, Pt, Pd, Au, etc.), but although some of these elements were anomalous none were of economic grade.

The talc resource appears to be a bulk-tonnage, medium-grade deposit. Talc grades estimated from a roadcut exposure of the multilithic breccia are on the order of 25 percent. GE brightness results are dependent on the magnetite content and weathering of the magnetite; magnetic separation of the magnetite could enhance the talc's brightness. Tonnages calculated from drill-hole intercepts and surface indications of the multilithic breccia assuming a conservative open-pit configuration are on the order of 1.8 million tons. An open-pit operation, little overburden, and anticipated ease of mining and ore separation favor low-cost production. Prospects for additional talc-mineralized zones within the Burks Mountain complex are good and would further enhance the mining economics.

The serpentinite has the potential for use as dimension stone or as a source of MgO for chemicals. The Burks Mountain serpentinite has been an economically viable source of MgO in the past. Open-pit development of the talc deposit would expose the underlying serpentinite to development, also.

The occurrence of exceedingly high concentrations of REE's, Ti and V in magnetite - ilmenohematite rich layers in the Burks Mountain complex is unusual if not unique. High concentrations of REE's are suggested for Ti-V-magnetite-rich layers in the Bushveld Complex. The extent of the occurrence in the Burks Mountain complex is unknown. Further studies are recommended to evaluate this occurrence.

## REFERENCES CITED

- Akpanika, O.I., Ukpong, E.E., and Olade, M.A., 1987, Mineralogy and geochemical dispersion in tropical residual soils overlying a talc deposit in southwestern Nigeria: *Chemical Geology*, v. 63, p. 109-119.
- Armstrong, R.L., and Dick, H.J.B., 1974, A model for development of thin overthrust sheets of crystalline rock: *Geology*, v. 2, p. 35-40.
- Bailey, E.H. and Everhart, D.L., 1964, Geology and quicksilver deposits of the New Almaden District, Santa Clara Co., California: U.S. Geological Survey Professional Paper 360, 260 pp.
- Blount, A.M. and Vassiliou, A.H., 1980, The mineralogy and origin of the talc deposits near Winterboro, Alabama: *Economic Geology*, v. 75, p. 107-116.
- Brown, C.E., 1973, Talc: U.S. Geological Survey Professional Paper 820, p. 619-626.
- Challis, G.A., 1965, The origin of the New Zealand ultramafic intrusions: *Journal of Petrology*, v. 6, p. 322-364.
- Chidester, A.H., 1962, Petrology and geochemistry of selected talc-bearing ultramafic rocks and adjacent country rocks in north-central Vermont: U.S. Geological Survey Professional Paper 345, 207 pp.
- Cocker, M.D., 1989a, Metamorphism and deformation of the Burks Mountain ultramafic complex, Columbia County, Georgia: *Geological Society of America Abstracts with Programs*, v. 21, no. 3, p. 8.
- Cocker, M.D., 1989b, Talc alteration of a serpentinite in the Burks Mountain ultramafic complex, Columbia County, Georgia: *Geological Society of America Abstracts with Programs*, v. 21, no. 3, p. 8.
- Cocker, M.D., 1989c, Geochemistry of a vertically zoned, metamorphosed and serpentinitized harzburgite: implications for the tectonic evolution of the southern Appalachian Piedmont: *Geological Society of America Abstracts with Programs*, v. 21, no. 7, p. A106.
- Cocker, M.D., 1990, Mineralogy, geochemistry and genesis of REE-Ti-V enriched iron oxides in the Burks Mountain complex, Columbia County, Georgia: *Geological Society of America Abstracts with Programs*, v. 22, no. 4, p. 8.
- Cocker, M.D., 1991a, Geology and origin of a talc prospect in the Burks Mountain Complex, Columbia County, Georgia: in Pickering, Jr., S.M., ed., *Proceedings of the Symposium on the Economic Geology of Southeastern Industrial Minerals*: Georgia Geologic Survey Bulletin 120, p. 107-133.
- Cocker, M.D., 1991b, Geology and geochemistry of altered serpentinites in the Burks Mountain complex, Columbia County, Georgia: *Georgia Geological Survey Bulletin* 124, 104 pp.
- Dallmeyer, R.D., Wright, J.E., Secor, D.T., Jr., Snoke, A.W., 1986, Character of the Alleghanian orogeny in the southern Appalachians: Part II. Geochronological constraints on the tectonothermal evolution of the eastern Piedmont in South Carolina: *Geological Society of America Bulletin*, v. 97, p. 1329-1344.
- Daniels, D.L., 1974, Geologic interpretations of geo-

- physical maps, central Savannah River area, South Carolina and Georgia: U.S. Geological Survey Geophysical Investigations Map GP-893.
- Eargle, D.H., 1955, Stratigraphy of the outcropping Cretaceous rocks of Georgia: United States Geological Survey Bulletin 1014, 101 pp.
- Evans, B.W. and Guggenheim, 1988, Talc, pyrophyllite and related minerals: *in* Bailey, S.W., ed., Hydrous Phyllosilicates (exclusive of micas): Mineralogical Society of America Reviews in Mineralogy, v.19, p. 225-294.
- Feiss, P.G., 1982, Geochemistry and tectonic setting of the volcanics of the Carolina slate belt: *Economic Geology*, v.77, p. 273-293.
- Frazier, W.J., and Schwimmer, D.R., 1987, Regional Stratigraphy of North America: Plenum Press, New York, 719 pp.
- Helz, R.T., 1985, Compositions of fine-grained mafic rocks, from sills and dikes associated with the Stillwater Complex, *in* Czamanske, G.K. and Zientek, eds., The Stillwater Complex, Montana: Geology and Guide: Montana Bureau of Mines and Geology Special Publication 92, p. 97-117.
- Higgins, M.W., Atkins, R.L., Crawford, T.J., Crawford, R.F., III, Brooks, R., Cook, R.B., 1988, The structure, stratigraphy, tectonostratigraphy, and evolution of the southernmost part of the Appalachian orogen: U.S. Geological Survey Professional Paper 1475, 173 pp.
- Hopkins, O.B., 1914, Asbestos, talc, and soapstone deposits of Georgia: Georgia Geologic Survey Bulletin 29, 319 pp.
- Howell, D.E., and Pirkle, W.A., 1976, Geologic section across the Modoc fault zone, Modoc, South Carolina: *in* Chowns, T.M., ed., Stratigraphy, structure, and seismicity in Slate Belt rocks along the Savannah River, Georgia Geologic Survey/Georgia Geological Society Field Trip Guide, p. 16-20.
- Hurst, V.J., Crawford, T.J., and Sandy, J., 1966, Mineral resources of the Central Savannah River area: U.S. Department of Commerce publication, 467 pp.
- Jahns, R.H., 1967, Serpentinities in the Roxbury district, Vermont: *in* Wyllie, P.J., ed., Ultramafic and Related Rocks: New York, John Wiley and Sons, p. 137-160.
- Kish, S.A., Butler, J.R., and Fullagar, P.D., 1979, The timing of metamorphism and deformation in the central and eastern Piedmont of North Carolina: Geological Society of America Abstracts with Programs, v. 11, p. 184-185.
- LeGrand, H.E., and Furcron, A.S., 1956, Geology and ground-water resources of central-east Georgia: Georgia Geologic Survey Bulletin 64, 174 pp.
- MacDonald, A.H., 1984, Water diffusion rates through serpentinized peridotites. Implications for reaction induced and chemical effects in ultramafic rocks: University of Western Ontario, unpublished Ph.D. Dissertation, 226 pp.
- Maher, H.D., Jr., 1978, Stratigraphy and structure of the Belair and Kiokee belts near Augusta, Georgia: *in* Snoke, A.W., ed., Geological investigations of the eastern Piedmont, southern Appalachians: South Carolina Geological Survey, Carolina Geological Society Guidebook for 1978, p. 47-54.
- Maher, H.D., Jr., 1987, Kinematic history of mylonitic rocks from the Augusta Fault Zone, South Carolina and Georgia: *American Journal of Science*, v. 287, p. 795-816.
- McLemore, W.H., 1965, Geology of the Pollard's Corner, Columbia County, Georgia, unpublished M.S. thesis, University of Georgia, 49 pp.
- O'Connor, B.J. and Prowell, D.C., 1976, The geology of the Belair Fault Zone and basement rocks of the Augusta, Georgia area: *in* Chowns, T.M., ed., Stratigraphy, structure, and seismicity in Slate Belt rocks along the Savannah River, Georgia Geologic Survey/ Georgia Geological Society Field Trip Guide, p. 16-20.
- Reynolds, I.M., 1985, Contrasted mineralogy and textural relationships in the uppermost titaniferous magnetite layers of the Bushveld Complex in the Bierkraal area north of Rustenburg: *Economic Geology*, v. 80, p. 1027-1048.
- Rice, S.J., 1957, Nickel: Mineral commodities of California: California Division Mines Bull. 176, p. 391-399.
- Roe, L.A., 1975, Talc and pyrophyllite: *in* Lefond, S.J., ed., Industrial Minerals and Rocks (Fourth Edition), A.I.M.E., Baltimore, Md., p. 1127-1147.
- Roe, L.A., and Olson, R.H., 1983, Talc: *in* Lefond, S.J., ed., Industrial Minerals and Rocks, (Fifth Edition) A.I.M.E., Baltimore, Md., p. 1275-1301.
- Rogers, J.J.W., 1982, Criteria for recognizing environments of formation of volcanic suites; Application of these criteria to volcanic suites in the Carolina slate belt, *in* Bearce, D.N., Black, W.W., Kish, S.A., and Tull, J.F., eds., Tectonic studies in the Talladega and Carolina slate belts, southern Appalachian orogen: Geological Society of America Special Paper 191,

- p. 99-107.
- Sacks, P.E., Maher, H.D., Jr., and Secor, D.T., 1987, The Burks Mtn. Belt of ultramafic rocks in the Kiokee Belt, Southern Appalachian Piedmont: Geological Society of America Abstracts with Programs, v. 19, p. 127.
- Sacks, P.E., Maher, H.D., Secor, D.T., Shervais, J.W., 1989, The Burks Mountain complex, Kiokee belt, southern Appalachian Piedmont of South Carolina and Georgia: *in* Mittwede, S.K. and Stoddard, E.F., eds., Ultramafic Rocks of the Appalachian Piedmont: Geological Society of America Special Paper 231, p. 75-86.
- Sanford, R.F., 1982, Growth of ultramafic reaction zones in greenschist to amphibolite facies metamorphism: American Journal of Science, v. 282, p. 543-616.
- Secor, D.T., Jr., 1987, Regional Overview: *in* Secor, D.T., Jr., ed., Anatomy of the Alleghanian orogeny as seen from the Piedmont of South Carolina and Georgia: Carolina Geological Society Field Trip Guidebook, p. 1-18.
- Secor, D.T., Jr., Samson, S.L., Snoke, A.W., and Palmer, A.R., 1983, Confirmation of the Carolina slate belt as an exotic terrane: Science, v. 221, p. 649-650.
- Secor, D.T., Jr., Snoke, A.W., Bramlett, K.W., Costello, O.P., and Kimbrell, O.P., 1986a, Character of the Alleghanian orogeny in the southern Appalachians: Part I. Alleghanian deformation in the eastern Piedmont of South Carolina: Geological Society of America Bulletin, v. 97, p. 1319-1328.
- Secor, D.T., Jr., Snoke, A.W., and Dallmeyer, R.D., 1986b, Character of the Alleghanian orogeny in the southern Appalachians: Part III. Regional tectonic relations: Geological Society of America Bulletin, v. 97, p. 1345-1353.
- Shelley, S.A., Shervais, J.W., and Secor, D.T., Jr., 1988, Geochemical characterization of metavolcanic rocks of the Carolina slate belt, central South Carolina: Geological Society of America Abstracts with Programs, v. 20, p. 314.
- Telford, W.M., Geldart, L.P., Sheriff, R.E., and Keys, D.A., 1976, Applied Geophysics, Cambridge University Press, New York, N.Y., 860 pp.
- Tschudy, R.H., and Patterson, S.H., 1975, Palynological evidence for Late Cretaceous, Paleocene and Early and Middle Eocene ages for strata in the kaolin belt, central Georgia: U.S. Geological Survey, Journal of Research, v. 3, p. 437-445.
- Vick, H.K., Channell, J.E.T., and Opdyke, N.D., 1987, Ordovician docking of the Carolina slate belt: Paleomagnetic data: Tectonics, v. 6, p. 573-583.
- Vincent, H.R., McConnell, K.I., Perley, P.C., 1990, Geology of selected mafic and ultramafic rocks of Georgia: a review: Georgia Geologic Survey Information Circular 82, 59 pp.
- Vitra, R.L., 1987, Talc and Pyrophyllite in 1986: U.S. Bureau of Mines Mineral Industry Surveys, 3 pp.
- Whitney, J.A., Paris, R.H., Carpenter, R.H., and Hartley, M.E., III, 1978, Volcanic evolution of the southern slate belt of Georgia and South Carolina - A primitive volcanic arc: Journal of Geology, v.86, p. 173-192.
- Wicks, F.J. and O'Hanley, D.S., 1988, Serpentine minerals: structures and petrology: *in* Bailey, S.W., ed., Hydrous Phyllosilicates (exclusive of micas): Mineralogical Society of America Reviews in Mineralogy, v. 19, p. 91-164.
- Worthington, J.E., 1964, An exploration program for nickel in the southeastern United States: Economic Geology, v. 59, p. 97-109.



## APPENDICES



## APPENDIX I.

### WHOLE ROCK CHEMISTRY - TALC

|                                | S1-132        | S5-163        | PC88-2<br>203 | PC88-2<br>128 |
|--------------------------------|---------------|---------------|---------------|---------------|
| SiO <sub>2</sub>               | 61.000        | 55.500        | 42.100        | 31.500        |
| Al <sub>2</sub> O <sub>3</sub> | 0.370         | 1.000         | 0.620         | 0.350         |
| Fe <sub>2</sub> O <sub>3</sub> | 1.100         | 3.400         | 4.800         | 2.900         |
| FeO                            | 1.500         | 1.300         | 1.100         | 1.500         |
| MgO                            | 30.500        | 30.200        | 24.100        | 28.500        |
| CaO                            | 0.022         | 0.820         | 8.400         | 7.000         |
| Na <sub>2</sub> O              | 0.100         | 0.040         | 0.040         | 0.040         |
| K <sub>2</sub> O               | 0.020         | 0.020         | 0.036         | 0.024         |
| LOI                            | 5.000         | 6.400         | 15.400        | 24.100        |
| TiO <sub>2</sub>               | 0.010         | 0.010         | 0.010         | 0.010         |
| P <sub>2</sub> O <sub>5</sub>  | 0.010         | 0.010         | 0.010         | 0.010         |
| MnO                            | 0.033         | 0.047         | 0.370         | 0.130         |
| SrO                            | 0.001         |               |               |               |
| Rb <sub>2</sub> O              | 0.001         |               |               |               |
| Ni                             |               |               | 0.130         | 0.195         |
| Cr                             |               |               | 0.210         | 0.220         |
| V(ppm)                         |               |               | 20.000        | 5.000         |
| <b>Total</b>                   | <b>99.266</b> | <b>98.747</b> | <b>97.326</b> | <b>96.479</b> |

(Values are in weight percent unless otherwise noted.)

| Sample:     | Sample locations:             |
|-------------|-------------------------------|
| S1-132      | DDH PC 87-1, depth - 132 feet |
| S5-163      | DDH PC 87-5, depth - 163 feet |
| PC88-2, 203 | DDH PC 88-2, depth - 203 feet |
| PC88-2, 128 | DDH PC 88-2, depth - 128 feet |

## APPENDIX II.

### TRACE ELEMENT GEOCHEMISTRY (Values are in ppm)

| Sample    | Au    | Ag    | Ni   | Cr   | Co  | Pt   | Pd   | Cu | Pb | Zn | As   | Hg   |
|-----------|-------|-------|------|------|-----|------|------|----|----|----|------|------|
| 1-74      | 0.03  | 5.8   | 2300 | 3150 |     | <0.1 | <0.1 |    |    |    |      |      |
| 1-132     |       |       | 1300 | 1250 |     |      |      |    |    |    |      |      |
| 1-160     | <0.02 | 0.4   | 2300 | 2000 |     | <0.1 | <0.1 |    |    |    |      |      |
| 1-173     |       |       | 1100 | 1050 |     |      |      |    |    |    |      |      |
| 4-23      |       |       | 4100 | 1700 |     |      |      |    |    |    |      |      |
| 4-47      |       |       | 1400 | 1200 |     |      |      |    |    |    |      |      |
| 4-90      | 0.686 | 3.8   | 1700 | 3100 | 70  | <0.1 | <0.1 |    |    |    |      |      |
| 4-140     | <0.02 | <0.34 | 2250 | 4450 | 90  | <0.1 | <0.1 |    |    |    |      |      |
| 4-170     |       |       | 930  | 1200 |     |      |      |    |    |    |      |      |
| 4-196     | <0.02 | <0.34 | 2250 | 2850 | 90  | <0.1 | <0.1 |    |    |    |      |      |
| 5-103     | <0.02 | <0.34 | 590  | 1250 | 15  | <0.1 | <0.1 |    |    |    |      |      |
| 5-147     | <0.02 | <0.34 | 670  | 870  | 15  | <0.1 | <0.1 |    |    |    |      |      |
| 5-149     | <0.02 | <0.34 | 1450 | 2050 | 30  | <0.1 | <0.1 |    |    |    |      |      |
| 5-185.5   | <0.02 | <0.34 | 2450 | 2800 | 85  | <0.1 | <0.1 |    |    |    |      |      |
| 5-177     |       |       | 700  | 200  |     |      |      |    |    |    |      |      |
| 5-205     | <0.02 | <0.34 | 2350 | 1750 | 95  | <0.1 | <0.1 |    |    |    |      |      |
| 5-236     | <0.02 | <0.34 | 2200 | 2950 | 105 | <0.1 | <0.1 |    |    |    |      |      |
| 5-257     | <0.02 | <0.34 | 2550 | 1450 | 135 | <0.1 | <0.1 |    |    |    |      |      |
| BM-1A     | <0.02 | <0.05 |      |      | 35  |      |      | <5 | <5 | 35 | <2   | 0.03 |
| BM-2A     | <0.02 | <0.05 |      |      | 30  |      |      | <5 | <5 | 25 | <2   | 0.03 |
| BM-2      | <0.02 | <0.05 |      |      | 60  |      |      | <5 | <5 | 35 | <2   | 0.02 |
| BM-3      | <0.02 | <0.05 |      |      | 25  |      |      | <5 | <5 | 20 | <2   | 0.02 |
| BM-4      | <0.02 | <0.05 |      |      | 10  |      |      | <5 | <5 | <5 | <2   | 0.04 |
| B-1000    | <0.02 | <0.05 |      |      | 55  |      |      | <5 | <5 | 35 | <2   | 0.02 |
| B-800     | <0.02 | <0.05 |      |      | 95  |      |      | <5 | <5 | 35 | <2   | 0.02 |
| DX-1      | <0.02 | <0.05 |      |      | 40  |      |      | <5 | <5 | 20 | <2   | 0.03 |
| D224      | <0.02 | <0.05 |      |      | 50  |      |      | 5  | <5 | 25 | <2   | 0.03 |
| E970-800S | <0.02 |       |      | 40   |     |      | 10   | <5 | <5 | 25 | <2   | 0.03 |
| W50-550S  | <0.02 |       |      | 20   |     |      | <5   | <5 | 10 | <2 | 0.02 |      |
| 88-2-203  |       | 1300  | 2100 |      |     |      |      |    |    |    |      |      |
| 88-2-128  |       | 1950  | 2200 |      |     |      |      |    |    |    |      |      |
| 88-3-1    |       |       | 990  | 3450 |     |      |      |    |    |    |      |      |
| 88-3-18   |       |       | 1650 | 2600 |     |      |      |    |    |    |      |      |
| 1010      |       |       | 2700 | 1850 |     |      |      |    |    |    |      |      |
| 88-1-0    |       |       | 830  | 2700 |     |      |      |    |    |    |      |      |
| 88-1-1    |       |       | 1600 | 3750 |     |      |      |    |    |    |      |      |
| 88-1-2    |       |       | 1700 | 2650 |     |      |      |    |    |    |      |      |
| 88-1-3    |       |       | 2650 | 2550 |     |      |      |    |    |    |      |      |
| 88-1-4    |       |       | 2000 | 360  |     |      |      |    |    |    |      |      |
| D139      |       |       | 1950 | 4600 |     |      |      |    |    |    |      |      |
| 88-2-60   |       |       | 2    | 295  |     |      |      |    |    |    |      |      |
| 88-2-104  |       | 1100  | 1200 |      |     |      |      |    |    |    |      |      |
| 88-2-115  |       | 2100  | 990  |      |     |      |      |    |    |    |      |      |
| 88-2-151  |       | 2350  | 1100 |      |     |      |      |    |    |    |      |      |
| 88-2-176  |       | 2050  | 770  |      |     |      |      |    |    |    |      |      |
| BM1       |       |       | 1650 | 2200 |     |      |      |    |    |    |      |      |
| B825      |       |       | 940  | 1250 |     |      |      |    |    |    |      |      |
| B850      |       |       | 210  | 100  |     |      |      |    |    |    |      |      |
| PC104-1   |       | 1100  | 1800 |      |     |      |      |    |    |    |      |      |

## APPENDIX II.

| Sample    | Sample Locations   |
|-----------|--|
| 1-74      | DDH PC 87-1, depth - 74 feet                               |
| 1-132     | DDH PC 87-1, depth - 132 feet                              |
| 1-160     | DDH PC 87-1, depth - 160 feet                              |
| 1-173     | DDH PC 87-1, depth - 173 feet                              |
| 4-23      | DDH PC 87-4, depth - 23 feet                               |
| 4-47      | DDH PC 87-4, depth - 47 feet                               |
| 4-90      | DDH PC 87-4, depth - 90 feet                               |
| 4-140     | DDH PC 87-4, depth - 140 feet                              |
| 4-170     | DDH PC 87-4, depth - 170 feet                              |
| 4-196     | DDH PC 87-4, depth - 196 feet                              |
| 5-103     | DDH PC 87-5, depth - 103 feet                              |
| 5-147     | DDH PC 87-5, depth - 147 feet                              |
| 5-149     | DDH PC 87-5, depth - 149 feet                              |
| 5-185.5   | DDH PC 87-5, depth - 185.5 feet                            |
| 5-177     | DDH PC 87-5, depth - 177 feet                              |
| 5-205     | DDH PC 87-5, depth - 205 feet                              |
| 5-236     | DDH PC 87-5, depth - 236 feet                              |
| 5-257     | DDH PC 87-5, depth - 257 feet                              |
| BM-1A     | Burks Mountain - surface                                   |
| BM-2A     | Burks Mountain - surface                                   |
| BM-2      | Burks Mountain - surface                                   |
| BM-3      | Burks Mountain - surface                                   |
| BM-4      | Burks Mountain - surface                                   |
| B-1000    | Burks Mountain - surface                                   |
| B-800     | Burks Mountain - surface                                   |
| DX-1      | Burks Mountain (Dixie Mountain) - outcrop                  |
| D224      | Old Petersburg Roadcut - outcrop                           |
| E970-800S | Outcrop on talc ridge 970 feet east of Old Petersburg Road |
| W50-550S  | Subcrop in field 50 feet east of Old Petersburg Road       |
| 88-2-203  | DDH PC 88-2, depth - 203 feet                              |
| 88-2-128  | DDH PC 88-2, depth - 128 feet                              |
| 88-3-1    | DDH PC 88-3, depth - 1 foot                                |
| 88-3-18   | DDH PC 88-3, depth - 18 feet                               |
| 1010      | E970-800S, outcrop 970 feet east of Old Petersburg Road    |
| 88-1-0    | DDH PC 88-1, depth - 0 feet                                |
| 88-1-1    | DDH PC 88-1, depth - 1 foot                                |
| 88-1-2    | DDH PC 88-1, depth - 2 feet                                |
| 88-1-3    | DDH PC 88-1, depth - 3 feet                                |
| 88-1-4    | DDH PC 88-1, depth - 4 feet                                |
| D139      | Old Petersburg Roadcut - outcrop                           |
| 88-2-60   | DDH PC 88-2, depth - 60 feet                               |
| 88-2-104  | DDH PC 88-2, depth - 104 feet                              |
| 88-2-115  | DDH PC 88-2, depth - 115 feet                              |
| 88-2-151  | DDH PC 88-2, depth - 151 feet                              |
| 88-2-176  | DDH PC 88-2, depth - 176 feet                              |
| BM1       | Burks Mountain - surface                                   |
| B825      | Burks Mountain - surface                                   |
| B850      | Burks Mountain - surface                                   |
| PC104-1   | Outcrop 100 feet east of Georgia Highway #104              |

(DDH is an abbreviation for diamond drill hole.)

## APPENDIX III.

### DRILLING RESULTS

The drilling program at Pollards Corner was conducted in two phases: 1) summer of 1987, and 2) summer of 1988. The initial phase consisted of 6 holes which were sited on areas which had surface indications of talc. The second phase consisted of 4 holes which were sited to test targets defined through detailed geologic and geophysical mapping. A total of 1623 feet were drilled with the footage as shown in Table 1.

Drilling was done with the Georgia Geologic Survey's Failing CF-15 drill rig using conventional wire-line drilling methods. The diameter of core drilled is NX (1.875 inches; 47.625 mm).

Table 1

| Diamond Drill Hole (DDH) | Total Depth |        |
|--------------------------|-------------|--------|
|                          | Feet        | Meters |
| DDH PC 87-1              | 285         | 87     |
| DDH PC 87-2              | 91          | 28     |
| DDH PC 87-3              | 68          | 21     |
| DDH PC 87-4              | 230         | 70     |
| DDH PC 87-5              | 282         | 86     |
| DDH PC 87-6              | 115         | 35     |
| DDH PC 88-1              | 120         | 36     |
| DDH PC 88-2              | 240         | 73     |
| DDH PC 88-3              | 66          | 20     |
| DDH PC 88-4              | 126         | 38     |
| Total drilled            | 1623        | 495    |

#### Recovery

Drill recovery is a measure of the amount of core retrieved from a drilled interval relative to the amount of hole drilled. This was obtained by direct measurement of the core divided by the difference between the footage recorded by the drilling crew on wood blocks. Percent recovery shown as greater than 100 percent resulted from incorrect marking of core blocks relative to the actual footage drilled. The percent recovery is a good indication of the amount of fracturing or cementation, because solid rock is less likely to fall out of a core barrel during drilling and core-barrel recovery than non-cemented or broken rock.

Drill recovery is plotted for each hole (Figures 29-37). DDH PC 87-6 is not included because of poor recovery during most of the drilling - only the lower 10 feet of core was recovered. The poor recovery in the upper parts of DDH's PC87-1, 87-4, 87-5, and 88-1 is attributed to drilling in the multilithic breccia. Extremely poor recovery in the upper parts of DDH's PC 87-2, 87-3, 87-6 may be due to the same cause. Drilling in Kiokee gneiss in the upper part of DDH PC 88-4 and PC 88-2 resulted in improved recovery although deep saprolitic weathering tends to inhibit good recovery. Other intervals of poor recovery are attributed to broken or crushed rock resulting from late-stage brittle faulting/fracturing. The best recovery appears to be in massive serpentinite, gneissic granite and quartzo-feldspathic gneisses.

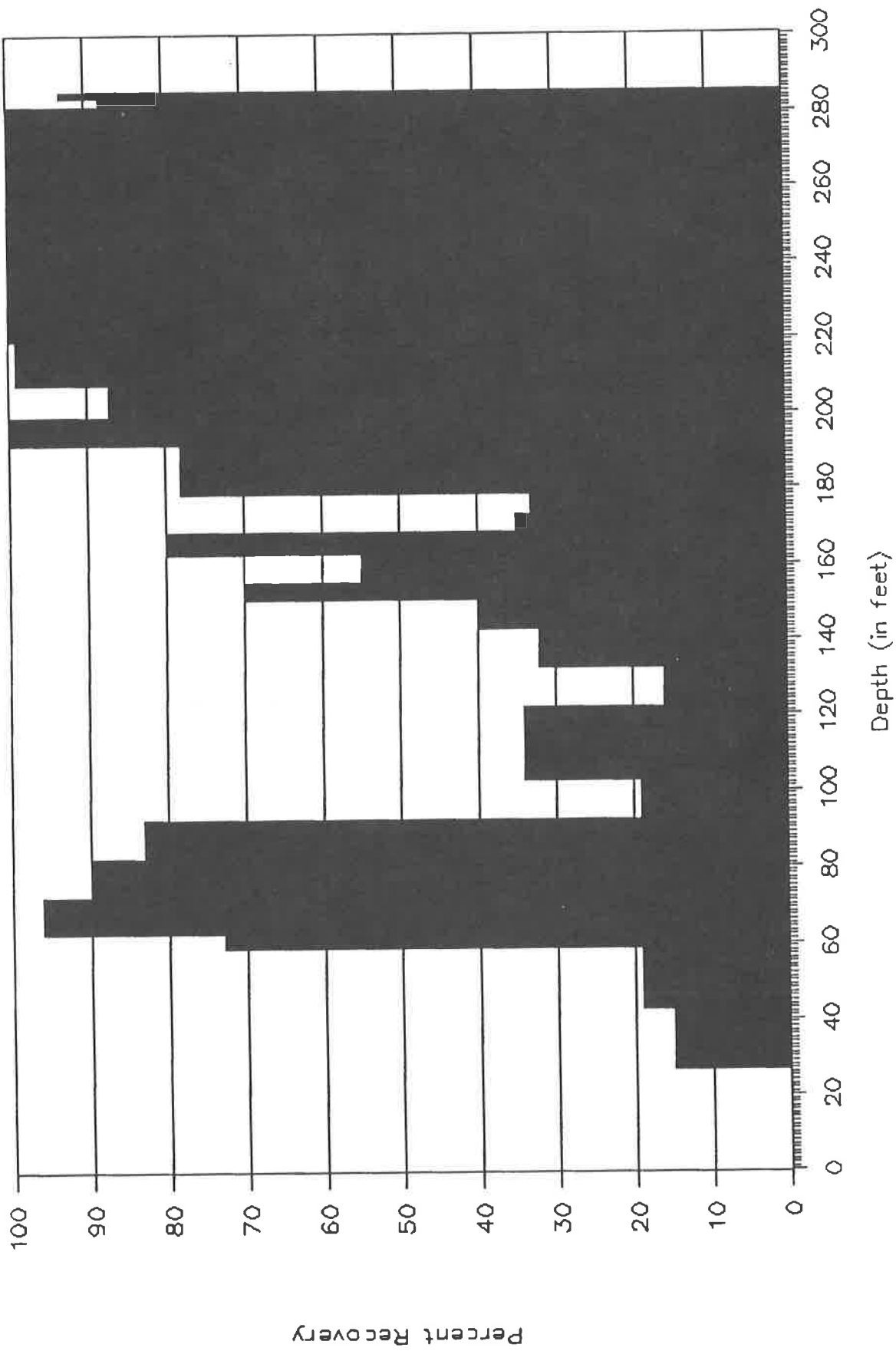


Figure 29. Recovery DDH PC87-1.

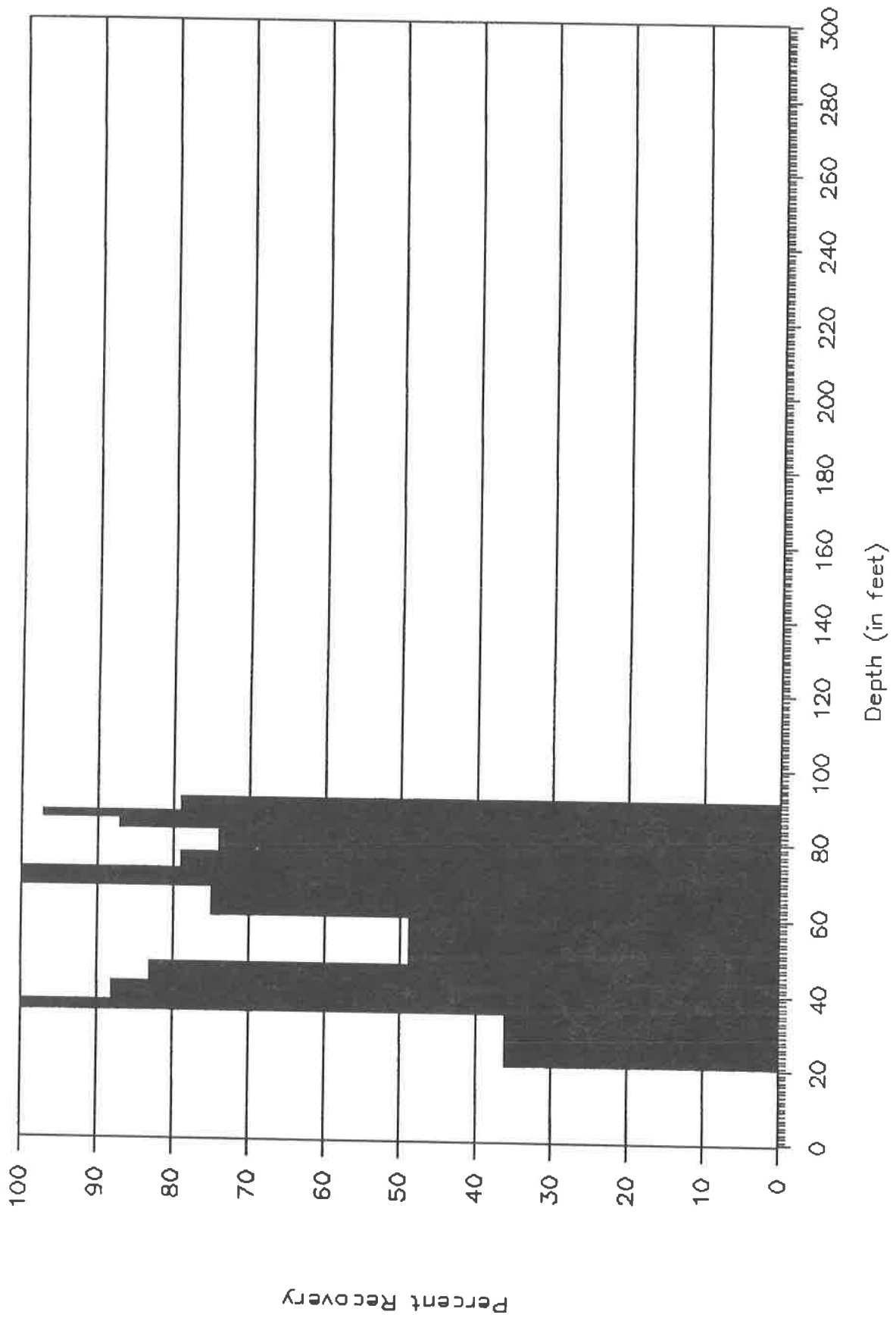


Figure 30. Recovery DDH PC87-2.



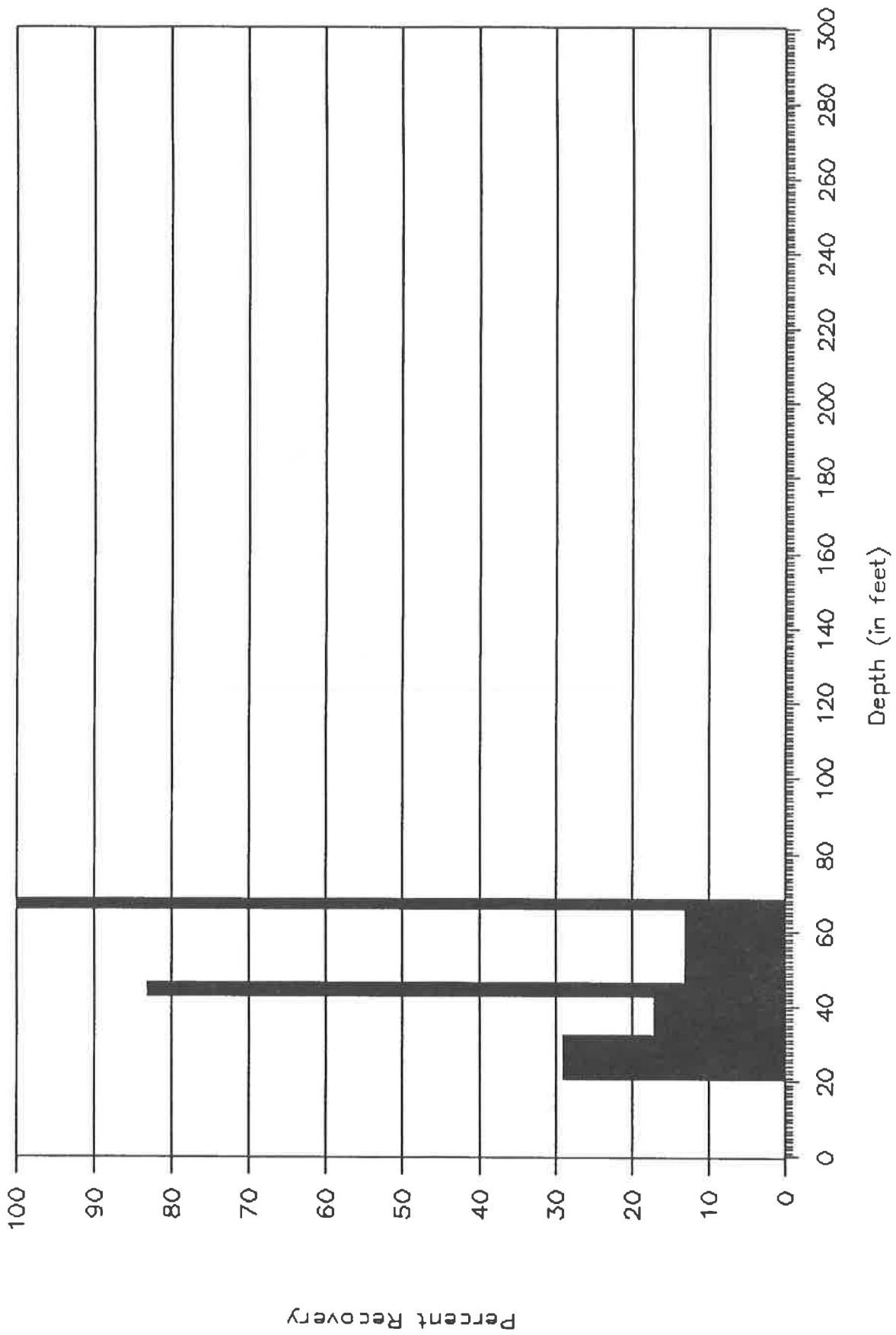


Figure 31. Recovery DDH PC87-3.

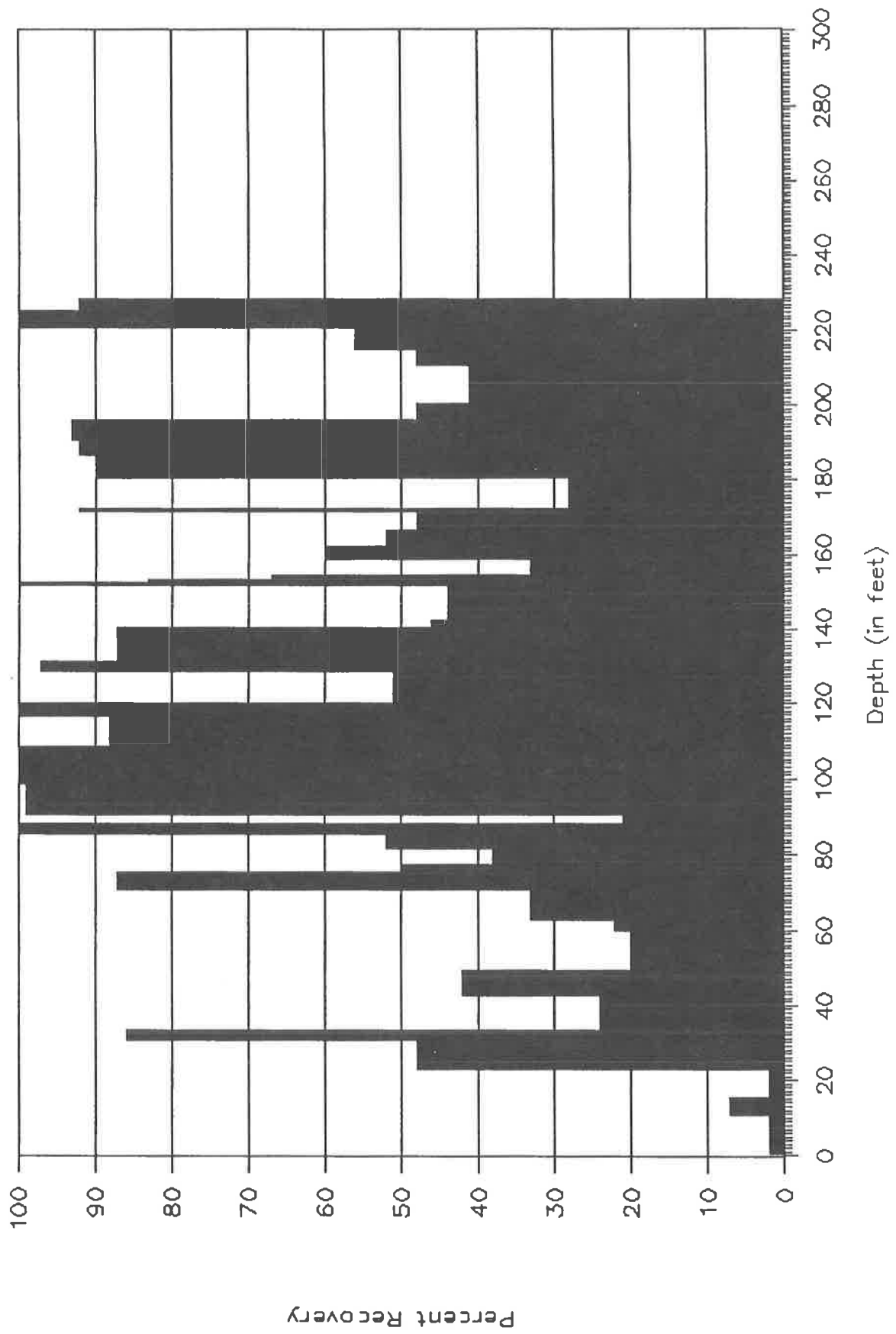


Figure 32. Recovery DDH PC87-4.

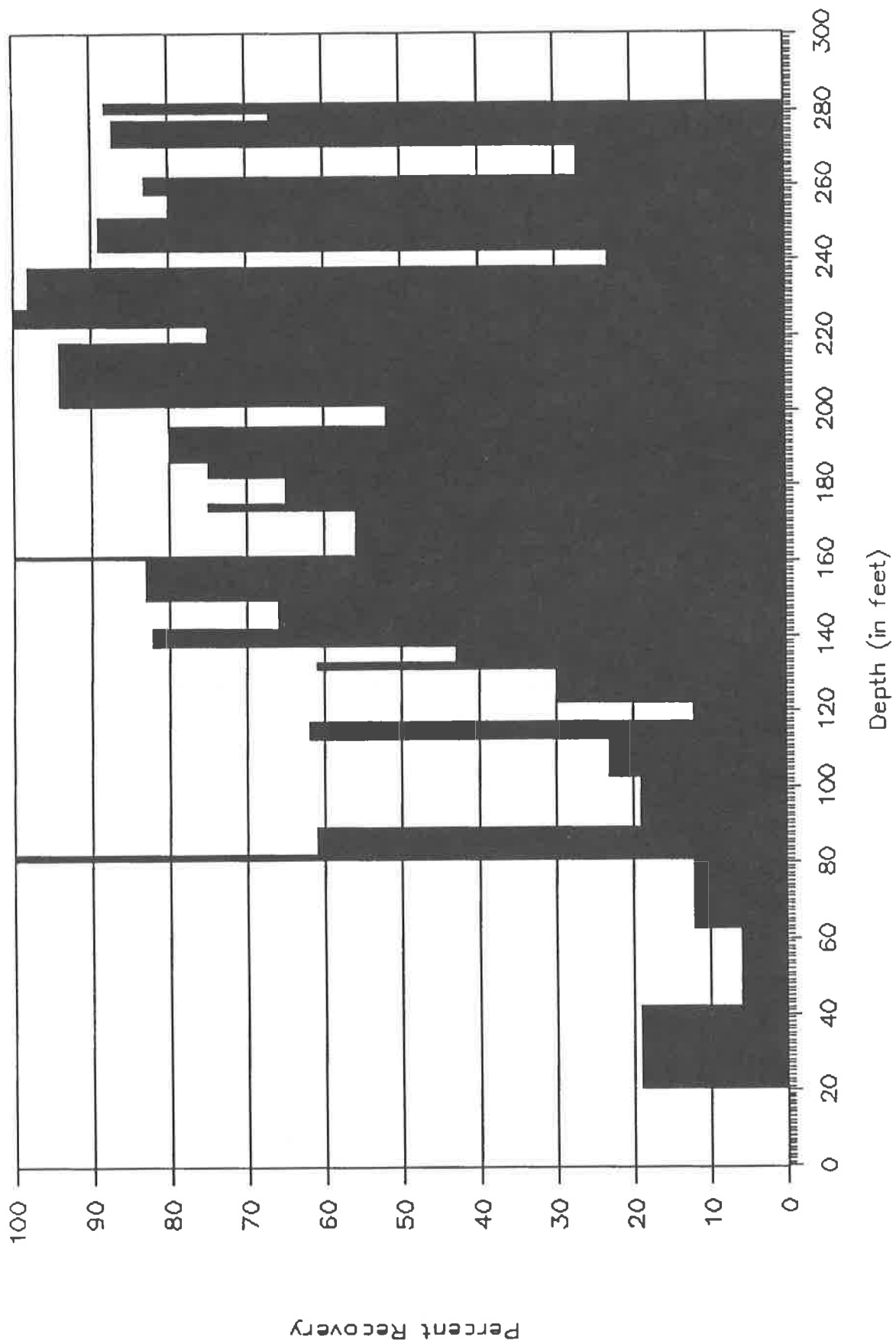


Figure 33. Recovery DDH PC87-5.

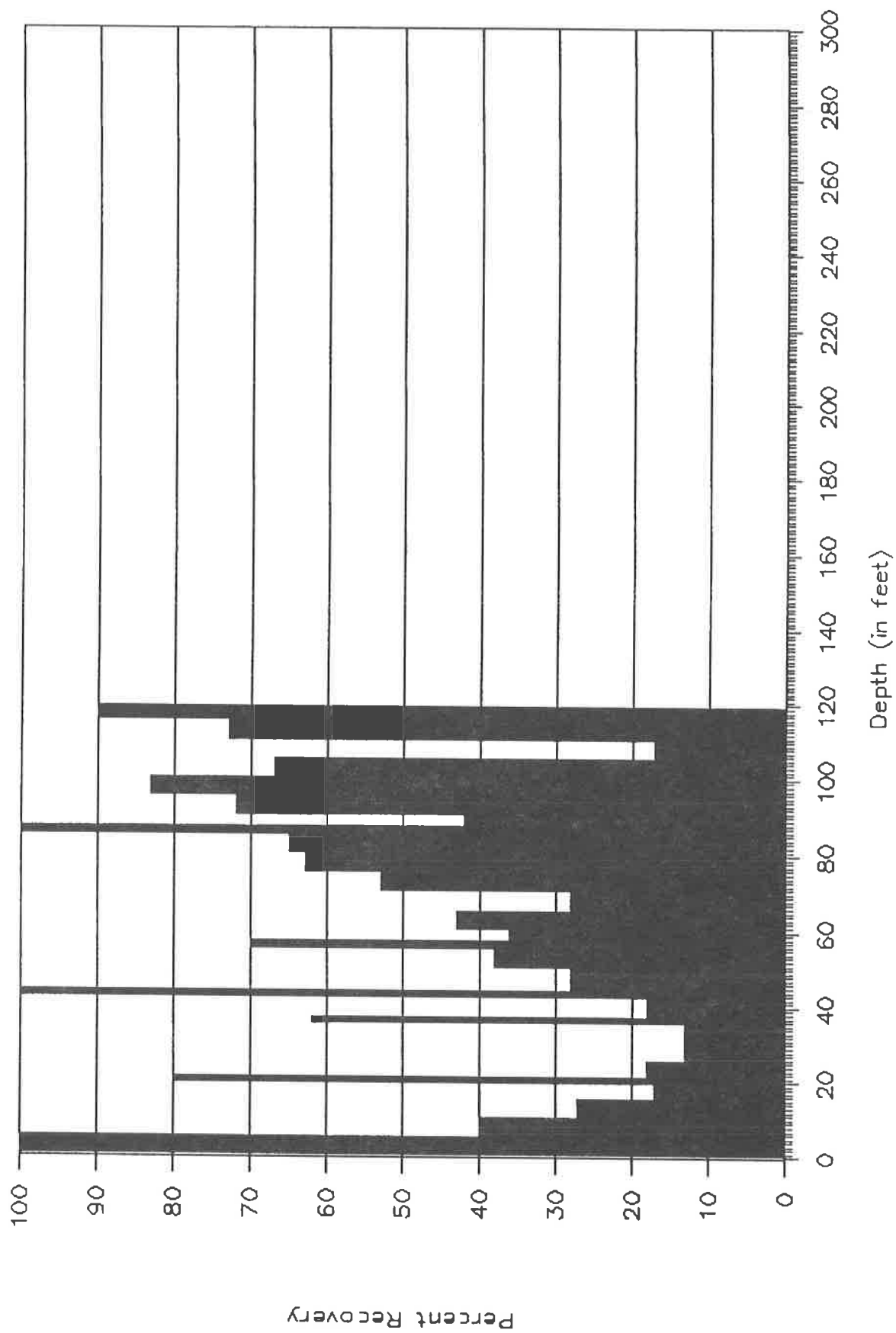


Figure 34. Recovery DDH PC88-1.

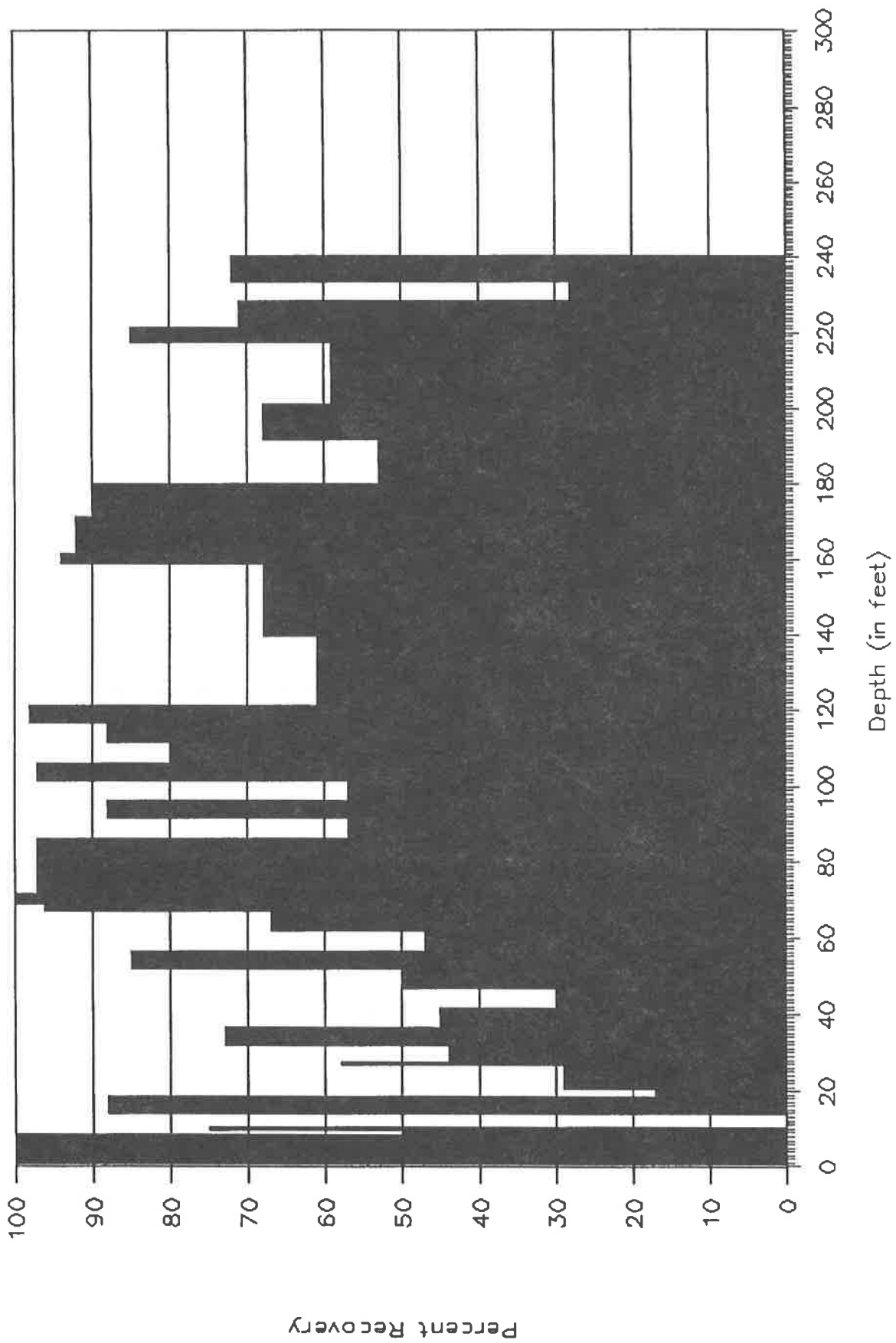


Figure 35. Recovery DDH PC88-2.

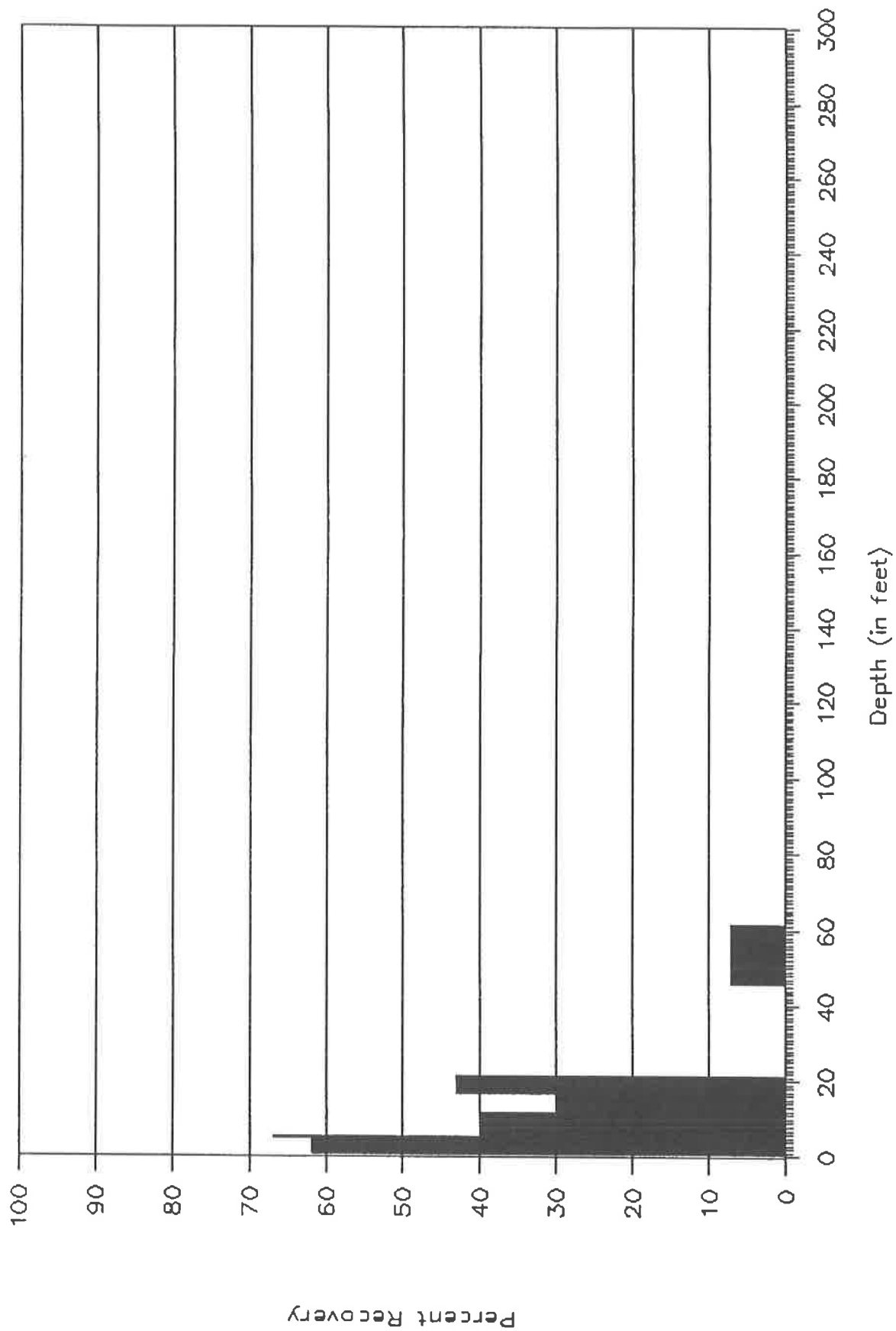


Figure 36. Recovery DDH PC88-3.

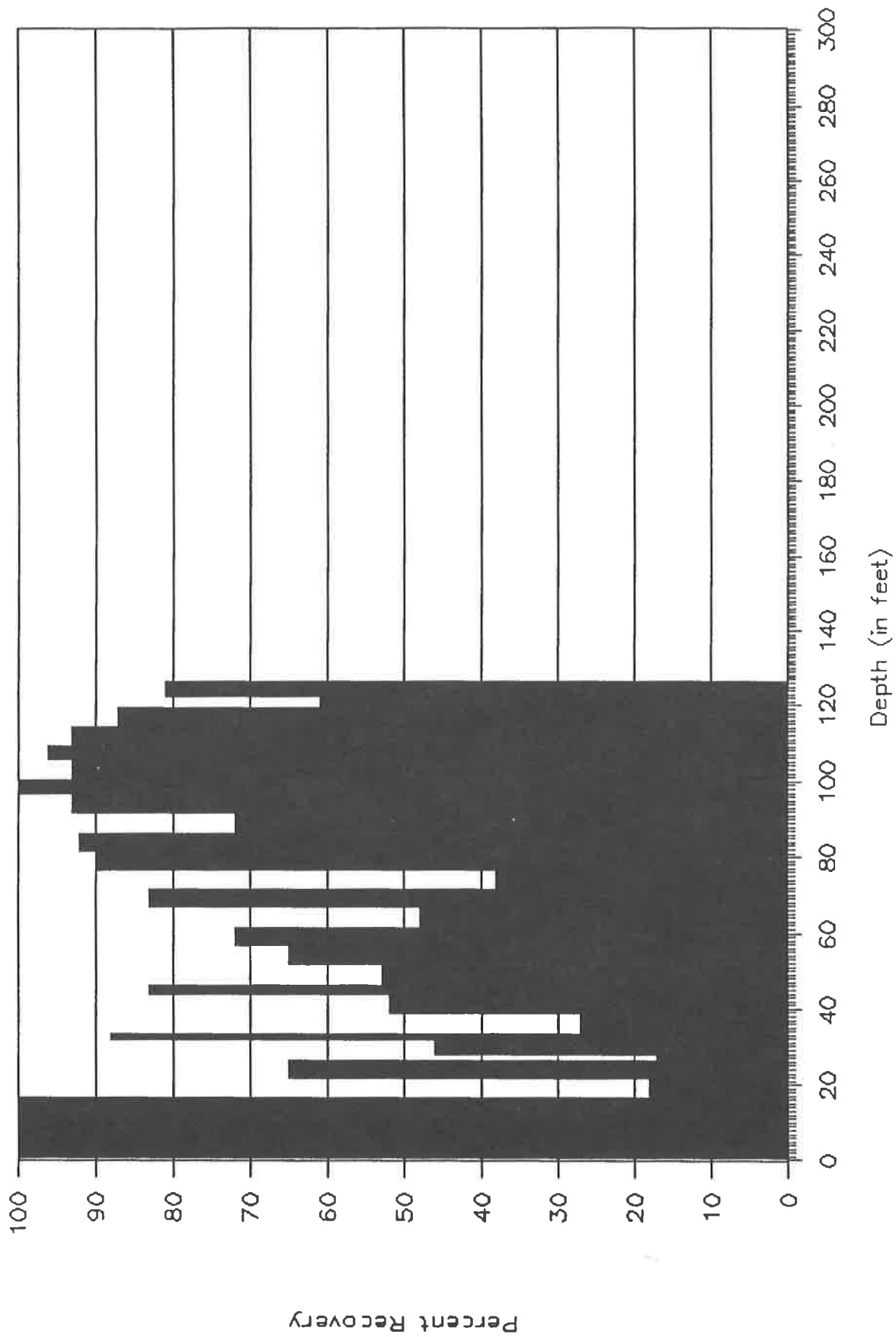


Figure 37. Recovery DDH PC88-4.

## APPENDIX IV.

### DRILL LOGS

#### Explanation for Drill Hole Logs

Depth is measured in feet because the drill core barrels and drilling depths, as indicated by core blocks, are measured in feet.

Measurements of small-scale features: grain sizes, layering, etc. are in millimeters or centimeters (mm or cm).

Estimated abundances are in percent shown either as a number in parentheses or as a number with a percent sign.

Angles of contacts, banding, etc. are measured in relation to the core axis (c.a.). To obtain the dip of the measured feature, subtract the angle to core axis from the inclination of the drill hole. In this investigation, all the drill holes are collared at  $-90^{\circ}$  and are assumed to have remained in a vertical orientation. No downhole surveys were conducted.

The logs are organized first by year, and then by number. They consist of: 1) lithologic descriptions, 2) alteration and mineralization, and 3) structure.



## APPENDIX IV. (cont.)

### Diamond Drill Hole PC 87-1

| <u>Depth</u><br>(in feet) | <u>Lithologic Description</u>  |
|---------------------------|--|
| 0.0 26.0                  | not recovered  |
| 26.0 42.5                 | pale tan and patchy gray serpentinite; 5-10 % disseminated magnetite   |
| 42.5 43.5                 | plagioclase cumulate(25) with intercumulate pyroxene(75); dark green to black  |
| 43.5 84.0                 | medium to dark green serpentinite; 5-10 % disseminated magnetite   |
| 84.0 86.0                 | hornblende + biotite(80)-feldspar + quartz(20) gneiss; grain size about 1 mm; 85 feet - banding 70 <sup>o</sup> c.a.   |
| 86.0 162.0                | medium to dark green serpentinite; 5-10 % disseminated magnetite   |
| 162.0 164.0               | coarse-grained chlorite  |
| 164.0 170.0               | medium to dark green serpentinite; 5-10% disseminated magnetite; 142-145 feet - alternating serpentinite and talc "banding" at 40 <sup>o</sup> c.a.  |
| 170.0 204.0               | hornblende(60)-biotite(10)-plagioclase(25)-quartz(5) gneiss; grain size about 1 mm; thinly banded; 178 feet - banding 75 <sup>o</sup> c.a.; 189 feet - banding 70 <sup>o</sup> c.a.  |
| 204.0 221.0               | quartz(60)-feldspar(30)-biotite(10) gneiss; local pegmatitic segregations of these minerals; 206 and 211 feet - banding 65 <sup>o</sup> c.a.   |
| 221.0                     | contact 80 <sup>o</sup> c.a.   |
| 221.0 231.0               | hornblende(30)-biotite(30)-feldspar + quartz(40) gneiss; interbanded with thin (<5 cm wide) felsic gneiss (< 20%); occasional migmatitic felsic segregations; 222 feet - banding at 80 <sup>o</sup> c.a., 226 feet banding at 65 <sup>o</sup> c.a., 229 feet - banding at 40 <sup>o</sup> c.a. |
| 231.0 239.0               | same as above but cut by numerous quartz(30)-feldspar(70) pegmatite dikes; grain size about 2 mm; local biotite and allanite(?); 294 feet - banding at 70 <sup>o</sup> c.a.; pegmatite contacts at 40, 50, 35, 50, 40 and 20 <sup>o</sup> c.a.   |
| 239.0 244.0               | hornblende(30)-biotite(30)-feldspar + quartz(40) gneiss; interbanded with thin (<5 cm wide) felsic gneiss (< 20%); occasional migmatitic felsic segregations; 242 feet - banding at 75 <sup>o</sup> c.a.   |
| 244.0                     | contact 75 <sup>o</sup> c.a.   |
| 244.0 252.0               | quartz(70)-feldspar(25)-opague(5) gneiss; marked by thin (<3 cm wide) bands of mafic gneiss; 246 feet - banding 75 <sup>o</sup> c.a.   |
| 252.0                     | contact 80 <sup>o</sup> c.a.   |
| 252.0 260.0               | hornblende(30)-biotite(30)-feldspar + quartz(40) gneiss; 257 feet - banding 75 <sup>o</sup> c.a.   |

DDH PC 87-1

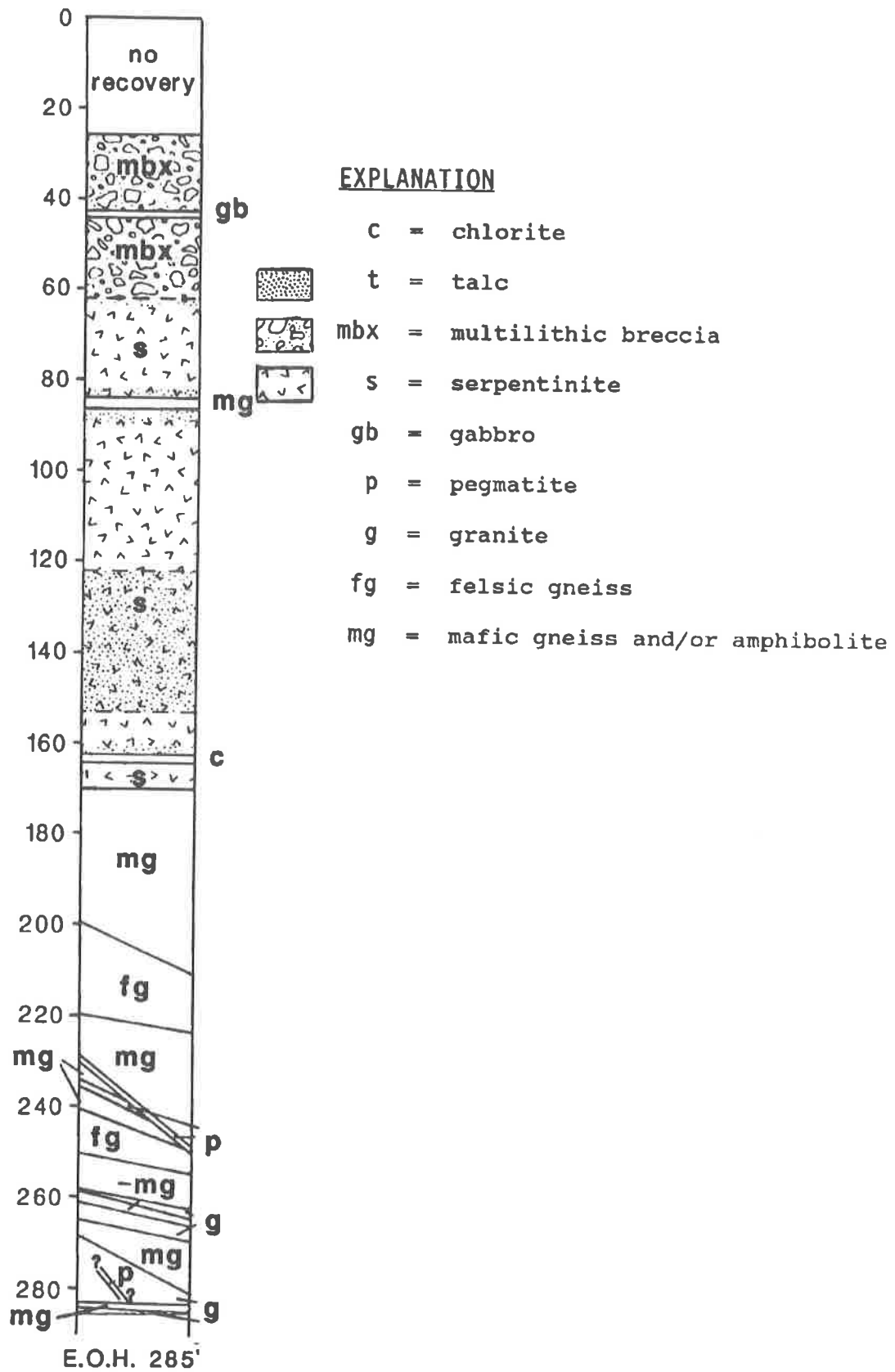


Figure 38. Graphic Log DDH PC87-1. The multilithic breccia is interpreted from the lithologies described in the lithologic log and from outcrop observations.

#### APPENDIX IV. (cont.)

| Depth | <u>Lithologic Description(cont.)</u> |  |
|-------|--------------------------------------|--|
| 260.0 |                                      | intrusive contact 75° c.a.   |
| 260.0 | 261.5                                | gneissic granite; quartz(55)-feldspar(35)-biotite(10) with feldspar phenocrysts(?)- trace pyrite and black opaque mineral; cut by 25 cm wide pegmatite dike at 60° c.a.                    |
| 261.5 | 263.0                                | biotite + hornblende(40)-quartz + feldspar(60) gneiss; 262 feet - banding 70° c.a.   |
| 263.0 |                                      | intrusive contact 80° c.a.   |
| 263.0 | 267.0                                | gneissic granite; quartz(55)-feldspar(35)-biotite(10) with feldspar phenocrysts(?)- trace pyrite and black opaque mineral; 265 feet - banding 65° c.a.                                     |
| 267.0 |                                      | irregular contact 80° c.a.   |
| 267.0 | 273.0                                | biotite + hornblende(40)-quartz + feldspar(60) gneiss; 270 feet - banding 55° c.a.   |
| 273.0 |                                      | intrusive contact 55 - 60° c.a.  |
| 273.0 | 280.0                                | gneissic granite; quartz(55)-feldspar(35)-biotite(10) with feldspar phenocrysts(?)- trace pyrite and black opaque mineral; biotite-rich inclusion at 278 feet; 276 feet - banding 65° c.a. |
| 280.0 |                                      | contact 40° c.a.   |
| 280.0 | 280.5                                | pegmatite  |
| 280.0 |                                      | irregular contact  |
| 280.5 | 283.0                                | gneissic granite; quartz(55)-feldspar(35)-biotite(10) with feldspar phenocrysts(?)- trace pyrite and black opaque mineral  |
| 283.0 |                                      | intrusive contact 5° c.a.  |
| 283.0 | 284.5                                | biotite + hornblende(40)-quartz + feldspar(60) gneiss; 284 feet - banding 65° c.a.   |
| 284.5 | 285.0                                | gneissic granite; quartz(55)-feldspar(35)-biotite(10) with feldspar phenocrysts(?)- trace pyrite and black opaque mineral; banding 50° c.a.  |

End of Hole at 285 feet

| Depth | <u>Alteration and mineralization</u> |  |
|-------|--------------------------------------|--|
| 26.0  | 62.0                                 | patchy talc disseminated in serpentinite; 10-20% |
| 62.0  |                                      | thin talc vein                                   |
| 65.0  |                                      | thin, 1 cm talc vein                             |

#### APPENDIX IV. (cont.)

| Depth | <u>Alteration and mineralization(cont.)</u> |   |
|-------|---|---|
| 70.0  | 74.0  | group of talc, chlorite and carbonate veins; 10, 25, 30, 30, 60 and 60° c.a.; 3 mm to 5 cm wide |
| 82.0  | 84.0  | massive talc  |
| 86.0  | 94.0  | group of talc veins; 10, 20, 25, 30, 30 and 75° c.a.; 3 mm to 5 cm wide                         |
| 92.0  | 121.0                                       | patchy talc disseminated in serpentinite; 10-20%  |
| 104.0 |   | talc vein; 2 cm wide; 60° c.a.  |
| 106.0 |   | talc and cross-fiber talc selvage; 2.5 cm wide; 70° c.a.  |
| 126.0 | 128.0                                       | three coarse chlorite veins and cross-fiber talc selvage; 5 cm wide; 35° c.a.                   |
| 121.0 |   | thin, talc veinlets, < 1 cm wide; 40° c.a.  |
| 121.0 | 154.0                                       | massive, light silvery gray talc  |
| 145.0 | 160.0                                       | numerous, irregular, thin, white to light gray quartz veins and carbonate veins; about 75° c.a. |
| 153.0 |   | coarse chlorite vein with 1 cm wide cross-fiber talc selvage; 10° c.a.                          |
| 158.0 | 160.0                                       | several irregular talc veinlets; 15° c.a.   |
| 160.0 |   | talc vein; 15° c.a.; 1 cm wide  |
| 162.0 |   | talc alteration adjacent to thick chlorite; 40° c.a.; 5 cm wide                                 |

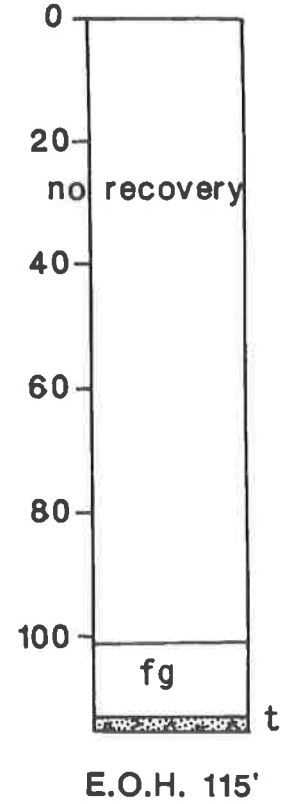
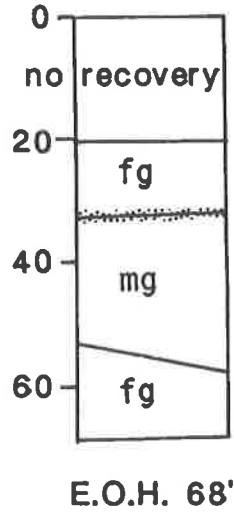
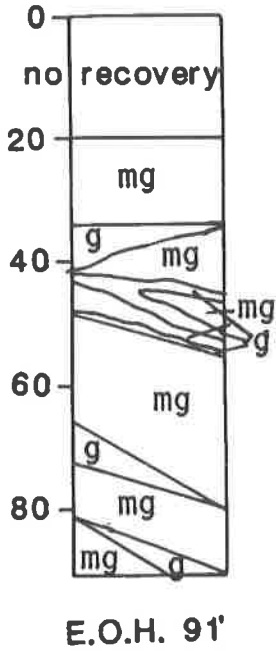
| Depth | <u>Structure</u> |   |
|-------|------------------|---|
| 42.0  | 68.0             | crushed and broken core                   |
| 66.0  |                  | weak fault; 20° c.a.                      |
| 83.0  | 85.0             | broken core                               |
| 89.0  |                  | weak shear and broken core; 70° c.a.      |
| 122.0 | 132.0            | broken core with much of interval missing |
| 142.0 | 150.0            | crushed and broken core; strong fault     |
| 152.0 |                  | strong shear and crushed core; 25° c.a.   |
| 162.0 |                  | moderate shear and slickensides; 45° c.a. |
| 170.0 | 171.0            | faulted contact; most core lost           |
| 173.0 | 175.0            | broken core                               |

## APPENDIX IV. (cont.)

### Diamond Drill Hole PC 87-2

| <u>Depth</u><br>(in feet) | <u>Lithologic Description</u>   |
|---------------------------|---|
| 0.0 20.0                  | core not recovered  |
| 20.0 34.0                 | biotite(40)-feldspar(35)-quartz(25) gneiss; grain size about 1 mm; local pegmatite segregations; moderately weathered to 34 feet; 21 feet - banding 85° c.a.                                      |
| 34.0 37.0                 | gneissic granite; quartz + feldspar(85)-biotite(15); weakly foliated; grain size about 1 mm   |
| 37.0                      | intrusive contact 35° c.a.  |
| 37.0 42.5                 | mafic gneiss; biotite + hornblende(70)-quartz + feldspar(30); irregularly banded; local quartz - feldspar-biotite pegmatitic segregations; 38 feet - banding 60° c.a.; 40 feet - banding 25° c.a. |
| 42.5                      | intrusive contact 75° c.a.  |
| 42.5 44.0                 | gneissic granite; quartz + feldspar(85)-biotite(15); weakly foliated; grain size about 1 mm   |
| 44.0                      | intrusive contact 60° c.a.  |
| 44.0 47.0                 | mafic gneiss; biotite + hornblende(60)-quartz + feldspar(40); irregularly banded; grain size (1-2 mm); 46 feet - banding 50° c.a.   |
| 47.0                      | contact 80° c.a.  |
| 47.0 48.5                 | gneissic granite; quartz + feldspar(85)-biotite(15); weakly foliated; grain size about 1 mm; cuts mafic gneiss; 48 feet - banding 70° c.a.  |
| 48.5                      | intrusive contact 50° c.a.  |
| 48.5 49.0                 | mafic gneiss; biotite + hornblende(60)-quartz + feldspar(40); irregularly banded; grain size (1-2 mm); banding 20° c.a.   |
| 49.0                      | intrusive contact 50° c.a.  |
| 49.0 50.0                 | gneissic granite; quartz + feldspar(85)-biotite(15); weakly foliated; grain size about 1 mm   |
| 50.0                      | intrusive contact 50° c.a.  |
| 50.0 51.0                 | mafic gneiss; biotite + hornblende(60)-quartz + feldspar(40); irregularly banded; grain size (1-2 mm)   |
| 51.0                      | contact 65° c.a.  |
| 51.0 51.5                 | gneissic granite; quartz + feldspar(85)-biotite(15); weakly foliated; grain size about 1 mm   |
| 51.5                      | contact 75° c.a.  |

DDH PC 87-2






- c = chlorite
-  t = talc
-  mbx = multilithic breccia
-  s = serpentinite
- gb = gabbro
- p = pegmatite
- g = granite
- fg = felsic gneiss
- mg = mafic gneiss and/or amphibolite

Figure 39. Graphic Logs DDH PC87-2, DDH PC87-3 and DDH PC87-6. The multilithic breccia is interpreted from the lithologies described in the lithologic log and from outcrop observations.

## APPENDIX IV. (cont.)

| <u>Depth</u> | <u>Lithologic Description (cont.)</u> |   |
|--------------|---------------------------------------|---|
| 51.5         | 73.0                                  | strongly folded, biotite(30)-quartz(40)-feldspar(30) gneiss; very variable in grain size from <1 to >5 mm; thin, regular banding to coarse, irregular banding; composition variable from low to high biotite; local pegmatitic segregations; 52 feet - banding 75° c.a. |
| 73.0         |                                       | contact 60° c.a.  |
| 73.0         | 76.0                                  | fine-grained (<1-2 mm), quartz(40)-feldspar(55)-biotite(5) gneiss   |
| 76.0         |                                       | contact 75° c.a.  |
| 76.0         | 86.0                                  | biotite(50)-quartz(35)-feldspar(15) mafic gneiss; regular, thin to medium banding; grain size (1-2 mm); locally more pegmatitic (2-5 mm grain size); 79 feet - banding 80° c.a.   |
| 86.0         |                                       | contact 70° c.a.  |
| 86.0         | 89.0                                  | fine-grained (<1-2 mm), quartz(40)-feldspar(55)-biotite(5) gneiss; cuts across foliation in lower unit  |
| 89.0         |                                       | contact cuts across banding 35° c.a.  |
| 89.0         | 91.0                                  | quartz(30)-feldspar(40)-biotite(25) gneiss; disseminated magnetite(5) and <1 % pyrite; grain size (2-5 mm); crudely layered; 90 feet - banding 70° c.a.   |

End of Hole at 91 feet

| <u>Depth</u> | <u>Structure</u> |   |
|--------------|------------------|---|
| 20.0         | 35.0             | moderately to strongly broken core                          |
| 42.0         |                  | weak fault, minor broken core                               |
| 45.0         |                  | weak fault, minor broken core                               |
| 59.0         | 60.0             | strong fault, crushed and broken core                       |
| 67.0         | 68.0             | moderate to strong fault, crushed and broken core           |
| 70.0         | 71.0             | moderate to strong fault, crushed and broken core; 65° c.a. |

## APPENDIX IV. (cont.)

### Diamond Drill Hole PC 87-3

| <u>Depth</u><br>(in feet) | <u>Lithologic Description</u>   |
|---------------------------|---|
| 0.0    20.0               | no recovery   |
| 20.0    32.0              | felsic gneiss(?); feldspar(50)-biotite + hornblende(25) - quartz(25); rock strongly weathered to about 44 feet; 15 cm wide pegmatite above 32 feet                    |
| 32.0    32.5              | 10-15 cm wide talc altered serpentinite; 5-10 % disseminated magnetite  |
| 32.5    51.0              | mafic gneiss; biotite + hornblende(70)-quartz + feldspar(30); thinly banded; moderately to strongly weathered; 48 feet - banding 65 <sup>o</sup> c.a.                 |
| 51.0    58.0              | no recovery; contact missing  |
| 58.0    68.0              | felsic gneiss; quartz + feldspar(90-95%)-biotite(5-10%); partially weathered near top; 59 feet - banding 85 <sup>o</sup> c.a., 61 feet - banding 80 <sup>o</sup> c.a. |

End of Hole at 68 feet

| <u>Depth</u> | <u>Structure</u>                      |
|--------------|---------------------------------------|
| 22.0    26.0 | broken and crushed core               |
| 32.0    43.0 | strong fault, broken and crushed core |



## APPENDIX IV. (cont.)

### Diamond Drill Hole PC 87-4

| Depth<br>(in feet) | Lithologic Description  |
|--------------------|---|
| 0.0 29.0           | sheared, broken and partially oxidized mixture of coarse-grained chlorite, talc altered serpentinite with disseminated magnetite, and fibrous talc                                    |
| 29.0 30.5          | coarse-grained quartz(70)-feldspar(10) pegmatite; feldspar bleached white in sheared upper 15 cm  |
| 30.5 48.5          | coarse-grained chlorite, sheared and/or crushed; locally oxidized/weathered serpentinite plus massive and fibrous talc  |
| 48.5 51.5          | coarse-grained quartz(70)-feldspar(10) pegmatite  |
| 51.5 59.0          | coarse-grained chlorite, sheared and/or crushed; locally oxidized/weathered serpentinite plus massive and fibrous talc  |
| 59.0 62.0          | dark green serpentinite   |
| 62.0 62.5          | black, fine-grained, magnetite-rich diorite/gabbro(?)   |
| 62.5 152.0         | medium to dark green serpentinite with 5-10% disseminated magnetite; coarse-grained chlorite at upper contact; color lighter above 120 feet; 142-152 feet appearance of chill zone(?) |
| 152.0              | contact 30 <sup>o</sup> c.a.  |
| 152.0 160.0        | weakly foliated granite; quartz(30)-feldspar(55)-biotite(15)  |
| 160.0 161.5        | coarse-grained chlorite   |
| 161.5 163.0        | weakly foliated granite; quartz(30)-feldspar(55)-biotite(15)  |
| 163.0 168.0        | serpentinite partially altered to talc  |
| 168.0 172.0        | coarse-grained chlorite   |
| 172.0 174.0        | serpentinite partially altered to talc  |
| 174.0              | contact 30 <sup>o</sup> c.a.  |
| 174.0 180.0        | quartz(35)-feldspar(35)-biotite(30) gneiss; coarse-grained (2-10 mm); strongly brecciated   |
| 180.0 180.5        | serpentinite partially altered to talc  |
| 180.5 182.0        | quartz(35)-feldspar(35)-biotite(30) gneiss; coarse-grained (2-10 mm); strongly brecciated   |
| 182.0 220.0        | dark green to brown serpentinite  |
| 220.0 225.0        | quartz(60)-feldspar(30)-biotite(10) gneiss; grain size (1-3 mm); moderately banded with local pegmatitic segregations; 222 feet - banding 70 <sup>o</sup> c.a.                        |

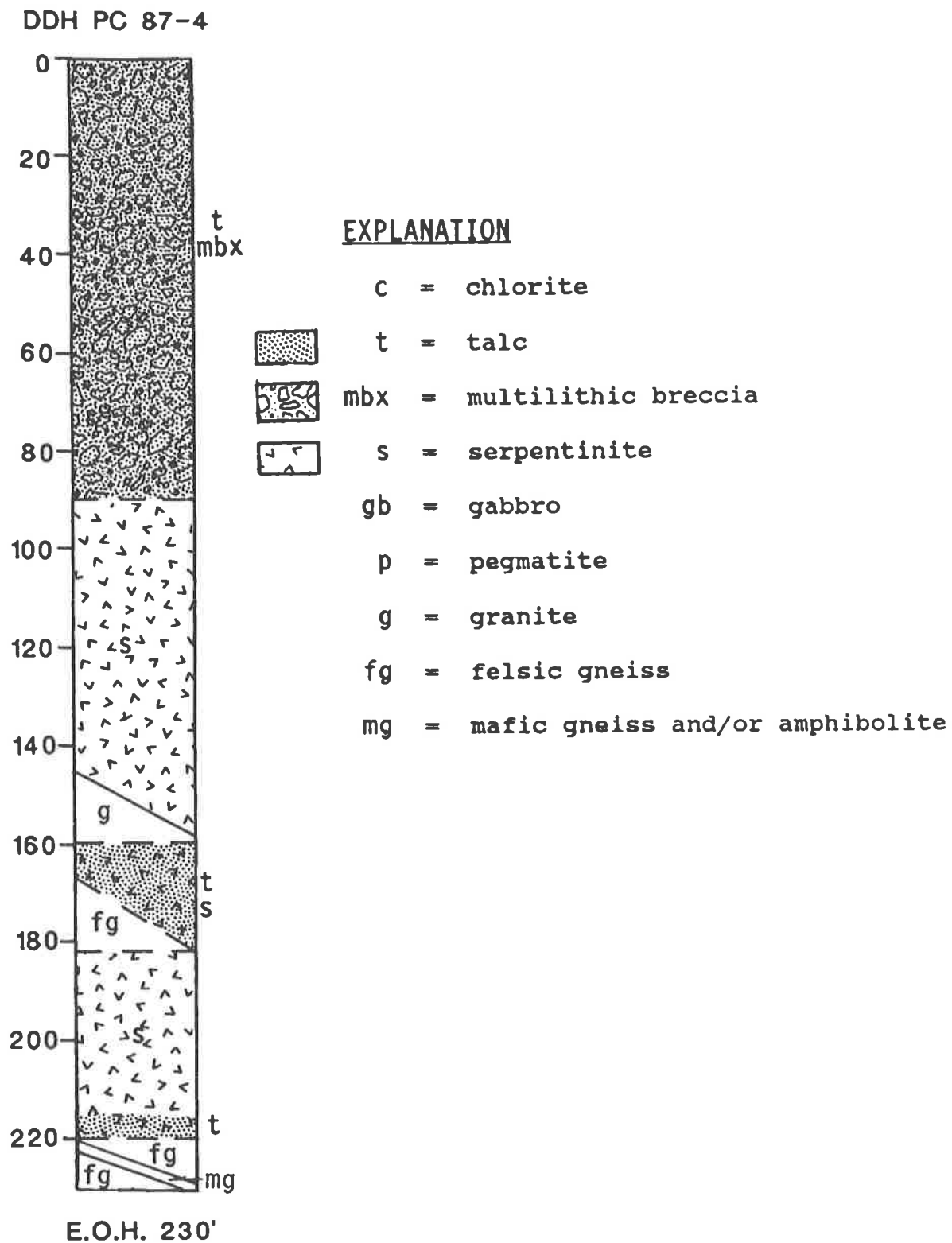


Figure 40. Graphic Log DDH PC87-4. The multilithic breccia is interpreted from the lithologies described in the lithologic log and from outcrop observations.

## APPENDIX IV. (cont.)

| Depth       | Lithologic Description (cont.)   |
|-------------|--|
| 225.0       | contact 70 <sup>o</sup> c.a.   |
| 225.0 227.0 | biotite + hornblende(?) (30)-quartz(30)-feldspar(10) gneiss                        |
| 227.0       | contact 60 <sup>o</sup> c.a.   |
| 227.0 230.0 | quartz(50)-feldspar(30)-biotite(20) gneiss; grain size (1-3 mm); moderately banded |

End of Hole at 230 feet

| Depth       | Alteration and Mineralization  |
|-------------|--|
| 22.0 52.0   | eight intervals of 7.5 to 26 cm wide massive talc +/- fibrous talc; core recovery poor and core is generally broken; one piece has fracture with coarse-grained chlorite with a talc alteration envelope; 70 <sup>o</sup> c.a. |
| 66.0 67.0   | massive talc adjacent to 2.5 cm wide chlorite fracture; 40 <sup>o</sup> c.a.   |
| 70.0 74.0   | four fractures containing chlorite 2.5-10 cm wide; 40, 45, 50, 70 <sup>o</sup> c.a.; fibrous talc and massive talc adjacent to fractures   |
| 75.0 140.0  | patchy disseminated talc   |
| 78.0 82.0   | four fractures containing chlorite 2.5-10 cm wide; 85 <sup>o</sup> c.a.; fibrous talc adjacent to two lower fractures, and massive talc adjacent to fractures  |
| 85.0 85.5   | massive talc   |
| 88.0 91.0   | several thin, 1 cm wide, chlorite fractures with thin, 2 mm wide, talc envelopes; 10-20 <sup>o</sup> c.a.  |
| 96.0 96.5   | massive talc   |
| 102.0       | massive talc, 5 cm wide (core broken and missing)  |
| 107.0       | coarse-grained chlorite, 2 cm wide, with 4 cm wide talc alteration envelope; 45 <sup>o</sup> c.a.  |
| 115.0       | talc, 15 cm wide, 45 <sup>o</sup> c.a.; cut by carbonate veinlets, 40-70 <sup>o</sup> c.a.   |
| 116.0       | quartz + carbonate vein, 1 cm wide; 35 <sup>o</sup> c.a.   |
| 116.5       | two quartz veins with carbonate, 1 cm wide; 10-20 <sup>o</sup> c.a.  |
| 124.0       | magnetite veinlet, 1-2 mm wide; 35 <sup>o</sup> c.a.   |
| 130.0       | thin chlorite fracture with 2.5 cm wide talc alteration envelope; 40 <sup>o</sup> c.a.   |
| 132.0 142.0 | numerous quartz and quartz + carbonate veinlets, 1-3 mm wide; 70-80 <sup>o</sup> c.a.  |

## APPENDIX IV. (cont.)

| Depth | Alteration and Mineralization (cont.)   |  |
|-------|---|--|
| 135.0 | carbonate vein, 1 cm wide; 60 <sup>o</sup> c.a.   |  |
| 137.0 | talc, 1-2 cm wide; 20 <sup>o</sup> c.a.   |  |
| 138.0 | chlorite fracture; 5-7.5 cm wide  |  |
| 139.0 | talc, 5-7.5 cm wide; 45 <sup>o</sup> c.a.   |  |
| 141.0 | chlorite fracture, 1 cm wide, with 2 cm wide talc alteration envelope; 30 <sup>o</sup> c.a. |  |
| 153.0 | 153.5   | coarse-grained chlorite at contact   |
| 153.5 | 160.0   | generally bleached with kaolinite? on fractures and chloritic alteration of biotite and feldspar?          |
| 160.0 | 161.5   | coarse-grained chlorite and broken talc  |
| 163.0 | 164.0   | irregular talc alteration  |
| 166.0 |   | chlorite fracture, 1 cm wide, with 2-3 cm wide talc alteration envelope; 10 <sup>o</sup> c.a.              |
| 168.0 | 172.0   | coarse-grained chlorite  |
| 173.0 | 175.0   | massive talc with 2 cm wide fibrous talc at contact  |
| 175.0 | 180.0   | biotite chloritized  |
| 182.0 | 220.0   | patchy disseminated talc, increasing from 10 to 30 % near base   |
| 182.0 |   | quartz vein, crustiform, 3 mm wide; 35 <sup>o</sup> c.a.   |
| 186.0 |   | quartz vein, crustiform, 2 mm wide; 50 <sup>o</sup> c.a.; 1 cm wide carbonate envelope                     |
| 188.0 |   | coarse-grained chlorite fracture, 1 mm wide, with 1 cm wide talc alteration envelope; 65 <sup>o</sup> c.a. |
| 189.0 |   | quartz vein, 3 mm wide; 40 <sup>o</sup> c.a.   |
| 190.0 |   | quartz vein, 1 mm wide; 20 <sup>o</sup> c.a.   |
| 192.0 |   | quartz-carbonate vein, 1 cm wide, with 2 cm wide carbonate envelope; 70 <sup>o</sup> c.a.                  |
| 197.0 |   | carbonate veinlet, 3 mm wide; 10 <sup>o</sup> c.a.   |
| 198.0 |   | massive talc, 10 cm wide; 90 <sup>o</sup> c.a.   |
| 200.0 | 204.0   | zone of quartz veining and weak talc alteration  |
| 210.0 |   | coarse-grained chlorite fracture, 1 cm wide, with 2 cm wide talc alteration envelope; 45 <sup>o</sup> c.a. |

## APPENDIX IV. (cont.)

| Depth          | <u>Alteration and Mineralization (cont.)</u>   |
|----------------|--|
| 212.0          | coarse-grained chlorite fracture, 2.5 cm wide, with 7.5 cm wide talc alteration envelope; 45° c.a. |
| 216.0          | coarse-grained chlorite fracture, 1 cm wide, with 2.5 cm wide talc alteration envelope; 45° c.a.   |
| 220.0    220.5 | massive talc above contact; actual contact missing - chlorite?                                     |

| Depth          | <u>Structure</u>                                     |
|----------------|--|
| 0.0    47.0    | crushed, broken and sheared core;                    |
| 50.0    67.0   | crushed and broken core                              |
| 71.0    72.0   | crushed and broken core                              |
| 73.0    74.0   | crushed and broken core                              |
| 80.0    86.0   | crushed and broken core                              |
| 102.0    103.0 | broken core  |
| 107.0    108.0 | broken core  |
| 113.0    127.0 | appears sheared, but healed prior to talc alteration |
| 117.0    118.0 | broken core  |
| 122.0    124.0 | broken core  |
| 138.0    139.0 | broken and crushed core                              |
| 142.0    149.0 | broken and crushed core                              |
| 151.0    152.0 | broken and crushed core                              |
| 153.0    154.0 | broken and crushed core                              |
| 156.0    165.0 | broken and crushed core                              |
| 168.0    172.0 | broken and crushed core                              |
| 174.0    176.0 | broken and crushed core                              |
| 176.0    180.0 | sheared and fractured gneiss                         |
| 200.0    201.0 | broken and crushed core                              |
| 203.0          | broken and crushed core                              |
| 218.0    220.0 | broken and crushed core                              |
| 222.0          | weak fault   |

## APPENDIX IV. (cont.)

### Diamond Drill Hole PC 87-5

| Depth<br>(in feet) | Lithologic Description  |
|--------------------|---|
| 0.0 20.0           | core not recovered  |
| 20.0 38.0          | oxidized/weathered coarse-grained chlorite  |
| 38.0 43.0          | serpentinite and talc   |
| 43.0 62.0          | no recovery   |
| 62.0 80.0          | biotite-quartz-feldspar gneiss; locally plagioclase and quartz segregations; strongly bleached in upper 5 feet  |
| 80.0 106.0         | serpentinite  |
| 106.0 115.0        | weakly foliated gneissic granite; quartz(50)-feldspar(40)-biotite(10)   |
| 115.0 121.0        | coarse-grained pegmatitic granite; quartz(50)-plagioclase(40)-biotite(10)   |
| 121.0 126.0        | silicified talc   |
| 126.0 128.0        | biotite-rich gneiss; brecciated   |
| 128.0 131.0        | silicified talc   |
| 131.0 137.0        | coarse-grained pegmatitic granite; quartz(50)-plagioclase(40)-biotite(10)   |
| 137.0 165.0        | medium to dark green serpentinite; 5% disseminated magnetite  |
| 165.0 173.0        | talc  |
| 173.0 219.5        | rusty brown serpentinite becoming dark green with depth   |
| 219.5 220.5        | granitic gneiss; strongly bleached  |
| 220.5 258.0        | dark green serpentinite   |
| 258.0 260.0        | coarse-grained (2-10 mm); biotite(5-25)-quartz + feldspar(75-95) gneiss; biotite locally more abundant; foliation banding generally not well developed but quite variable |
| 260.0              | contact 30° c.a.  |
| 260.0 262.0        | dark green serpentinite   |
| 262.0              | contact 50° c.a.  |
| 262.0 274.0        | coarse-grained (2-10 mm); biotite(5-25)-quartz + feldspar(75-95) gneiss; biotite locally more abundant; foliation banding generally not well developed but quite variable |

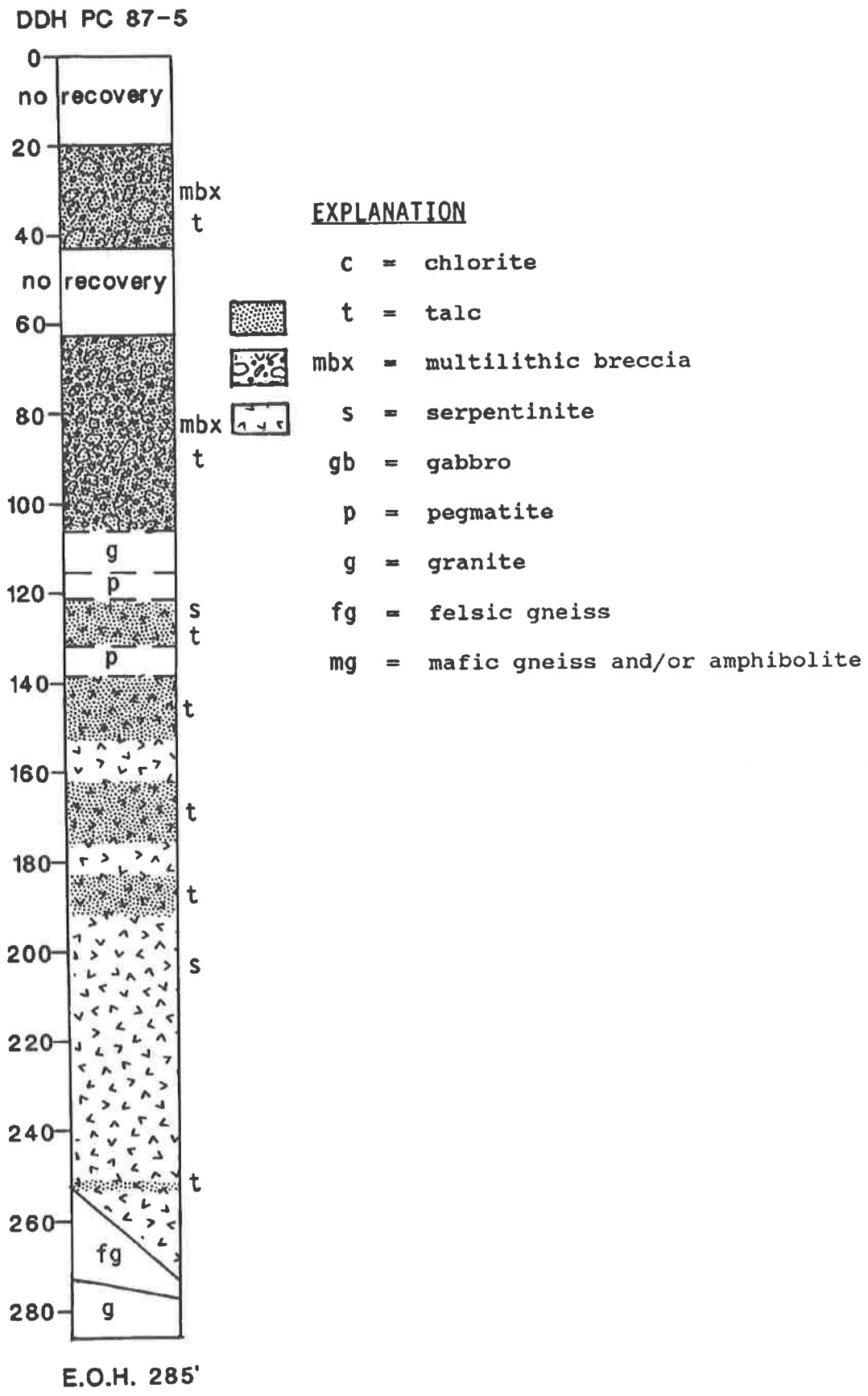


Figure 41. Graphic Log DDH PC87-5. The multilithic breccia is interpreted from the lithologies described in the lithologic log and from outcrop observations.

#### APPENDIX IV. (cont.)

| Depth       | Lithologic Description (cont.)  |
|-------------|---|
| 274.0       | irregular contact 80° c.a.  |
| 274.0 285.0 | fine-grained (1-2 mm) gneissic granite; quartz + feldspar(75) + biotite(25); weakly foliated; inclusion of coarse-grained biotite(30) + quartz + feldspar(70) gneiss; 281 feet - banding 80° c.a. |

End of Hole at 285 feet

| Depth       | Alteration and Mineralization   |
|-------------|---|
| 28.0 38.0   | masses of massive talc up to 2 feet thick   |
| 40.0 42.0   | thin talc veins; 10 - 30° c.a.  |
| 62.0 68.0   | strongly bleached   |
| 80.0 87.0   | gneiss and granite clasts bleached +/- argillized(?); serpentinite altered to talc with coarse-grained chlorite in fractures and breccia matrix |
| 88.0 93.0   | massive talc envelope adjacent to 1 foot wide coarse-grained chlorite fracture  |
| 93.0 96.0   | silicified  |
| 121.0 126.0 | silicified  |
| 128.0 131.0 | silicified  |
| 137.0 139.0 | quartz replacing talc along 5 mm - 3 cm wide veinlets; 60, 70 and 80° c.a.  |
| 140.0 149.0 | principally talc with some serpentinite and secondary quartz  |
| 151.0 153.0 | numerous veinlets of chlorite with talc envelopes; 30 - 60° c.a.; massive talc toward base;   |
| 153.0 162.0 | patchy, disseminated talc alteration  |
| 159.0 160.0 | irregular massive talc  |
| 161.0       | talc veinlets, 5 mm wide; 60° c.a.  |
| 162.0 164.0 | massive talc  |
| 164.0 165.0 | coarse-grained chlorite   |
| 165.0 174.0 | massive talc  |
| 174.0 175.0 | talc veinlets   |



#### APPENDIX IV. (cont.)

| Depth | <u>Alteration and Mineralization (cont.)</u> |  |
|-------|--|--|
| 175.0 | 180.0  | coarse-grained chlorite  |
| 180.0 |  | talc alteration; 2 cm wide   |
| 182.0 | 185.0  | numerous talc veinlets cut by carbonate veinlets   |
| 186.0 | 187.0  | coarse-grained chlorite  |
| 187.0 | 188.0  | quartz   |
| 188.0 | 192.0  | talc + chlorite + quartz; generally massive; alteration contact averages 30 <sup>o</sup> c.a.                    |
| 192.0 |  | 5 cm wide chlorite vein; 60 <sup>o</sup> c.a.  |
| 195.0 | 197.0  | disseminated patchy carbonate  |
| 195.0 |  | 1 cm wide carbonate vein; 35 <sup>o</sup> c.a.   |
| 197.0 | 255.0  | disseminated, patchy talc; 10-20 %   |
| 205.0 | 211.0  | 2 mm to 2 cm wide creamy carbonate veinlets; 35, 30, 30, 75, 30 <sup>o</sup> c.a.                                |
| 218.0 | 221.0  | irregular, thin, creamy carbonate veinlets; weak talc alteration adjacent to veinlets; 10 - 20 <sup>o</sup> c.a. |
| 222.0 |  | 1 cm wide chlorite fracture with 13 cm wide talc envelop; 50 <sup>o</sup> c.a.                                   |
| 222.0 | 223.0  | thin, creamy, carbonate veinlets; 60 <sup>o</sup> c.a.   |
| 227.0 | 228.0  | thin, creamy, carbonate veinlets   |
| 230.0 |  | 1-2 mm wide quartz vein; 80 <sup>o</sup> c.a.  |
| 232.0 |  | thin, creamy carbonate veinlet; 70 <sup>o</sup> c.a.   |
| 239.0 |  | 2-3 mm wide, carbonate veinlet; 20 <sup>o</sup> c.a.   |
| 232.0 |  | 5 cm wide chlorite fracture; 70 <sup>o</sup> c.a.  |
| 232.0 | 248.0  | 2-10 mm wide, creamy carbonate veinlet; 5, 40, 80, 30, 40 <sup>o</sup> c.a.                                      |
| 252.0 | 260.0  | numerous white and cream carbonate veinlets; irregular and thin <5 mm wide; about 40 <sup>o</sup> c.a.           |
| 261.0 | 262.0  | coarse-grained chlorite fracture; 50 <sup>o</sup> c.a.   |

APPENDIX IV. (cont.)

| <u>Depth</u> | <u>Structure</u>                  |
|--------------|-----------------------------------|
| 38.0         | crushed core                      |
| 89.0 94.0    | crushed and broken core           |
| 97.0 110.0   | crushed and broken core           |
| 111.0 112.0  | crushed core                      |
| 116.0 137.0  | well broken core                  |
| 142.0 145.0  | broken core                       |
| 152.0 153.0  | broken and partially crushed core |
| 164.0 170.0  | sheared and partially broken core |
| 175.0 180.0  | sheared and partially broken core |
| 185.0 188.0  | sheared and partially broken core |
| 220.0        | broken core                       |
| 251.0 252.0  | moderate sheared zone             |
| 257.0 258.0  | well broken core                  |
| 260.0 262.0  | sheared and broken core           |
| 268.0 272.0  | mainly broken core                |

**APPENDIX IV. (cont.)**

**Diamond Drill Hole PC 87-6**

| <u>Depth</u><br>(in feet) |       | <u>Lithologic Description</u>  |
|---------------------------|-------|--|
| 0.0                       | 20.0  | core not recovered   |
| 20.0                      | 101.0 | represented in cuttings saved in 2x4" cloth bags; 20 foot intervals per bag; very poor condition; material looks like overburden but could be fault gouge or Coastal Plain sediments |
| 101.0                     | 113.0 | quartz(45)-feldspar(40)-biotite(15) gneiss; appears intensely crushed and weathered  |
| 113.0                     | 115.0 | massive talc   |

End of Hole at 115 feet

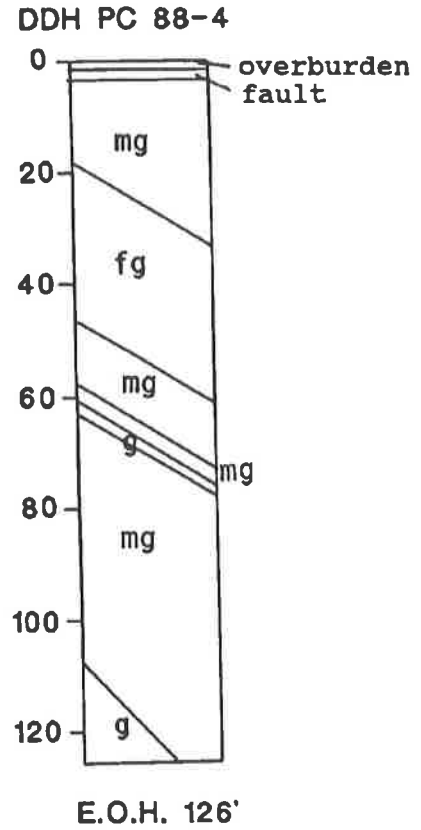
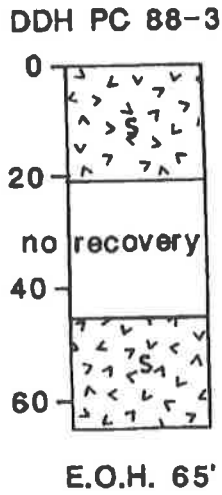
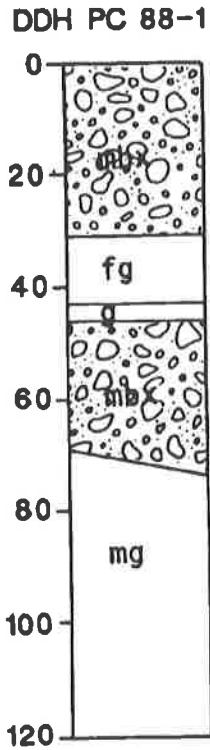
| <u>Depth</u> |       | <u>Alteration and Mineralization</u> |
|--------------|-------|--------------------------------------|
| 113.0        | 115.0 | massive talc                         |

| <u>Depth</u> |       | <u>Structure</u>                 |
|--------------|-------|----------------------------------|
| 101.0        | 115.0 | strongly sheared and broken core |

## APPENDIX IV. (cont.)

### Diamond Drill Hole PC 88-1

| Depth<br>(in feet) | Lithologic Description   |
|--------------------|--|
| 0.0    4.0         | weathered chlorite   |
| 4.0    19.0        | dominantly chlorite with minor talc, < 5% disseminated magnetite in talc   |
| 19.0   21.0        | schist, biotite + feldspar altered to kaolinite  |
| 21.0   26.0        | talc   |
| 26.0   31.0        | mixture of talc, biotite-quartz-feldspar gneiss, chlorite; poor recovery in this interval - probably mainly chlorite |
| 31.0   43.0        | biotite(50)-feldspar(50)-quartz(30) granite; fine-grained (< /= 1 mm); feldspar altered to clay                      |
| 43.0   44.0        | similar to above interval but has weak foliation, also   |
| 44.0   46.0        | coarse-grained (1-3 mm) biotite(20)-feldspar(50)-quartz(30) gneiss   |
| 46.0   50.0        | chloritized biotite  |
| 50.0   51.0        | clast of fibrous talc  |
| 51.0   51.5        | coarse-grained, biotite(30)-feldspar(40)-quartz(30) gneiss clast   |
| 51.5   52.0        | clast of fibrous talc  |
| 52.0   52.5        | fine-grained, biotite(20)-feldspar(50)-quartz(30) gneiss clast   |
| 52.5   55.5        | talc clast with fibrous talc rim   |
| 56.0   56.5        | coarse-grained, biotite(30)-feldspar(40)-quartz(30) gneiss clast   |
| 56.5   58.0        | fine-grained, biotite(20)-feldspar(50)-quartz(30) gneiss clast + quartz-feldspar pegmatite                           |
| 58.0   59.0        | coarse-grained chlorite  |
| 59.0   61.0        | two talc clasts + quartz-feldspar pegmatite clast  |
| 61.0   62.5        | coarse-grained chlorite  |
| 62.5   63.0        | talc clast with fibrous talc rim   |
| 63.0   71.0        | diorite(?); pyroxene(30)-feldspar(70); grain size 1-4 mm   |
| 71.0   72.0        | 15-30 cm wide talc with approximately 0.6 cm chlorite at contact   |
| 72.0   75.0        | biotite schist (?) altered to chlorite   |



### EXPLANATION

- c = chlorite
- t = talc
- mbx = multilithic breccia
- s = serpentinite
- gb = gabbro
- p = pegmatite
- g = granite
- fg = felsic gneiss
- mg = mafic gneiss and/or amphibolite

Figure 42. Graphic Logs DDH PC88-1, DDH PC88-3 and DDH PC88-4. The multilithic breccia is interpreted from the lithologies described in the lithologic log and from outcrop observations.

## APPENDIX IV. (cont.)

| <u>Depth</u> | <u>Lithologic Description (cont.)</u>  |
|--------------|--|
| 75.0 94.0    | mafic gneiss; biotite(25)-hornblende(40)-feldspar + quartz(35); medium grained (1-4 mm) - occasionally coarser grained (to 6 mm); strong foliation banding (1-3 mm wide); magnetite concentrated in layers   |
| 94.0 95.0    | biotite-rich schist  |
| 95.0 120.0   | mafic gneiss; biotite(25)-hornblende(40)-feldspar + quartz(35); medium grained (1-4 mm) - occasionally coarser grained (to 6 mm); strong foliation banding (1-3 mm wide); magnetite concentrated in layers; at 108 feet approximately 1% magnetite; appears to be more strongly banded below 111 feet; quartz-feldspar bands become thicker and more common below 115 feet |

End of Hole at 120 feet

| <u>Depth</u> | <u>Alteration and Mineralization</u>  |
|--------------|---|
| 0.0 4.0      | coarse-grained chlorite   |
| 4.0 19.0     | dominantly coarse-grained chlorite with minor massive talc +/- fibrous talc |
| 19.0 21.0    | feldspar altered to kaolinite   |
| 21.0 26.0    | dominantly talc   |
| 26.0 31.0    | talc and coarse-grained chlorite  |
| 31.0 43.0    | feldspar altered to kaolinite   |
| 46.0 50.0    | biotite altered to chlorite   |
| 51.5 52.0    | fibrous talc  |
| 55.5 56.0    | massive talc with fibrous talc rim  |
| 58.0 59.0    | coarse-grained chlorite   |
| 59.0 61.0    | talc  |
| 61.0 62.5    | coarse-grained chlorite   |
| 62.5 63.0    | talc with fibrous talc rim  |
| 71.0 72.0    | talc with minor coarse-grained chlorite                                     |
| 72.0 75.0    | biotite altered to chlorite   |

#### APPENDIX IV. (cont.)

| <u>Depth</u> |       | <u>Structure</u>                      |
|--------------|-------|---------------------------------------|
| 0.0          | 31.0  | broken and sheared core               |
| 42.0         | 44.0  | broken core                           |
| 50.0         | 52.0  | broken core                           |
| 56.0         |       | broken core                           |
| 65.0         | 66.0  | broken core; strong fault             |
| 89.0         | 91.0  | broken core; weak shear, 20° c.a.     |
| 104.0        | 110.0 | broken core; moderate to strong fault |

APPENDIX IV. (cont.)

Diamond Drill Hole PC 88-2

| <u>Depth</u><br>(in feet) |       | <u>Lithologic Description</u>   |
|---------------------------|-------|---|
| 0.0                       | 2.0   | overburden  |
| 2.0                       | 13.0  | weathered gneiss; predominantly felsic; abundant quartz + weathered biotite   |
| 13.0                      | 14.0  | fine-grained(about 1 mm) equigranular granite; quartz(50)-feldspar(40)-biotite(10)  |
| 14.0                      | 15.0  | fine to coarse-grained migmatitic gneiss; biotite(30)-quartz(40)-feldspar(30); banding 80° c.a.   |
| 15.0                      | 20.0  | fine to medium-grained (<1-2 mm), very weakly foliated gneissic granite; quartz(60)-feldspar(30)-biotite(10)  |
| 20.0                      | 27.0  | mafic gneiss; thinly banded (1-3 mm); biotite + hornblende(70)-quartz(20)-feldspar(10); 24 feet- banding 75° c.a.   |
| 27.0                      | 34.0  | biotite(25)-feldspar(25)-quartz(50) migmatitic gneiss; irregularly banded; thin to medium (1-4 mm); grain size (<1-2 mm); cut by coarse-grained feldspar dikes (1-4 cm wide); 31 feet banding 70° c.a.  |
| 34.0                      | 51.0  | biotite(35)-feldspar(25)-quartz(50) gneiss; thinly banded; often biotite-rich; fine- to medium grained (<1-2 mm); 40 feet - banding 70° c.a.  |
| 51.0                      | 54.0  | medium-grained, biotite(20)-feldspar(30)-quartz(50) gneiss; weakly foliated   |
| 54.0                      | 57.0  | biotite(20)-feldspar(30)-quartz(50) gneiss; irregular banding; fine-grained; 55 feet - banding 75° c.a.   |
| 57.0                      | 60.0  | biotite(20)-hornblende(10)-feldspar(10)-quartz(10); irregular banding; fine- to medium-grained  |
| 60.0                      | 60.0  | 2.5-3 cm wide layer of epidote(30)-plagioclase(70); contacts at 75° c.a.  |
| 60.0                      | 96.0  | fine- to medium-grained, biotite(30)-hornblende(20)-feldspar(10)-quartz(40) gneiss; irregularly banded; locally more quartz-feldspar rich, coarser grained and banded; grain size (<1-2 mm) locally to 5 mm; 68 feet - banding 80° c.a.; 76 feet - banding 80° c.a.; 84 feet - banding 80° c.a.; 94 feet - banding 60° c.a. |
| 96.0                      | 104.0 | hornblendite gneiss; hornblende(60)-biotite(10)-quartz(20)-feldspar(10); generally fine-grained (approximately 1 mm) and massive; occasionally banding present; 103 feet - banding 80° c.a.   |
| 104.0                     |       | contact 80° c.a.  |
| 104.0                     | 109.0 | talc(80)-chlorite(10)-magnetite(5)-serpentine(5); generally massive talc with fibrous talc; 2-3 cm wide crushed chlorite at upper contact   |



DDH PC 88-2

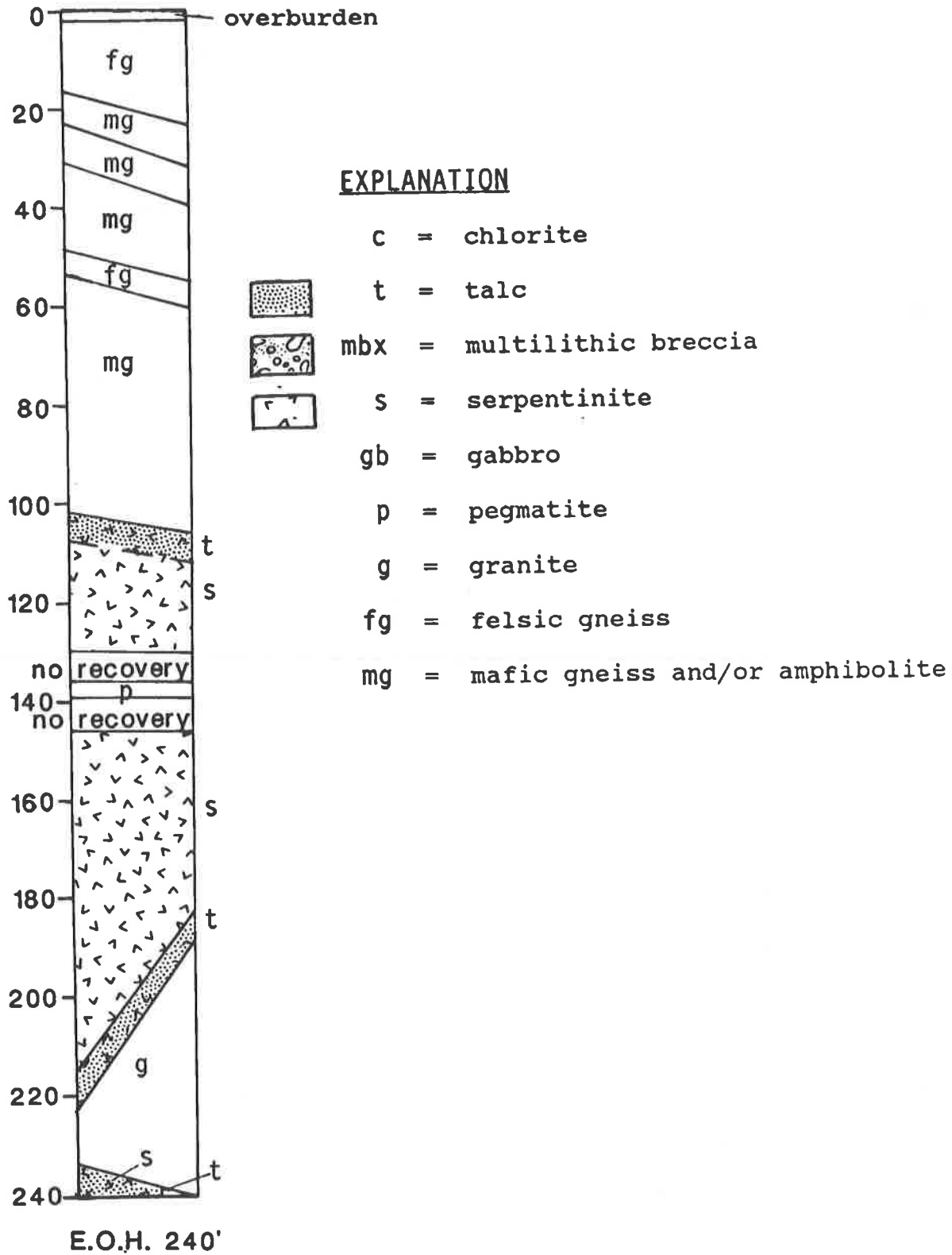


Figure 43. Graphic Log DDH PC88-2. The multilithic breccia is interpreted from the lithologies described in the lithologic log and from outcrop observations.

**APPENDIX IV. (cont.)**

| <u>Depth</u>            | <u>Lithologic Description (cont.)</u>  |
|-------------------------|--|
| 109.0 130.0             | fine-grained, dark green to black, serpentinite with 5-10% disseminated magnetite; 1 cm wide black serpentinite at 119 feet - 35 <sup>o</sup> c.a.; layered magnetite at 128-129 feet - 80 <sup>o</sup> c.a. |
| 130.0 136.0             | gap  |
| 136.0 139.0             | pegmatitic quartz + feldspar   |
| 139.0 146.0             | gap  |
| 146.0 196.0             | black to dark green serpentinite; 5-10% disseminated magnetite; 159 feet - 20% disseminated magnetite  |
| 196.0                   | contact 80 <sup>o</sup> c.a.   |
| 196.0 197.0             | pegmatitic quartz(45)-biotite(25)-feldspar(30)   |
| 197.0 199.0             | gap  |
| 199.0 205.0             | impure talc (approximately 70%); clast of crushed biotite +/- chlorite at upper contact  |
| 205.0                   | contact 10 <sup>o</sup> c.a.   |
| 205.0 236.0             | massive granite with 5-10% disseminated biotite; appears quartz-rich; fine-medium grained (1-3 mm); may be very weakly foliated; 7 cm coarse chlorite/biotite at upper contact                               |
| 236.0 236.5             | 15 cm wide clay/chlorite gouge   |
| 236.5 240.0             | talc; 238 feet - foliation 40 <sup>o</sup> c.a.  |
| End of Hole at 240 feet |  |

| <u>Depth</u> | <u>Alteration and Mineralization</u>   |
|--------------|--|
| 104.0 110.0  | talc massive and minor fibrous talc and chlorite   |
| 107.0        | chlorite, 7.5 cm   |
| 108.0        | silicified talc, 10 cm   |
| 112.0 113.0  | coarse-grained chlorite fracture with massive talc and fibrous talc; 60 <sup>o</sup> c.a.                            |
| 113.0        | carbonate vein, 3-4 mm wide, cutting talc; 50 <sup>o</sup> c.a.  |
| 115.0        | quartz and dolomite vein, 5-10 mm wide; 30 <sup>o</sup> c.a.   |
| 116.0        | quartz vein, 3-5 mm wide; 60 <sup>o</sup> c.a.   |
| 118.0 119.0  | zone of irregular quartz veinlets; light gray to white, crystalline to opaline; 1-3 mm wide; 40-80 <sup>o</sup> c.a. |

#### APPENDIX IV. (cont.)

| Depth       | <u>Alteration and Mineralization (cont.)</u>  |
|-------------|---|
| 121.0       | chlorite fracture with minor talc and fibrous talc; 65° c.a.  |
| 126.0       | quartz vein cuts bleached contact; 35° c.a.   |
| 126.0 130.0 | bleached light green to greenish gray   |
| 146.0 155.0 | patchy disseminated talc, 10-20%  |
| 152.0       | orange carbonate vein, 3 mm wide, 30° c.a.  |
| 155.0 161.0 | bleached and partially altered to talc(50) + carbonate(20)  |
| 155.0 156.0 | irregular quartz veins cutting carbonate veins; also 1 cm wide carbonate + talc? vein; 40° c.a.                         |
| 166.0       | talc vein; 1 cm wide; 15° c.a.  |
| 167.0 169.0 | talc veins, 5 mm wide; 10 and 60° c.a.  |
| 172.0       | quartz vein, 1 mm wide; 25° c.a.  |
| 174.5 175.0 | massive talc  |
| 177.0       | talc veins, 5 mm wide, 25 and 55° c.a.  |
| 181.0       | chlorite fracture, 2 cm wide; 35° c.a.  |
| 181.5       | chlorite fracture, 1.5 cm wide; 15° c.a.; cut by 2-3 mm wide quartz vein; 2-3 mm wide, fibrous talc alteration envelope |
| 181.0 196.0 | serpentinite bleached light to medium gray, with varying amounts of talc, 10-90%, plus minor fibrous talc and chlorite  |
| 191.0       | chlorite fracture, 2.5 cm wide; fibrous talc envelope; 40° c.a.   |
| 192.0       | chlorite fracture, 2.5 cm wide; fibrous talc envelope; 70° c.a.   |
| 195.0       | fibrous talc vein; 80° c.a.   |
| 201.0 205.0 | massive talc  |
| 201.0 201.5 | coarse-grained chlorite   |
| 203.0       | coarse-grained chlorite fracture, 2.5 cm wide, with fibrous talc alteration envelope, 4 mm wide; 35° c.a.               |
| 204.0       | coarse-grained chlorite fracture, 2.5 cm wide, with fibrous talc alteration envelope, 4 mm wide; 35° c.a.               |

**APPENDIX IV. (cont.)**

| <u>Depth</u>   | <u>Structure</u>  |
|----------------|---|
| 18.0    19.0   | broken core   |
| 66.0    66.5   | crushed and broken ore  |
| 85.0           | weak to moderate fault/shear; 50° c.a.  |
| 89.0    91.0   | crushed and broken core; 60° c.a.   |
| 96.0           | broken core   |
| 105.0          | weak shear; 30° c.a.  |
| 111.0          | weak shear; 60° c.a.  |
| 120.0          | moderate shear; 30° c.a.  |
| 129.0    130.0 | strong fault?; sheared and brecciated serpentinite and chlorite at base; 60° c.a. |
| 172.0    174.0 | broken core   |
| 198.0          | slicks near contact; 75° c.a.   |
| 205.0          | chlorite gouge, 2.5-3 cm, cuts coarse chlorite; 35° c.a.                          |
| 208.0    209.0 | broken core   |
| 212.0    217.0 | broken and bleached core  |
| 228.0    232.0 | broken core   |
| 236.0    236.5 | clay gouge; slicks 75° c.a.   |

## APPENDIX IV. (cont.)

### Diamond Drill Hole PC 88-3

| <u>Depth</u><br>(in feet) | <u>Lithologic Description</u>  |
|---------------------------|--|
| 0.0    5.0                | strongly oxidized, poorly consolidated, silicified, serpentinite   |
| 5.0    21.0               | strongly silicified serpentinite; quartz(95)-disseminated magnetite(5); weathering produces a boxwork pseudogossan   |
| 21.0    45.0              | no recovery  |
| 45.0    66.0              | strongly silicified serpentinite; quartz(95)-disseminated magnetite(5); weathering produces a boxwork pseudogossan - more highly developed than above; rock often broken down to "sandy" texture |

End of Hole at 66 feet

| <u>Depth</u> | <u>Alteration and Mineralization</u>   |
|--------------|--|
| 5.0    66.0  | more or less silicified serpentinite   |
| 11.0         | silicified talc; 10-20 cm wide         |
| 12.0         | drusy quartz vein; 1 mm wide; 20° c.a. |
| 14.0    18.0 | quartz veinlets; 55, 45, 40, 80° c.a.  |

| <u>Depth</u> | <u>Structure</u>   |
|--------------|--|
| 0.0    7.0   | well broken core   |
| 7.0    9.0   | strong fault; 20° c.a.   |
| 19.0    21.0 | broken core  |
| 21.0    45.0 | not recovered, but rock is apparently well broken/ fractured causing poor recovery and loss of circulation |
| 45.0    60.0 | well broken core   |

## APPENDIX IV. (cont.)

### Diamond Drill Hole PC 88-4

| Depth<br>(in feet) | Lithologic Description   |
|--------------------|--|
| 0.0    2.0         | red-brown, sandy unconsolidated soil(?)  |
| 2.0    4.0         | reddish-brown clay zone - fault(?)   |
| 4.0    20.0        | weathered bedrock; generally sandy quartz-feldspar-biotite gneiss; some shearing apparent; saprolitic to 20 feet   |
| 20.0    26.0       | quartz + feldspar(80)-biotite(20) migmatitic gneiss; local segregations of quartz-feldspar; grain size 1-4 mm; distinctly foliated   |
| 26.0    54.0       | quartz + feldspar(97)-biotite(3) gneiss; very weakly foliated; grain size 2-10 mm  |
| 54.0               | contact 60 <sup>o</sup> c.a.   |
| 54.0    65.5       | quartz + feldspar(80)-biotite(20) migmatitic gneiss; weakly friable; thinly banded; 58 feet - banding 40-50 <sup>o</sup> c.a.  |
| 65.5    66.0       | medium-grained quartz-feldspar segregation(?)  |
| 66.0    69.0       | hornblende(20)-biotite(10)-quartz + feldspar(70) migmatitic gneiss; local quartz-feldspar segregations   |
| 69.0               | contact 65 <sup>o</sup> c.a.   |
| 69.0    71.0       | coarse-grained quartz-feldspar segregation(?)  |
| 71.0    95.0       | quartz + feldspar(60)-biotite(25)-hornblende(15) migmatitic gneiss; very irregularly banded (1-15 cm thick); hornblende locally concentrated; 78 feet - banding 55 <sup>o</sup> c.a.; 87 feet - banding 55 <sup>o</sup> c.a.   |
| 95.0               | contact 25 <sup>o</sup> c.a.   |
| 95.0    96.0       | quartz-feldspar rich layer   |
| 95.0    105.0      | quartz + feldspar(60)-biotite(25)-hornblende(15) migmatitic gneiss; very irregularly banded (1-15 cm thick); hornblende locally concentrated; 97 feet - banding 40 <sup>o</sup> c.a.   |
| 105.0    106.5     | quartz-feldspar rich layer   |
| 106.5              | contact 30 <sup>o</sup> c.a.   |
| 106.5    121.0     | quartz + feldspar(60)-biotite(25)-hornblende(15) migmatitic gneiss; very irregularly banded (1-15 cm thick); hornblende locally concentrated; 113 feet - banding 45 <sup>o</sup> c.a.; 119 feet - banding 40 <sup>o</sup> c.a. |
| 121.0              | contact 45 <sup>o</sup> c.a.   |

## APPENDIX IV. (cont.)

| <u>Depth</u> | <u>Lithologic Description (cont.)</u>       |
|--------------|---|
| 121.0 126.0  | granite; quartz + feldspar(95)-magnetite(5) |

End of Hole at 126 feet

| <u>Depth</u> | <u>Structure</u>                     |
|--------------|--------------------------------------|
| 2.0 4.0      | strong fault?; red brown clayey zone |
| 4.0 20.0     | broken core                          |
| 23.0 24.0    | broken core                          |
| 27.0 28.0    | broken core                          |
| 39.0 40.0    | broken and crushed core              |
| 50.0 51.0    | broken core                          |
| 61.0 62.0    | crushed and broken core              |
| 64.0 65.0    | crushed and broken core              |
| 71.0 73.0    | crushed and broken core              |
| 80.0 81.0    | crushed and broken core              |
| 90.0 91.0    | crushed and broken core              |
| 96.0 97.0    | broken core                          |
| 101.0 102.0  | broken core                          |
| 103.0 105.0  | broken core                          |
| 119.0 122.0  | broken core                          |







For convenience in selecting our reports from your bookshelves, they are color-keyed across the spine by subject as follows:

|            |  |
|------------|--|
| Red        | Valley and Ridge mapping and structural geology        |
| Dk. Purple | Piedmont and Blue Ridge mapping and structural geology |
| Maroon     | Coastal Plain mapping and stratigraphy                 |
| Lt. Green  | Paleontology   |
| Lt. Blue   | Coastal Zone studies                                   |
| Dk. Green  | Geochemical and geophysical studies                    |
| Dk. Blue   | Hydrology  |
| Olive      | Economic geology                                       |
|            | Mining directory                                       |
| Yellow     | Environmental studies                                  |
|            | Engineering studies                                    |
| Dk. Orange | Bibliographies and lists of publications               |
| Brown      | Petroleum and natural gas                              |
| Black      | Field trip guidebooks                                  |
| Dk. Brown  | Collections of papers                                  |

Colors have been selected at random, and will be augmented as new subjects are published.

Cartographers: Mark D. Cocker and Donald L. Shellenberger

\$2924/500

The Department of Natural Resources is an equal opportunity employer and offers all persons the opportunity to compete and participate in each area of DNR employment regardless of race, color, religion, sex, national origin, age, handicap, or other non-merit factors.